Interferon-gamma/Hypoxia Primed Mesenchymal Stem Cells for an Improved Immunosuppressive Cell Therapy

Holly Wobma

Submitted in partial fulfillment of the
requirements for the degree of
Doctor of Philosophy in the
Graduate School of Arts and Sciences

COLUMBIA UNIVERSITY
2018

ABSTRACT

Interferon-gamma/Hypoxia Primed Mesenchymal Stem Cells for an Improved Immunosuppressive Cell Therapy

Holly Wobma

Mesenchymal stem cells (MSCs) are promising candidates for treating diverse inflammatory disorders due to their capacity to be immunosuppressive. This phenotype is not present at baseline but develops in response to instructive cues. To date, clinical trials use cells grown in basic culture conditions, anticipating the cells will acquire a useful phenotype in response to *in vivo* cues. This strategy has failed to produce any FDA approved therapies, based on inconsistent efficacy. This thesis explores whether priming MSCs prior to administration can lead to a more uniformly therapeutic phenotype, and it details the design of an optimal *in vitro* priming regimen. Because interferon gamma (IFN-γ) is known to induce an anti-inflammatory state in MSCs, hypoxia can confer survival benefits, and both cues coexist in known situations of immune tolerance, we hypothesized dual IFN-γ/hypoxia priming would yield a superior immunosuppressive MSC therapy. We show that priming MSCs with hypoxia or IFN-γ alone improves their ability to inhibit T-cells *in vitro*, but combining these cues results in additive improvements. We next characterize the proteomic and metabolomic changes MSCs undergo when exposed to single or dual IFN-γ/hypoxia priming. While IFN-γ induces MSCs to suppress inflammation and fibrosis, hypoxia leads to cell adaptations to low oxygen, including upregulation of proteins involved in anaerobic metabolism, autophagy, angiogenesis, and cell migration. Dual priming results in additive effects, with many instances of synergy. Finally, we show initial evidence that dual primed MSCs are better able to inhibit disease progression in a mouse model of acute graft-vs-host disease (GvHD).

TABLE OF CONTENTS

LIST OF TABLES

LIST OF FIGURES

COMMONLY USED ABBREVIATIONS

APC	antigen presenting cell
BMM	bone marrow media
CALM	Center for Advanced Laboratory Medicine
COX-2	cyclooxygenase 2
DC	dendritic cell
DE	differential expression
ECM	extracellular matrix
ETC	electron transport chain
FSE	full skin equivalent
GLUT1	glucose transporter 1
GvHD	graft-vs-host-disease
Gy	gray: a radiation unit
HCT	hematopoietic cell transplantation
HLA	human leukocyte antigen
IDO	indoleamine 2,3-dioxygenase
IFN-γ	interferon gamma
iPSC	induced pluripotent stem cell
KC	keratinocyte
Log2FC	log2 fold change
MLR	mixed lymphocyte reaction
MSC	mesenchymal stromal cell
NSG	NOD-*scid IL2rγ*^{null} mice strain
PBMC	peripheral blood mononuclear cell
PD-L1	programmed death ligand 1
PGE2	prostaglandin-E2
TBI	total body irradiation
TCA	tricarboxylic acid [cycle]

Chapter 1

Introduction

1.1 Mesenchymal Stem Cells (MSCs)

Mesenchymal stem cells are multipotent progenitor cells that can be isolated from a wide range of tissues, most commonly from bone marrow, adipose tissue, or umbilical cords,[1,2] although they can also be differentiated from embryonic and induced pluripotent stem cells.[3,4] While there is some debate surrounding how to best define them, demonstration of tri-lineage differentiation capacity into osteocytes, adipocytes, and chondrocytes is thought to be a minimal criterion.[1] They should additionally have surface expression of CD73, CD90, and CD105 and lack expression of hematopoietic markers (CD11b, CD14, CD19, CD34, CD45 and HLA-DR).[1]

Because they are easy to isolate, do not raise the same ethical concerns as embryonic stem cells, do not form tumors (teratomas), and can be differentiated into a wide variety of cell types (**Figure 1**),[5] MSCs have traditionally been explored as a source cell to be differentiated into mature cell types for tissue engineering and regenerative medicine applications.

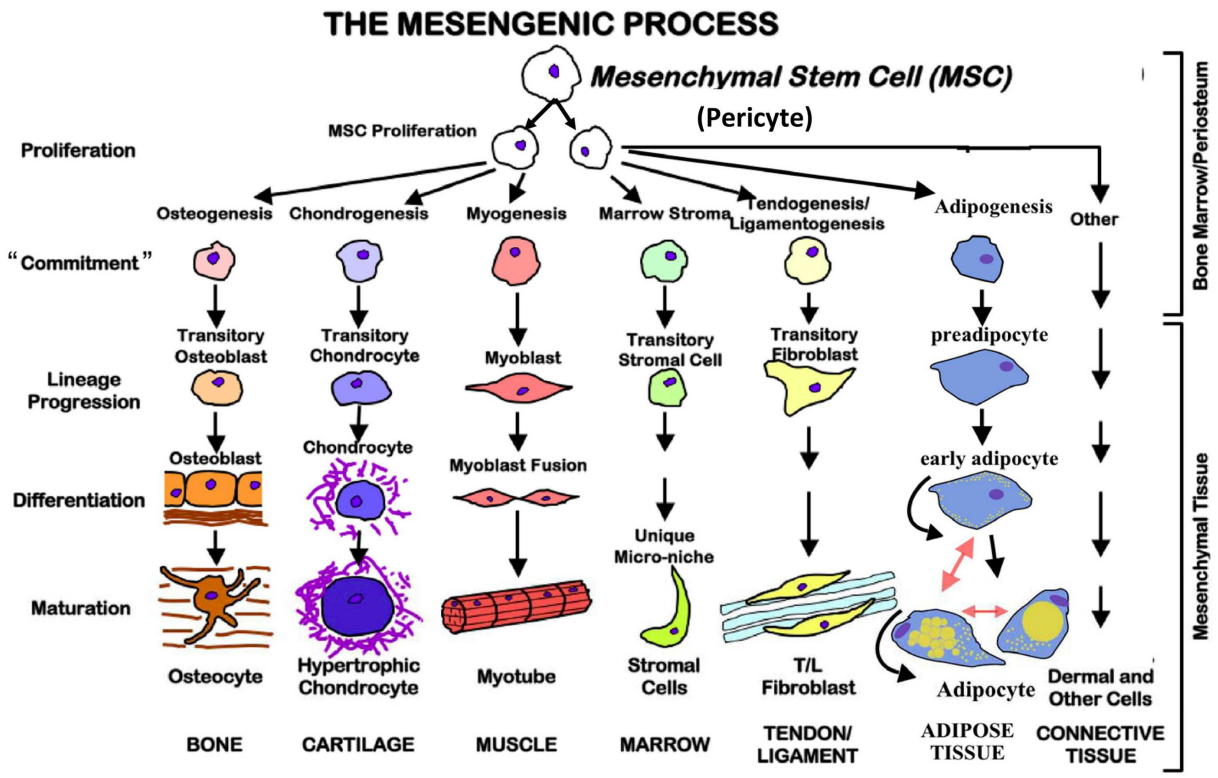

Figure 1 Demonstration of the diverse differentiation potential of MSCs (DiMarino et al.[5])

In the field of tissue engineering, many groups have used MSCs for engineering bone, cartilage, and other connective tissues.[6,7] Others have tried to use differentiated MSCs as mature cell therapies, creating neurons for central and peripheral nervous system damage,[8–10] cardiomyocytes for treating heart damage,[11] and so forth.

Despite their multipotent differentiation potential, it is not clear that endogenous MSCs naturally differentiate to aid in tissue repair *in vivo*. Indeed, there is a growing appreciation that their normal physiological role may have more to do with their paracrine effects,[2,12] based on *in vivo* observations that MSC delivery without differentiation and engraftment into injured tissues still leads to regeneration via alternative therapeutic mechanisms.[13–15] MSCs have been shown to release numerous growth factors (GFs) (e.g., EGF, FGF) and angiogenic factors (e.g., VEGF,

PDGF), and express immunomodulatory proteins and lipids capable of subduing both the innate and adaptive immune response (e.g., IDO, PGE2, HGF).[16] Because of these paracrine effects, MSCs could potentially be used to treat a wide variety of conditions, including acute inflammation, autoimmune disease, and graft rejection.

1.2 MSCs as Immunomodulatory Cells

1.21 Immune privileged or not?

Around 1998, researchers at Osiris Therapeutics started to present evidence that allogeneic MSCs could inhibit T-cells in gold standard immune activation assays and that MSCs were

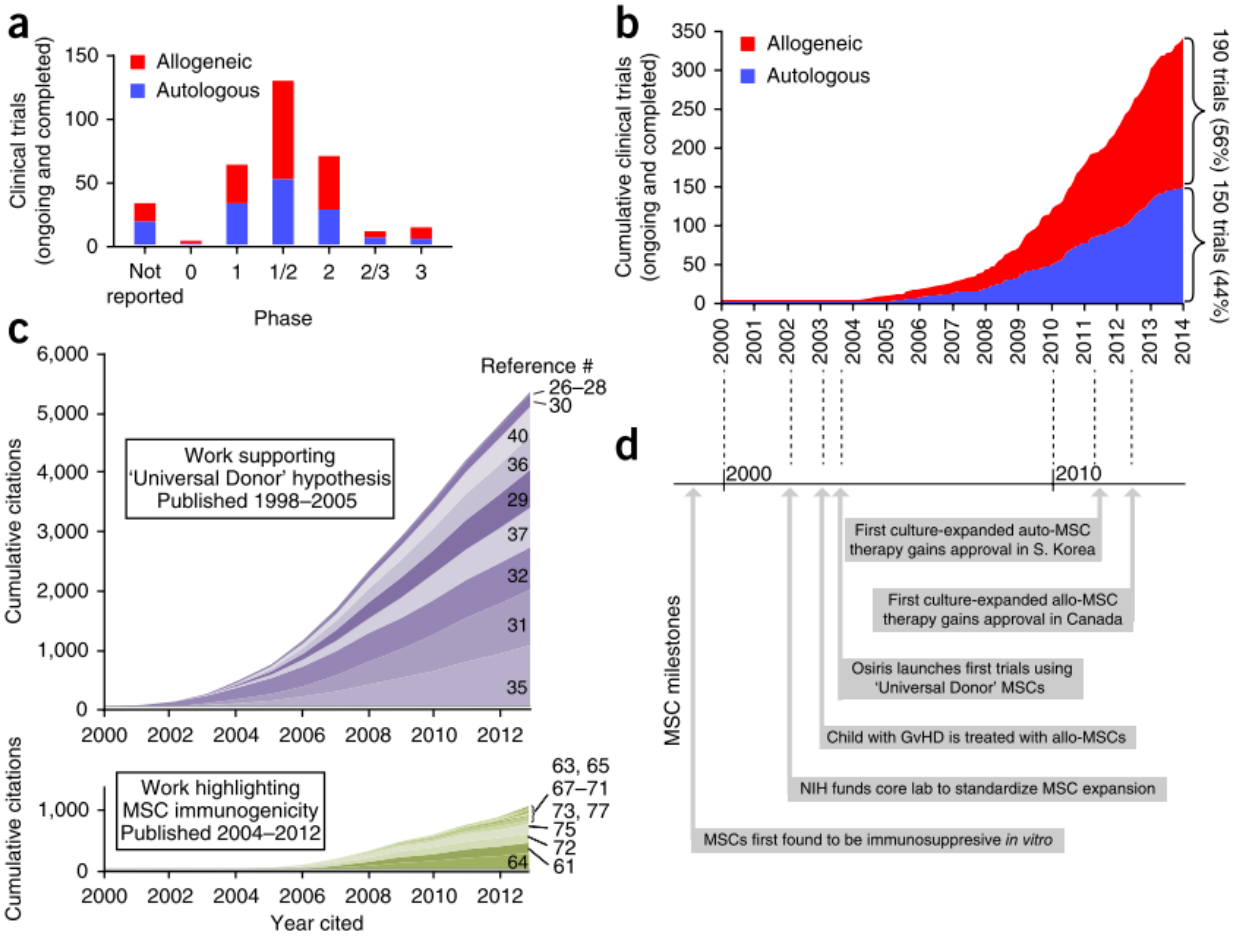

Figure 2 Historical perspective on the universal donor hypothesis for allogeneic MSCs (Ankrum et al.[16])

"immune priviledged".[16] They subsequently proposed the notion of universal, allogeneic MSC therapies, a striking contrast to the related field of hematopoietic stem cell transplantation, where human-leukocyte antigen (HLA) matching between donor and recipient is paramount.

Over the next 5 years, the scientific community latched onto the notion of MSCs being immune privileged, even capable of showing an immunosuppressive effect in xenogeneic models without any negative sequelae related to rejection.[17,18] More recent evidence, however, supports that allo- and xeno-MSCs do express immunogenic proteins, but the influence of these is partially offset by the expression of a variety of immunosuppressive and immune protective factors **(Figure 2).**[16] Notably, even if a slight allogeneicity increases the clearance rate of allo or xeno-MSCs, they still have a lasting impact on the immune system. This has been described as the "hit-and-run" effect,[19,20] and it is one reason why clinicians are optimistic that even single doses of MSCs could provide a long-term benefit to patients.

1.2.2 Mechanisms of immunomodulation

Early studies provided evidence that MSCs act through paracrine mechanisms such as through the secretion of exosomes and immunosuppressive proteins. While true, several surface (e.g. PD-L1[21]) and intracellular (e.g. IDO[22]) factors have been identified as being critical to the therapeutic function of MSCs, and there is also evidence that they may mediate their effect through the formation of apoptotic bodies.[23] While the relative importance of these diverse mechanisms is hard to quantify, it is at least clear that the repertoire by which MSCs act as immunomodulatory cells is highly diverse. We summarize factors that have been associated with MSC immunosuppression in **Table 1.**

Table 1 The numerous immunomodulatory factors implicated in the ability of MSCs to be immunosuppressive and immune protected. * Mϕ – macrophage; APC – antigen presenting cell; DC – dendritic cell; T-reg – regulatory T-cell; NK cell – Natural Killer Cell

Factor	Immunomodulatory Effects	Target
IDO[22,23]	• Limits T and NK cell proliferation • Induction of tolerogenic DCs & Tregs • Promotes Th1→ Th2 switch • Promotes M2 Mϕ polarization • Assists with microbial clearance	Tryptophan; catabolizes to kynurenine
HLA-G[24]	• Inhibition of T & B cell proliferation • Inhibition of cytolysis by $CD8^+$ & NK cells • Induction of T-regs	ILT2 ILT4 KIR2DL4 CD160
HLA-E[25]	• Can activate (NKG2C) or inhibit (NKG2A) NK cell mediated lysis; higher affinity for inhibitory receptor • Blocks lysis by $CD8^+$ T cells	CD94/NKG2A CD94/NKG2C
TGF-β[26]	• Induction of T-regs	TGFBR1
HGF[27]	• Decreases cytotoxic activities of NK & $CD8^+$ T cells • Increases neutrophil migration & activity • Reduces antigen presentation by APCs • Promotes pro-tolerogenic DCs & T-regs • Promotes tissue repair by macrophages • B cell differentiation (once activated)	c-Met
LIF[28]	• Inhibits lymphocyte proliferation • Contributes to T-reg formation	LIF-R
PGE2[26]	• Suppression of T cell activation & proliferation • Can alter Mϕ phenotype • Inhibits Th17 differentiation	EP2 EP4
NO[26]	• Acts short distance to inhibit T cell proliferation & induce T cell apoptosis • May be more important in mice than humans	Many via forming reactive nitrogen species
TSG-6[15]	• Participates in extracellular matrix remodelling • Anti-inflammatory/limits pro-inflammatory response • Modulates leukocyte migration	CD44
CD59[29]	• Blocks formation of membrane attack complex, protecting cell from complement mediated destruction	C9
PD-L1[21]	• Co-inhibitory signal in activated T-cells • Promotes T-cell anergy & apoptosis	PD-1

1.2.3 Homing of cells

Beyond the ability to directly modulate immune cell activity, MSCs have also been shown to mimic leukocytes in their ability to home to inflamed sites. Detailed studies of MSC homing

suggest that there are both active and passive mechanisms at play.[30] Inflamed tissues exhibit vasodilation such that blood flow is shunted towards the damaged site. Leukocytes exit circulation via the expression of surface adhesion molecules on activated endothelium (and leukocytes),[31] and MSCs may leave circulation in a similar manner (active). However, they may also migrate due to more physical forces (passive). MSCs are large cells, with a diameter that can be larger than the lumen of microvasculature. Thus, as they attempt to flow through, their course will be naturally slowed, and they may transmigrate through the endothelium rather than continue through the lumen of the blood vessel.[32] This could be facilitated by the leaky vasculature common to inflamed tissues and the remodeling of the local extracellular matrix (ECM). There is some speculation that chemokines could also contribute to MSC homing. For example, the SDF-1/CXCR4 axis could contribute to migration towards the bone marrow. However, MSCs do not seem to uniformly express this chemokine receptor, and thus investigators that have wanted to augment cell migration have done so by genetically engineering the cells to overexpress the desired chemokine receptor.[33–36]

1.2.4 Summary of potential as an immunomodulatory cell therapy

Given that MSCs home to the diseased site, exhibit a diverse repertoire of immunomodulatory factors, and can be used allogeneically, they appear to be ideal candidates for treating conditions where there is an overactive immune response. Intuitive examples of such disorders include organ rejection, sepsis, and autoimmune disease. However, pathological inflammation plays a role in many other disease processes, including conditions as disparate as depression and atherosclerosis.[37,38] While our understanding of how to use MSCs in patients is still in its infancy, clinical trials are starting to provide some insights.

1.3 Human Clinical Trials and their Challenges

1.3.1. Clinical trials show inconsistent and unclear efficacy

Over the past decade, there have been over 800 registered clinical trials (clinicaltrials.gov) using MSCs to treat a wide variety of pathologies.[23] While trials have clearly demonstrated a strong safety record,[39] the efficacy of MSCs has been modest and inconsistent.[40,41] For example, one of the most extensively explored applications has been for treatment of heart disease.

Initial preclinical studies in large animal models (porcine, canine, ovine) showed promising data for treatment of acute myocardial infarction (MI),[42,43] subacute MI,[44,45] and chronic ischemia,[46] using standard benchmarks of cardiac health such as ejection fraction, left ventricular end-diastolic volume, contractility, scarring, and vascular density.

Similar studies were then conducted in human patients such as the phase I/II POSEIDON trial, which showed improved ejection fraction, fewer arrhythmic events, and reduced cardiac hypertrophy in patients after acute MI.[47] Results for chronic ischemia followed the same trends, as the PROMETHEUS and TAC-HFT trials all showed significant decrease in scar size after injection of MSCs, leading to better perfusion and contractility.[48,49] Based on these and other promising phase I/II data, phase III trials followed. However, these results were less encouraging. For example, the BOOST trial showed that intracoronary delivery of MSCs improved left ventricle ejection but this difference was no longer significant after 18 months.[50] This questionable efficacy was not unique to cardiac studies. Two phase III trials of Prochymal, a commercial MSC therapy developed by Osiris Therapeutics, did not meet their primary end point for treatment of graft-vs-host-disease, and in other indications, Osiris's testing did not fare much better. A phase III trial geared toward Crohn's disease was discontinued, while treatment of chronic obstructive pulmonary disease also failed to meet its efficacy end point.[51,52] To this

day, there are still no FDA approved MSC therapies, although many companies and academic clinicians are actively pursuing clinical trials.

1.3.2 Cited reasons for poor clinical trial outcomes

Many explanations have been offered for why MSCs continue to fail in clinical trials despite encouraging animal model data.[21,22,53] For example, contrary to animal studies which use fresh, low-passage MSCs, most clinical trials have used industrially manufactured, frozen MSCs. Given the higher quantities of cells needed in human (vs. mouse) studies, the cells may be over-expanded, and MSC immunomodulatory capacity is known to decline with increasing passage number (cell senescence).[23,52] Most manufactured products are also cryopreserved and thawed only hours before transfusion into patients. Prochymal was found to have a viability of about 70% upon thawing, but many believe that even the "live" cells are dysfunctional, with lowered metabolism and immunomodulatory capacity.[54]

A final consideration is that MSCs are not immunosuppressive at baseline and only adopt this phenotype in response to instructive cues.[23] Since clinical trials have used "naïve" MSCs, the therapeutic capacity reached by the cells is entirely dependent on an individual patient's internal microenvironment. Compared to in-bred mice, humans show much greater biological variation, which may explain the lack of consistent benefit MSCs have shown in human clinical trials. A strategy that could potentially mitigate such variation would be to "prime" cells with instructive cues before injection. This could induce uniformly therapeutic cells, which would no longer rely on patient-specific *in vivo* cues. In further support of this notion, studies have shown that priming MSCs can also revitalize senescent cells to become usefully immunomodulatory again,[55] overcoming one of the previously listed obstacles.

1.4 Our Strategy

1.4.1 Objective

Considering the many ways by which priming MSCs could improve upon current therapies, our goal was to design an optimal *in vitro* priming regimen that could eventually be developed for testing in clinical trials. We first examined the microenvironmental cues common to biological scenarios where immune escape and immune tolerance are present, such as solid tumors.[56–58] Across diverse malignancies, hypoxia and inflammation are commonly present, suggesting that the combination of these two environmental cues may be ideal for inducing immunosuppressive cell phenotypes. In support of this notion, there have been several studies of priming MSCs with one of these two priming cues.[22,59,60]

The pro-inflammatory cytokine interferon-γ (IFN-γ) has been the most extensively investigated factor for priming MSCs.[22,23,61] Indeed, the International Society for Cellular Therapy (ISCT) recommends it as a standard priming method for evaluating the immunosuppressive capacity of MSCs *in vitro,* with induction of the tryptophan catabolizing enzyme indoleamine-2,3-dioxygenase (IDO) as a readout.[23] In addition to IFN-γ, hypoxia priming has been shown to enhance the immunomodulatory capacity of MSCs, their ability to promote angiogenesis and tissue repair, and survival in animal models of ischemia.[59,62–64]

1.4.2 Hypothesis

Based on the above observations, we hypothesized that combining IFN-γ and hypoxia priming would lead to MSCs that are more effective as an immunosuppressive cell therapy than if either cue were used alone.

1.4.3 Specific Aims

We first sought to test our hypothesis by comparing how IFN-γ and hypoxia directly alter the immunomodulatory phenotype of MSCs. This led to our First Aim:

Aim 1: To evaluate the effect of single vs. dual IFN-γ/hypoxia priming on the immunomodulatory capacity of MSCs

However, the "therapeutic" quality of MSCs for treating immune and non-immune disorders depends on more than their anti-inflammatory features, as cell survival and homing also play important roles. We thus wanted to obtain a more comprehensive understanding of how various priming regimens altered the MSC phenotype. This led to our Second Aim:

Aim 2: To conduct a global proteomic and metabolomic characterization of single vs. dual IFN-γ/hypoxia primed MSCs

Finally, we sought to assess whether dual priming MSCs would lead to a significant improvement in their ability to treat GvHD. For these studies, we planned to use a well-established xenogeneic mouse model of GvHD. We additionally wanted to leverage the skills of our lab to develop an *ex vivo* engineered model of GvHD of the skin, which is a model that is still in development. These aspirations are summarized in our Third Aim:

Aim 3: To compare the ability of dual IFN-γ/hypoxia primed vs. unprimed MSCs to prevent disease progression in models of acute GvHD

Chapter 2

Methods for MSC Culture and Priming

2.1 MSC line validation

Frozen vials of MSCs from eight separate fully de-identified human lipoaspirates (LaCell, New Orleans, LA) were used in experiments. Given the trend towards using adipose-derived MSCs in clinical trials, we used cells from this source for our studies.[12] However, many previous studies of MSC priming have used MSCs from alternative tissue sources[9,11,13,16], and so we will retain the acronym "MSC" to emphasize the likely generalizability of our findings.

Cell lines were initially tested for tri-lineage differentiation as well as positive expression of *in vitro* MSC surface markers. Adipogenic, chondrogenic, and osteogenic differentiation was performed as previously described.[65] For immunophenotyping, MSCs were stained for standard MSC markers (CD29, CD73, CD90, CD105*)* as well as for HLA-DR, both before and after priming. Cells were stained in BD BSA Stain Buffer for 20 minutes at 4 °C and then washed twice in this same buffer. All data collection was performed on a BD FACS CANTOII flow

cytometer followed by analysis in FlowJo (Ashland, OR). Representative data from one of the most commonly used MSC lines is shown in **Figure 3**. MSC lines were also regularly tested to be mycoplasma negative (MycoAlert, Lonza).

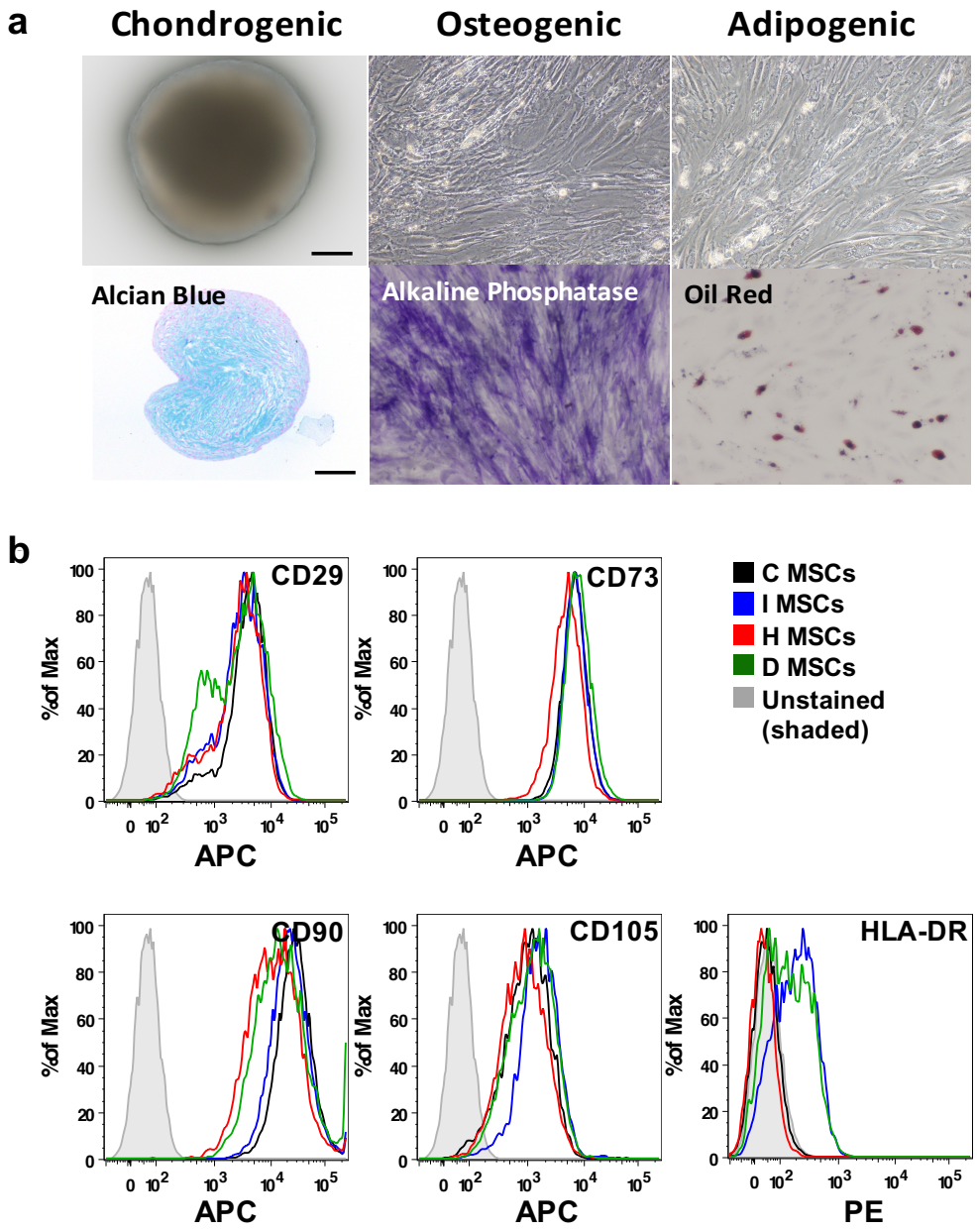

Figure 3 (a) Demonstration of tri-lineage differentiation capacity of control adipose-derived MSCs. **(b)** Expression of MSC surface markers and HLA-DR upon exposure to different priming conditions.

2.2 MSC culture and priming

MSCs were expanded to P3 and cryopreserved. MSC expansion media consisted of high glucose DMEM 11965 (ThermoFisher), 10% FBS, and 1% Penicillin/Streptomycin. Cryopreservation media consisted of 50% MSC media, 40% FBS, and 10% DMSO. For a given experiment, P3 vials were thawed, sub-cultured to P4 (seeding density 5,000 cells/cm^2) and, upon near-confluence, were either kept in control conditions or exposed to 1% O_2 (New Brunswick Galaxy 14S or 48R incubator), 25-100 ng/mL IFN-γ (Peprotech), or both conditions. Cells were then collected for characterization or functional assays, as shown in **Figure 4**. Regardless of priming condition, MSCs always had a viability of >95%.

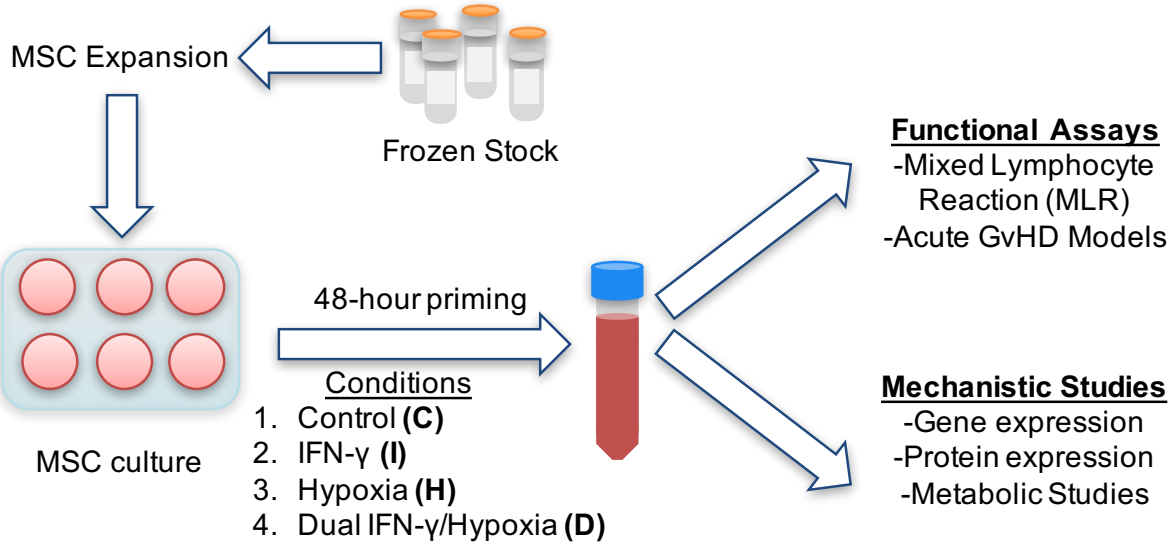

Figure 4 Experimental Design. Primed MSCs were evaluated for their ability to inhibit T-cells in MSC-mixed lymphocyte reaction co-cultures (MSC-MLR). To then discern the origin of group differences in immunosuppressive capacity, numerous mechanistic studies were pursued.

2.3 Optimizing priming duration

Initial pilot studies were conducted to determine the optimal duration of priming. First, two vs. four day priming regimens were compared. The fold increase in expression of six immunosuppressive genes upon dual IFN-γ/hypoxia priming was determined by polymerase chain reaction (PCR). Since none of the genes had higher induction at day four vs. day two, it

was deemed unnecessary to prime cells for longer than two days **(Figure 5)**.

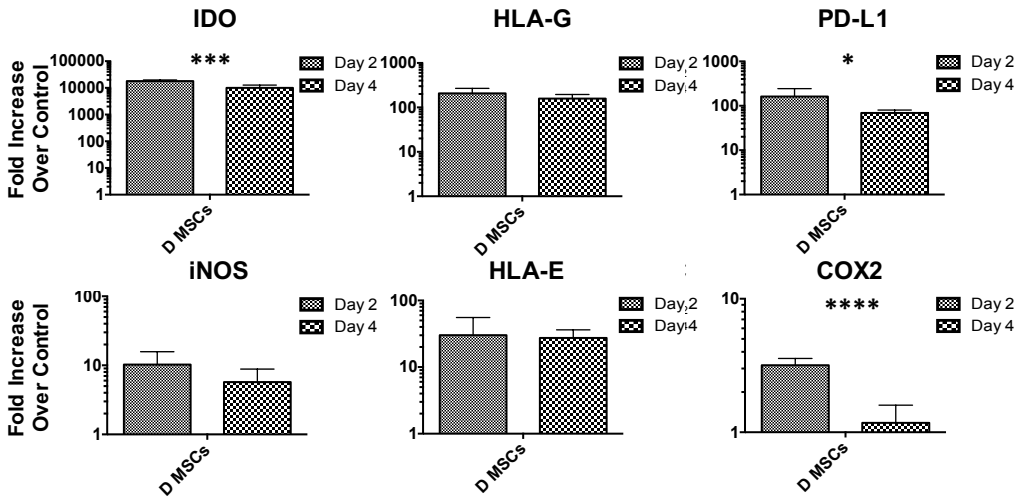

Figure 5 Comparison of the fold increase ($2^{-\Delta\Delta Ct}$) in immunosuppressive gene expression in dual primed over control MSCs using a two-day vs. four-day priming regimen.

The gene most highly induced at day two was indoleamine-2,3-dioxygenase (IDO). Since this protein is thought to be very important for MSC function,[23] the kinetics of IDO upregulation were subsequently tracked by both PCR and flow cytometry (**Figure 6a and b**).

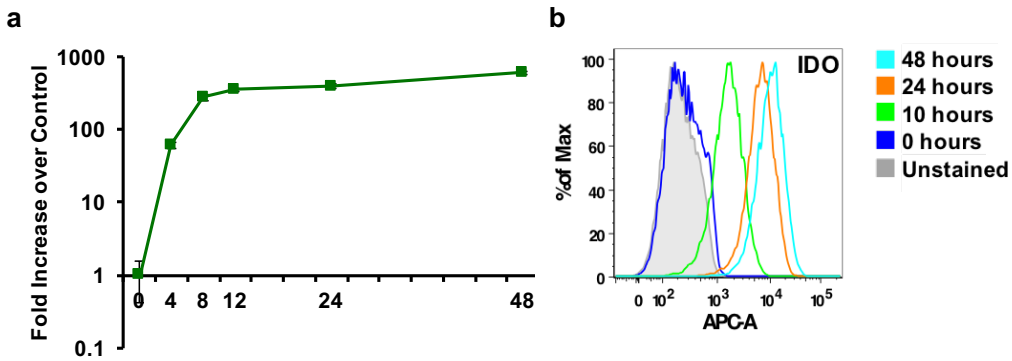

Figure 6 IDO onset kinetics. MSCs were exposed to dual IFN-γ/hypoxia for different durations before samples were collected for **(a)** PCR analysis and **(b)** flow cytometry analysis.

While significant induction occurred by 8-12 hours of exposure, expression levels were still higher from 48 hours of priming. For this reason, a 48-hour priming regimen was chosen for all further experiments.

Chapter 3

Aim 1: To evaluate the effect of single vs. dual IFN-γ/hypoxia priming on the immunomodulatory capacity of MSCs

3.1 Overview

In the literature, the notion of "licensing" or priming MSCs towards an immunosuppressive phenotype is almost exclusively done with pro-inflammatory cytokines.[66–68] While some studies have used TNF-α, LPS, or other toll-like receptor agonists to accomplish this feat, the most commonly cited method is to use IFN-γ.[22,23] Nevertheless, there are a growing number of studies focusing on the potential benefits of hypoxia for MSC therapies. For example, some describe its ability to promote a more primitive MSC phenotype in the long term, enabling MSCs to better maintain their stemness and avoid senescence as they are expanded to clinically relevant numbers.[69] Other studies have shown a survival benefit to hypoxia preconditioning, as it appears

to prolong the lifespan of MSCs injected into animal models of ischemia.[70,71] However, few studies have explicitly focused on how hypoxia affects the immunosuppressive function of MSCs,[72,73] even though there is reason to believe this might be true.

Two of the best natural examples of immune escape and tolerance are solid-tumors and the maternal-fetal interface.[74,75] In addition to the presence of inflammatory cells, these physiological states demonstrate a low oxygen tension. Because tumors often grow at a faster pace than their neovasculature, they tend to have hypoxic cores.[57] Hypoxia is also characteristic of the first trimester of pregnancy.[76] It thus seems plausible that hypoxia supports survival and growth in these settings by helping to prevent immune attack. Mechanistically, some studies have suggested a correlation between hypoxia and anti-inflammatory macrophages.[77] Others have implicated hypoxia in the upregulation of HLA-G, an immune tolerance promoting protein found in both biological scenarios. MSCs are also known to be able to express HLA-G, and the confluence of these observations led us to suspect that hypoxia preconditioning of MSCs may do more than just influence their stemness and survival skills *in vivo* – it could also directly impact their immunomodulatory capacity. Our first aim was thus to determine if – as with IFN-γ – hypoxia could induce an immunosuppressive phenotype in MSCs, and if so, whether combining both cues would yield even more potent immunosuppression.

3.2 Materials and Methods

3.2.1 Mixed lymphocyte reactions (MLRs)

For MLRs, a peripheral blood mononuclear cell (PBMC) cryo-bank was made using fully de-identified samples from 10 different donors, to generate different sets of stimulator-responder pairs. PBMCs were isolated from fresh leukopaks (New York Blood Center, New York, NY)

using Histopaque-1077 (Sigma, St. Louis, MO) based on density gradient centrifugation, washed twice with bone marrow medium (BMM; Media 199 (Thermo Fisher) containing 1% HEPES, 1% Penicillin/Streptomycin, and 20 kU DNAse I (Sigma), treated with ACK lysis buffer (Thermo Fisher) for red cell lysis, and cryopreserved.

MSCs were trypsinized after 48-hour priming and seeded at either 1×10^6/mL or 2×10^6/mL in 40 μL (i.e. 40,000 or 80,000 cells total) in 96-well U-bottom plates in complete AIM-V (Thermo Fisher) supplemented with 5% heat-inactivated human AB serum (Sigma), 1% Penicillin/Streptomycin, 1% HEPES, and 50 μM 2-mercaptoethanol (cAIM-V). Two batches of allogeneic PBMCs were thawed in 1:1 BMM:cAIM-V and washed twice. Responder PBMCs were stained with BD Violet Proliferation Dye (Becton Dickson (BD) Canaan, CT) per manufacturer's instructions (final concentration: 1 μM). Stimulator PBMCs were inactivated using 30 Gy X-ray irradiation with an X-RAD 320 irradiator (Precision X-ray Inc., North Branford, CT) or 10 mg/mL Mitomycin C (always provided similar results in comparison studies). Stimulator and responder PBMC cell concentrations were adjusted to 2.5×10^6/mL, and 80 μL of each cell suspension (i.e. 200,000 cells) was layered on top of previously plated MSCs. Thus, the stimulator to responder ratio was 1:1 and the MSC to responder ratio was 1:2.5 or 1:5.

MLR experiments were run for 5 days, with 50 μL of cAIM-V added halfway through. For end-point analysis, two antibody panels were used: CD3/4/8/25/107a (activation/cytotoxicity) and CD3/4/45RA and CCR7 (naïve vs. memory). Primary conjugated antibodies (BD) were used at the recommended test size, except for CD4 and CD8, which were used at 1:80 and 1:40 dilutions, respectively (see **supp**. **Table S1** for clones). All surface staining was done without fixation in BD BSA Stain buffer. Flow cytometry analysis was done within 30 minutes of staining. When analyzing CD4+ and CD8+ subpopulations, each group was

normalized to that of the MLR with no MSCs (positive control set to 100%) by dividing each experiment's % divided (violet negative), % CD25+, or % CD107+ by the corresponding values for the MLR only condition. These group data were then averaged over 7-11 experiments.

For some experiments, extra MLR-MSC reactions were set up for various Day 1 and Day 3 analyses. Pro-inflammatory cytokine levels were detected using a Human Cytokine 16-Plex ELISA kit (PBL Assay Science, Piscataway, NJ). Supernatant glucose levels were determined by the Hormone and Metabolite Core Laboratory at Columbia University Medical Center. Supernatant lactate levels were determined by the colorimetric L-Lactate Assay Kit (Abcam, Cambridge, MA), following an initial deproteinization step (as instructed) and dilution 1:3 to be within the range of the kit. Cells from Day 1 and Day 3 MSC-MLR experiments were also collected, fixed, permeabilized, and stained for the GLUT1 transporter.

3.2.2 qRT-PCR

A list of 15 genes implicated in MSC-based immunosuppression/protection was established based on published studies (primers shown in **Table S2)**.[16,28,78–83] MSC priming experiments were repeated 4 times using MSCs from 3 different donors. RNA was isolated using the RNAqueous Micro Kit (Thermo Fisher) and quantified using a Nanodrop ND1000 (Wilmington, DE). RNA was treated with DNase I, Amplification Grade Kit (Thermo Fisher) and converted to cDNA using the High Capacity cDNA Reverse Transcription Kit (Thermo Fisher). qRT-PCR analysis was performed using 20 ng cDNA per reaction and SYBR Green Master Mix (Thermo Fisher). The expression of target genes at each time point was normalized to GAPDH, which has been shown to be robust as a housekeeping gene for MSCs in hypoxic conditions,[84] and subsequently to the unprimed phenotype at its baseline time point ($2^{-\Delta\Delta Ct}$).

3.2.3 IDO activity assay

MSCs that had just been primed for 48 hours were re-plated in fresh control MSC media at 10,000 cells per well in 96-well plates and left overnight to attach. Measurement of IDO activity was achieved via a kit (BPS Bioscience, San Diego, CA) as per the manufacturer's protocol, with the modification that no transfection of IDO was performed, and it was simply measured in the MSCs of different priming conditions. Samples were performed in replicates of 6.

3.2.4 HLA-G Western blot

After washing twice with PBS, primed MSCs were lysed on ice for 30 minutes with NP-40 Lysis buffer containing phosphatase and protease inhibitors each at a 1:50 ratio (Thermo Fisher). Lysates were centrifuged at 4 °C, 13,600 × g for 15 minutes. Protein concentrations were determined via a BCA protein assay (Thermo Fisher). After the protein concentrations from different MSC priming groups were normalized, the supernatant was diluted 1:1 with 2x Laemmli Sample Buffer (Bio-Rad, Hercules, CA) and boiled at 95 °C for 5 minutes. Protein samples were resolved by SDS-PAGE in a 4–20% precast polyacrylamide gel (Bio-Rad) and electrotransferred onto a polyvinylidene difluoride membrane. After transfer, the membrane was blocked with 5% BSA TBST for 1 hour and probed with anti-HLA-G primary antibody (1:500; OriGene Technologies) at 4 °C overnight. The membrane was then washed with TBST x3 and exposed to goat anti-rabbit IgG AlexaFluor 680 secondary antibody (1:10,000; Thermo Fisher) for 1 hour. The membrane was then imaged on a Licor Odyssey scanner (Lincoln, NE).

3.2.5 Flow cytometry for functional proteins

MSCs were stained for immunomodulatory proteins that had shown up-regulation at the

mRNA level from qRT-PCR (HLA-G, COX-2, IDO, PD-L1, HLA-E; also GLUT1 for metabolic studies). For intracellular proteins, cells were fixed, permeabilized and stained using the reagents in the BD Cytofix/Cytoperm kit. For surface staining, cells were stained in BD BSA Stain Buffer for 20 minutes at 4 °C and then washed twice with stain buffer. All data collection was performed on a BD FACS CANTOII flow cytometer followed by analysis in FlowJo. A complete list of antibody clones and dilutions can be found in **Table S1**.

3.2.6 HGF ELISA

MSC supernatant collected at the end of 48 hour priming was collected, spun down to pellet cell debris, and then transferred to fresh tubes for storage at -80 °C. ELISA samples were brought to room temperature and used undiluted with the Invitrogen Human HGF ELISA kit (Carlsbad, CA), as per manufacturer's instructions.

3.2.7 Seahorse assays

Seahorse assays were conducted to determine whether priming affected MSC metabolism, as this could possibly explain differences in immune modulatory capacity. Differently primed MSCs were plated on Seahorse tissue culture plates (10,000 cells in 100 µL) and incubated overnight at 37 °C in a standard 5 % CO_2 incubator. The following day, wells were washed twice with Seahorse Assay medium (100 mL) containing (1 mL of 200 mM L-glutamine, 1 mL of 100 mM Sodium Pyruvate, and 400 µL of 45% D-Glucose; pH 7.4) and the plate was kept in a non-CO_2 incubator for 2 hours prior to running the MitoStress Assay (Oligomycin 1 µM, FCCP 1 µM, Rotenone/Antimycin 1 µM). Data were analyzed using Wave (Agilent, Santa Clara, CA).

3.2.8 Lactic acid titration

PBMCs were thawed, as previously described, and stained in HEPES-buffered saline at 37 °C for 30 minutes with pHrodo® Red AM (Thermo Fisher) as per manufacturer's instructions (1000x dilution of dye). After a single wash with HEPES buffer, samples were divided into 5 eppendorf tubes, spun down, and resuspended in cAIM-V with L-lactic acid (Sigma) added to make concentrations of: 0 mM, 5 mM, 10 mM, 20 mM, and 30 mM. Cells were resuspended in these new media and incubated at 37 °C for 30 minutes. Immediately prior to each flow cytometry reading, each sample was diluted 1:9 with BD Stain Buffer and mixed well. This neutralized external pH and diluted media components without permitting time for intracellular lactate to be exported. For lymphocyte proliferation experiments, PBMCs were thawed and stained with BD Violet Proliferation dye, as described previously, and resuspended in cAIM-V with L-lactic acid added to the concentrations above. Cells were plated in 96-well U-bottom plates at 200,000 cells per well. Concanavalin A was added to be 5 μg/mL, and PBMCs were analyzed by flow cytometry on Day 3.

3.2.9 Mass spectrometry

MSC plates were washed x3 with ice-cold PBS to remove residual FBS and added cytokines. Lysis buffer consisting of TBS with 3% SDS and 50 μL protease inhibitors (Sigma) was added to each MSC plate. The lysate was collected and proteins were precipitated in chloroform/methanol. Mass spectrometry was performed at the Quantitative Proteomics and Metabolomics Center at Columbia University with an UltiMate 3000 RSLCNano ultrapressure liquid chromatograph coupled to a Q Exactive HF (Orbitrap) mass spectrometer.

3.2.10 Statistical analysis

One-way ANOVA analysis in conjunction with Tukey post-hoc tests was used to compare the MLR, PCR, Flow cytometry, ELISA, glucose, and lactate results from different priming groups using GraphPad Prism 6 software (La Jolla, CA). Data were presented as mean ± standard deviation, and a p value <0.05 was considered statistically significant.

3.3 Results

3.3.1 MSC priming with IFN-γ or hypoxia leads to similar improvements in T-cell inhibition over control MSCs, while dual primed MSCs show twice the functional improvement

Addition of control MSCs to MLRs resulted in mild inhibition of both CD4+ and CD8+ T cell proliferation (% Divided) and activation (% CD25+) at Day 5 of MSC-MLR co-cultures (**Figure 7a & 7b**). When IFN-γ or hypoxia primed MSCs were instead used, MSCs were consistently ~25-30% more effective at inhibiting proliferation and activation of CD4+ T-cells (i.e. determined by % divided primed MSCs/% divided C MSCs), and ~20% more effective at inhibiting CD8+ T-cells. This inhibitory advantage approximately doubled for MLRs with dual-primed MSCs. Doubling the dose of MSCs by using a 1:2.5 MSC:PBMC ratio led to greater T-cell inhibition regardless of priming regimen, although the relative inhibitory capacities amongst the priming groups were notably maintained. Dual primed MSCs also showed significantly greater inhibition of CD8+ T-cell cytotoxicity (%CD107+) compared to control MSCs, although this was only seen at the 1:5 MSC:PBMC ratio.

The effect of MSC:MLR co-culture on differentiation of responding T cells was studied by analyzing the expression of CCR7 and CD45RA. By day 5, the responder-only group (negative control; no allogeneic PBMCs present) had 48% of the CD4+ T cells in the naïve sub-

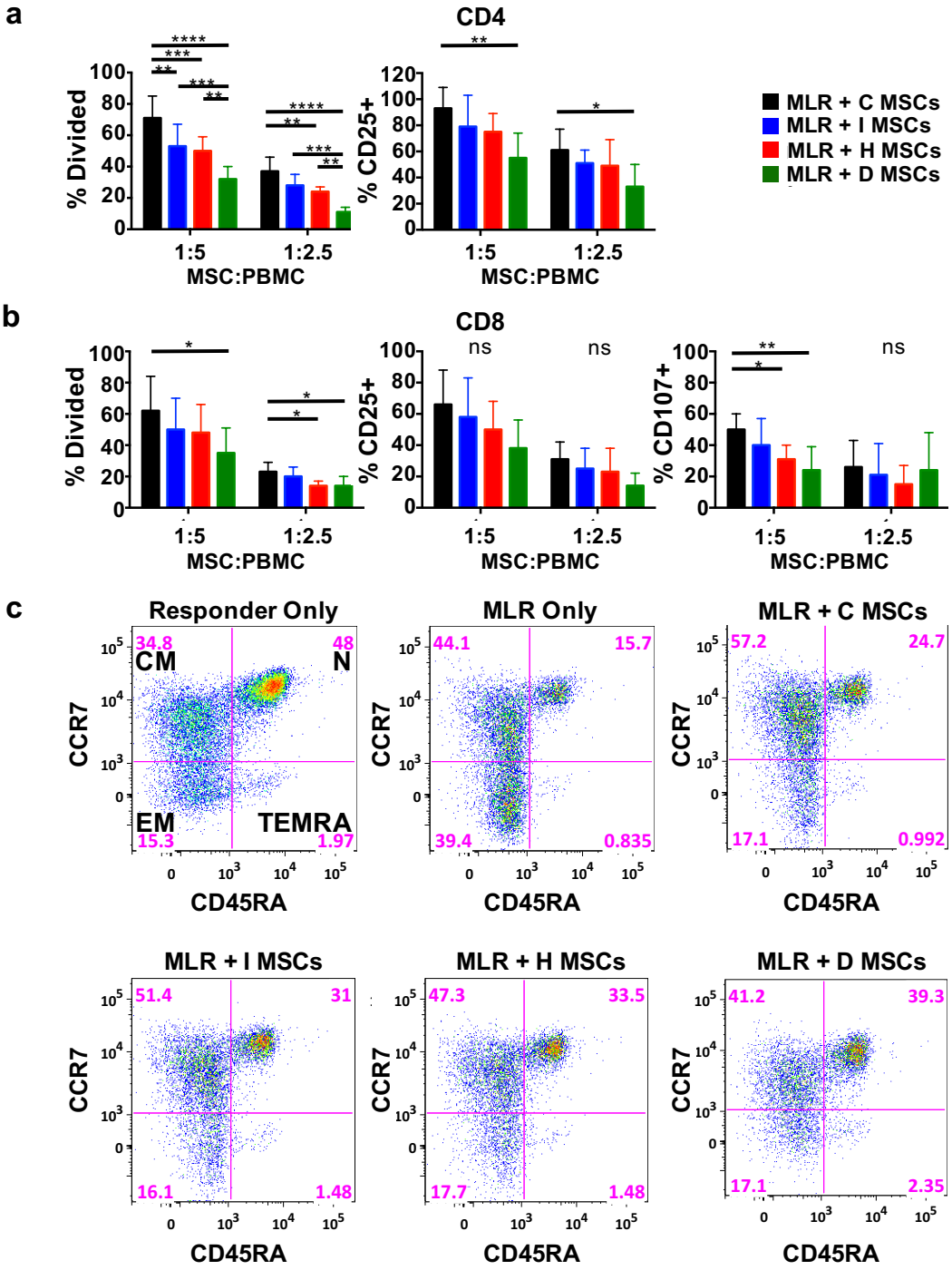

Figure 7 End-point analyses for MSC-MLR co-culture. The variable inhibition by control (black) and primed MSCs (colored) is evident by comparing their violet- population (% divided) to that of the MLR alone condition (set to 100% division) at day 5. T-cell activation status (% CD25+) and cytotoxic capacity (% CD107+) were similarly determined at day 5. **(a)** Shows activation and proliferation data for the CD4+ T-cell fraction. **(b)** Shows these same data for the CD8+ T-cell fraction. **(c)** Representative memory panel data for the CD4 subset at Day 5 of an MLR-MSC co-culture study. The "responder only" group was a negative control that lacked allogeneic stimulator PBMCs. N:naïve; CM: central memory; EM: effector memory; TEMRA; terminal effector; n = 7-11 $p < 0.05$ *, < 0.01 **, < 0.001 ***, < 0.0001 ****

-set (CCR7+CD45RA+), while the MLR (positive control) had only 15.7% cells in this subset. Co-culture with MSCs inhibited the loss of naïve phenotype **(Figure 7c)**, as 24.7%, 31%, 33.5%, and 39.3% of the responding CD4+ T-cells remained in the naïve subset after co-culture with C MSCs, I MSCs, H MSCs, and D MSCs, respectively. These differences in the naïve fraction reflected a shift from the central memory T-cell compartment, as the central memory fraction decreased as the naïve fraction increased.

To investigate how early in the MSC-MLR experiments T-cells exhibited different activation patterns, we looked at two indicators of T-cell activation that preceded the end-point analysis at Day 5 (i.e. % division): GLUT1 expression and pro-inflammatory cytokine levels in the supernatant. The glucose transporter, GLUT1, is upregulated in activated T-cells to fuel glycolysis. As expected, T-cells in the MLR (no MSCs) condition did not upregulate GLUT1 over the responder-only group until Day 3, reflecting slow activation **(Figure 8a, supp. Table S3)**. When MLRs were instead co-cultured with MSCs, there was a rapid increase in T-cell GLUT1 expression even at Day 1, likely due to the T-cells sensing competition for resources. Nevertheless, at Day 1 and Day 3, there were differences depending on the MSC priming condition. While single-primed MSCs led to less T-cell GLUT1 expression than control MSCs, dual-primed MSCs were associated with significantly lower T-cell GLUT1 expression levels than all other MSC conditions. Indeed, at Day 1 they were not significantly different from the responder-only group, and they were still the most similar to this group by Day 3. Differences in pro-inflammatory cytokine levels were only apparent by Day 3 **(Figure 8b)**, and MSC-MLRs with dual-primed MSCs had lower levels than single-primed MSCs. MLRs with control MSCs had higher supernatant concentrations of pro-inflammatory cytokines than MLRs without MSCs,

suggestive of an initial allogeneicity. However, the control MSCs were still inhibitory in MLRs, possibly due to an immunosuppressive reactivity to the pro-inflammatory milieu that developed.

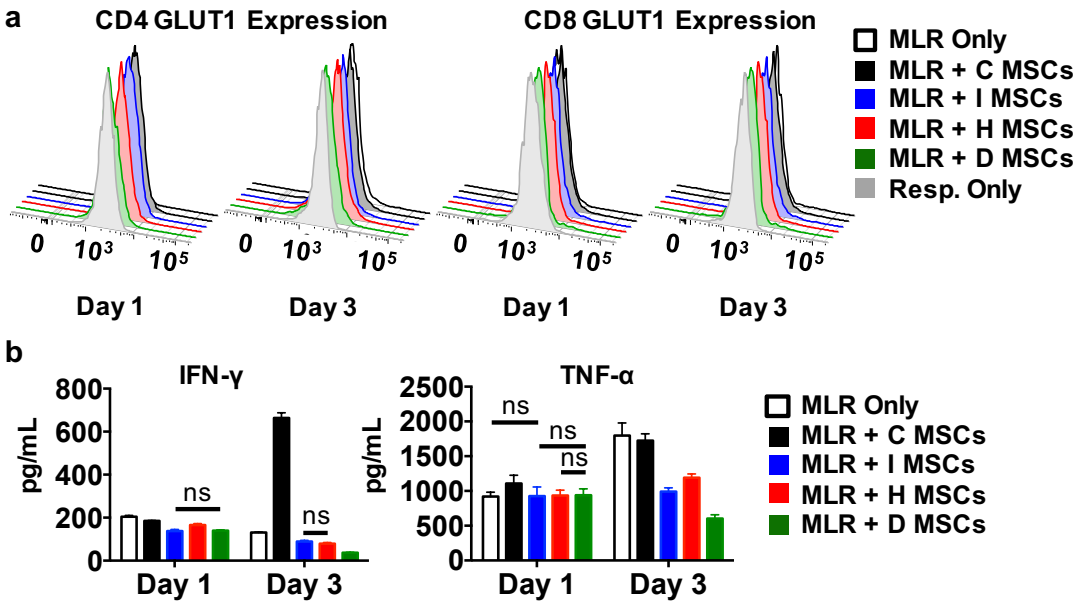

Figure 8 Early and mid-point analyses for MSC-MLR co-culture. **(a)** GLUT1 expression in CD4+ and CD8+ T-cells at Day 1 and Day 3 of MSC-MLR co-cultures. The mean ± SD intensity data can be found in Table S3 of the SI (significance determined by ANOVA analysis). **(b)** Pro-inflammatory cytokine levels measured at Day 1 and 3 of MSC-MLR co-cultures. All pairwise comparisons were significant except where indicated. Cytokine concentrations for the responder only group were below the detection limit and are thus not shown. n = 4

3.3.2 IFN-γ and hypoxia priming differentially upregulate immunomodulatory genes

To uncover how IFN-γ and hypoxia enhanced MSC immunosuppression, both as individual priming cues and in combination, we conducted qRT-PCR for 15 genes previously implicated in MSC-based immunosuppression **(Figure 9)**. IFN-γ priming led to >5-fold induction of HLA-G, HLA-E, HGF, iNOS, and, most markedly, PD-L1 and IDO, which were induced by 730-fold and 31,000-fold, respectively. In contrast, hypoxia priming led to greater induction of HLA-G than IFN-γ priming (10^2 fold vs. 5 fold) and induction of COX-2.

Overall, the combination of the two priming conditions resulted in an amalgamation of the two transcriptional upregulation patterns obtained by IFN-γ and hypoxia individually. The effects were not precisely additive, as the expression of some genes (e.g. IDO, HLA-E, PD-L1)

induced by IFN-γ was partially subdued by dual priming, while the induction of HLA-G was instead potentiated.

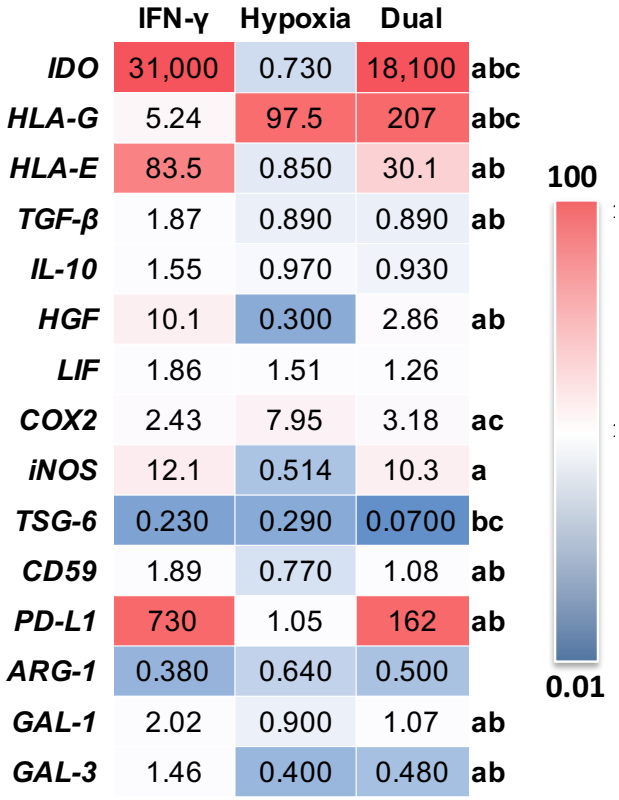

Figure 9 Differential expression of genes related to immunosuppression after 48 hours of single or dual priming. mRNA data obtained by qRT-PCR are shown after 48 hours of priming by IFN-γ, hypoxia, or dual IFN-γ/hypoxia in a representative experiment. Data are normalized to the expression in control MSCs (normoxia and regular MSC media). The color bar scales the fold difference from 0.01 to 100 (and saturates at either end). Significant differences between groups, as determined by ANOVA and Tukey post-hoc tests ($p < 0.05$), are shown at the right of each gene as indicated: **(a)** for IFN-γ vs. hypoxia stimulation, **(b)** for IFN-γ vs. dual stimulation, and **(c)** for hypoxia vs. dual stimulation. n = 4-6

3.3.3 Genes upregulated by dual priming at the mRNA level show strong induction at the protein level

We next investigated the mRNA trends from MSC priming at the protein level. Some trends were confirmed. For example, HGF protein was only detectable in the supernatant of IFN-γ-primed cells, **(Figure S1).** Notably, PD-L1, IDO, and HLA-E, which had less mRNA induction from dual priming than from IFN-γ priming, showed similar or greater induction by dual priming **(Figure 10a, Table S4)**. In fact, IDO protein expression was significantly greater after dual priming than after exposure to IFN-γ alone. This unanticipated result was confirmed by an IDO activity assay **(Figure 10b)**, where dual-primed MSCs showed significant enhancement of IDO activity over IFN-γ-primed MSCs.

Enhancement of the two genes induced by hypoxia at the mRNA level (COX-2 and HLA-G) was analyzed by flow cytometry. COX-2 protein expression was equally enhanced by all priming regimens, and protein levels were only slightly greater than those for control MSCs.

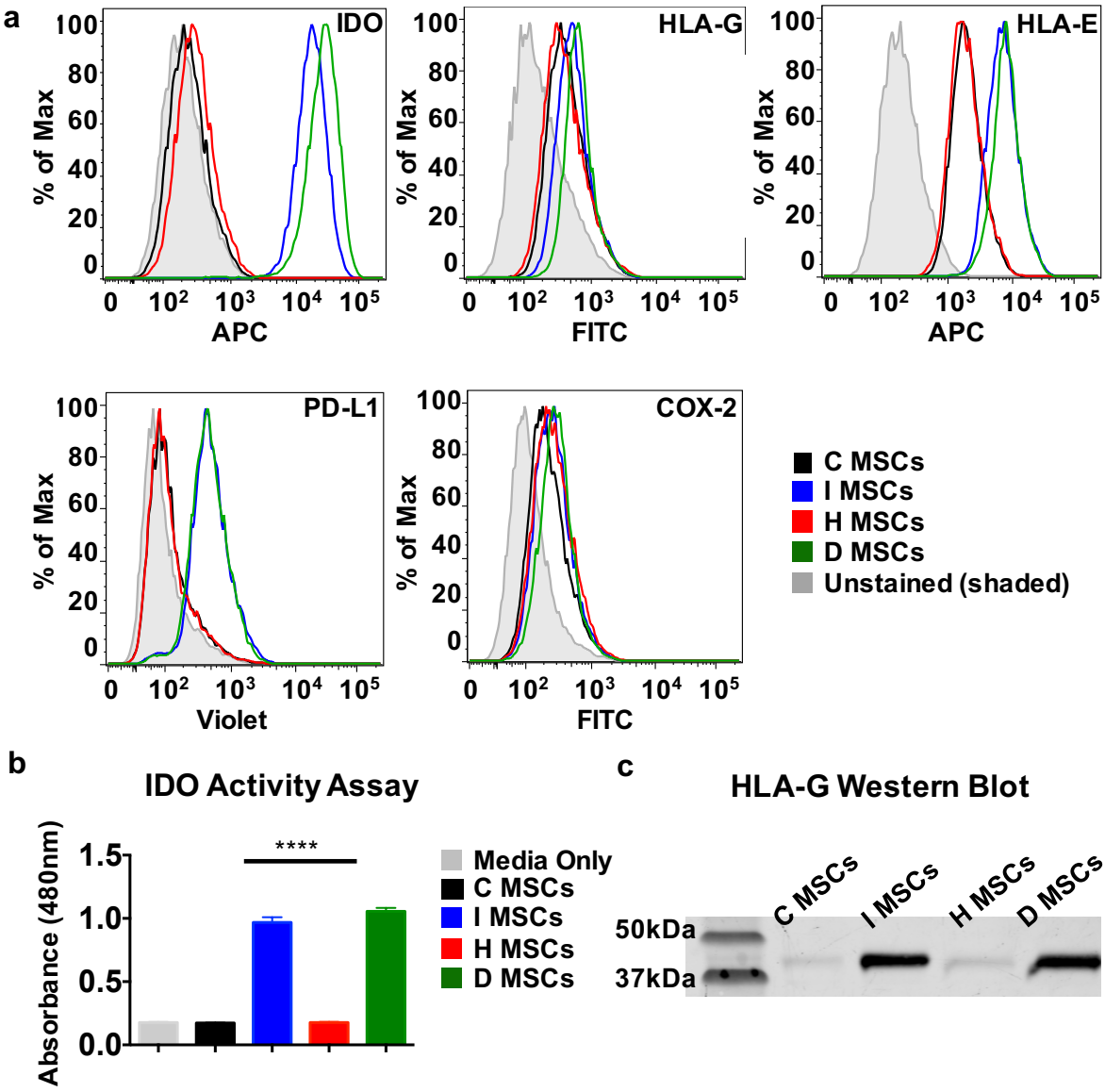

Figure 10 Protein expression after 48 hours of single or dual priming. (a) Histograms are shown from a representative experiment with 20,000 events (same experiment conducted n = 3 times). All pairwise comparisons for IDO, HLA-G, HLA-E, and PD-L1 were significant except control vs. hypoxia ($p<0.0001$). By contrast, only control vs. hypoxia was significant for COX-2 ($p<0.01$). **(b)** Relative IDO activity in MSCs replated after 48 hours of different priming regimens. IDO activity corresponds to detecting the tryptophan byproduct kynurenine via absorbance at 480 nm. 6 wells were averaged per condition. **(c)** Western blot showing relative HLA-G protein levels in MSC lysate after 48-hours of different priming regimens. Each lane was initially loaded with the same amount of protein (per BCA assay). $p<0.0001$ ****

While MSC HLA-G protein levels were the greatest after dual priming, consistent with the PCR data, protein levels were greater from priming by IFN-γ than by hypoxia, opposite to the PCR findings. This result was confirmed by Western blot analysis, which showed that HLA-G was substantively induced by both IFN-γ and dual priming at the protein level (but not by hypoxia) **(Figure 10c)**. Thus, an important overall finding was that hypoxia did not upregulate any of the studied immunosuppressive proteins more than IFN-γ.

3.3.4 Hypoxia and dual priming induce a metabolic shift to glycolysis

We next explored possible metabolic explanations for hypoxia-induced immunosuppression by investigating how different priming regimens affected major metabolic pathways in MSCs.

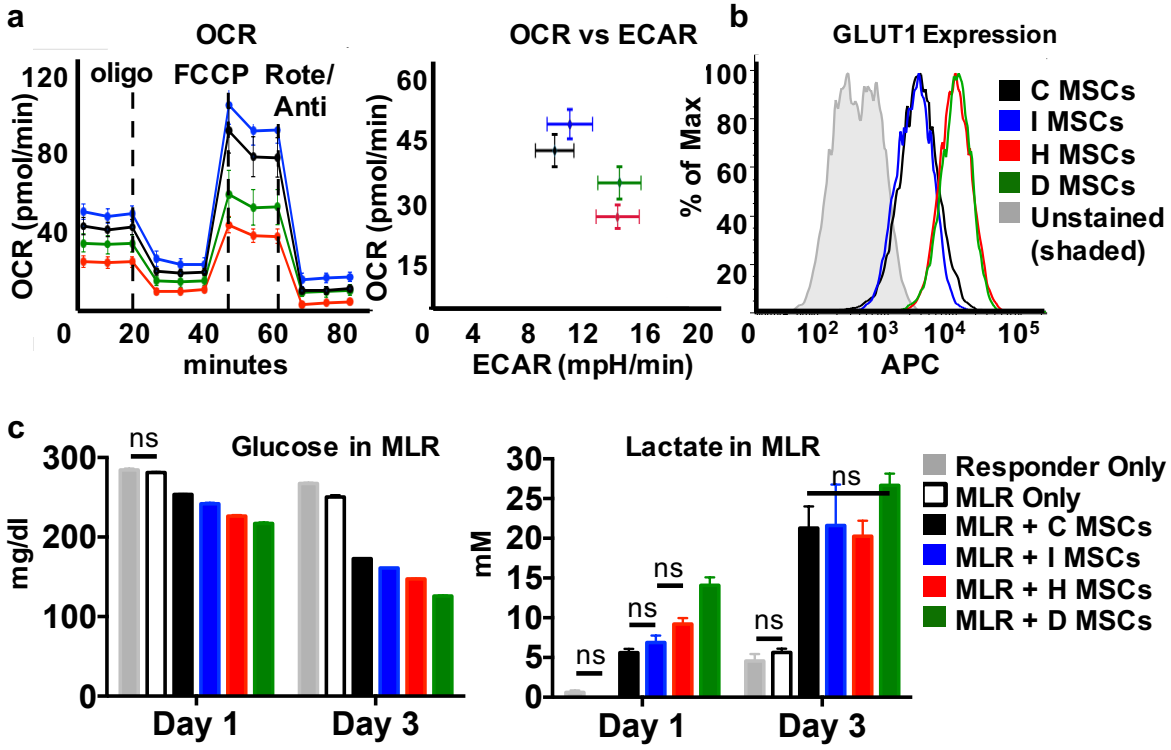

Figure 11 Influence of MSC priming on cell metabolism. (a) After 48 hours of priming, MSCs were replated at 10,000 cells per well into Seahorse Tissue Culture plates and evaluated by the Seahorse Mitostress kit. n=5 **(b)** GLUT1 expression in MSCs after 48 hours of priming. **(c)** Glucose and lactate levels in MSC-MLR co-culture experiments at Day 1 and Day 3. n = 2. All pairwise comparisons are significant at $p<0.001$ except where indicated (note: error bars for glucose graph are so small they are often not visible).

IFN-γ-primed MSCs had the highest oxygen consumption rate (OCR, by Seahorse Analysis), which is a marker for oxidative phosphorylation. The OCR decreased from control MSCs to dual-primed MSCs and was lowest for hypoxia-primed MSCs **(Figure 11a)**. Importantly, while hypoxia-primed and dual-primed MSCs had a reduced OCR relative to MSCs not exposed to hypoxia, they both had a significantly higher extracellular acidification rate (ECAR), which is a metric for glycolytic metabolism (acid from lactate production). The shift towards glycolysis in hypoxia-primed and dual-primed MSCs was further supported by unique upregulation of GLUT1, the inducible glucose transporter also required for T-cell glycolysis **(Figure 11b)**.

We then investigated if the observed metabolic changes could explain the trends seen in the MSC-MLR co-cultures **(Figure 7)**, specifically (*i*) why hypoxia-primed MSCs were as inhibitory as IFN-γ-primed MSCs and (*ii*) if metabolic changes could explain the additive immunosuppressive efficacy of dual-primed MSCs. Glucose and lactate levels were measured at Days 1 and 3, time points that precede T-cell division (to maintain consistent cell numbers amongst groups) but during which T cells may become activated. As expected, by Day 3, activated PBMCs in the MLR (no MSCs) had higher glucose consumption than the responder only group, and they further showed a trend suggestive of higher lactate production, although this difference was not significant **(Figure 6c)**. Addition of MSCs had a large influence on glucose and lactate levels. Dual-primed and hypoxia-primed MSCs led to the greatest glucose depletion and lactate production by Day 1, consistent with higher GLUT1 expression and induction of glycolysis. Notably, dual-primed and hypoxia-primed MSCs led to a 3-fold and 2-fold, respectively, increase of lactate in the supernatant relative to control MSCs (~15 mM and 10 mM vs. 5 mM). Glucose levels continued to decline between Days 1 and 3, while the rate of consumption during this phase was similar amongst MSC-MLR groups (drop of ~40 mg/dL for

control, IFN-γ and hypoxia-primed MSC-MLR co-cultures; 45 mg/dL for dual-primed; **Table S4**). Lactate accumulation started to plateau between Days 1 and 3, although the highest levels were still found in MSC-MLR reactions with dual-primed MSCs.

To explore the consequences of a high extracellular lactate concentration, we looked at its effect on intracellular pH (pHi) and proliferation of T-cells in titration experiments. Increasing extracellular lactic acid levels in fresh cAIM-V media (see Methods) led to a dose-dependent drop in T-cell pHi, which started to become pronounced at 15 mM, and by 30 mM, dropped dramatically along with media pH **(Figure 12a; Table S6)**.

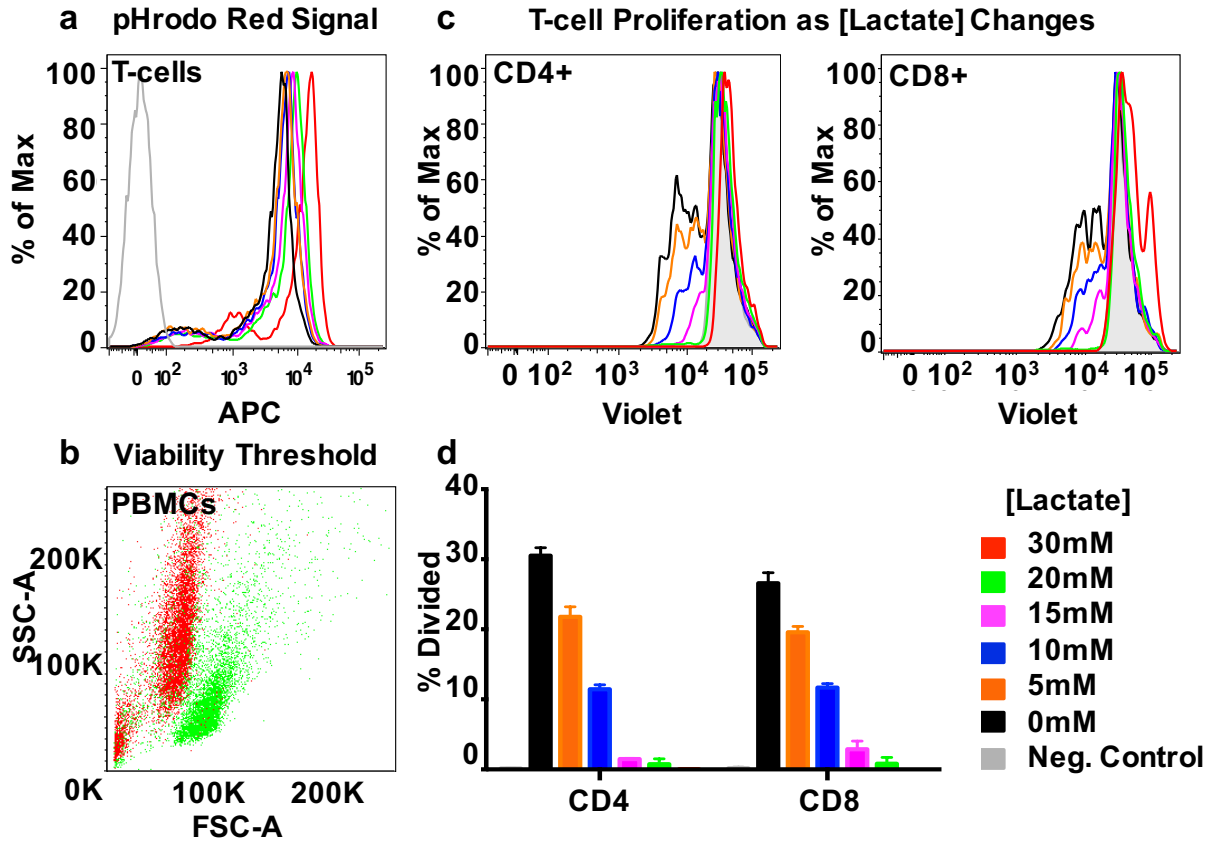

Figure 12 Effect of external lactate concentration on PBMCs (a) Effect of external L-lactic acid concentration on intracellular pH as revealed by increasing pHrodo Red dye intensity with declining pH. Representative overlay shown for n = 3 **(b)** Change in ungated PBMC scatter properties as the external L-lactic acid concentration reaches 30 mM. The shift is suggestive of dying cells. **(c & d)** Effect of lactic acid concentration on T-cell division in response to Concanavalin A. n = 3. "Negative control" in the legend refers to unstained cells for **(c)** and unstimulated cells for **(d).**

As the lactic acid concentration increased from 20 mM to 30 mM, there was also a notable change in the scatter properties of the T-cells, consistent with cells undergoing apoptosis **(Figure 12b)**. Titrating lactic acid into the media also attenuated both CD4+ and CD8+ T-cell division in response to the strong mitogen Concanavalin A **(Figure 12c & d)**. At 10 mM lactate, T-cell division was reduced to 30-45% of the maximum rate, and at 15 mM, T-cell division was almost completely eliminated **(Figure 12c & d)**.

3.3.5 Mass spectrometry confirms that hypoxia influences MSC metabolism but does not upregulate proteins with direct immunosuppressive capacity

To further evaluate our metabolic hypothesis for hypoxia-induced MSC immunosuppression and for why dual-primed MSCs showed additive improvements in immunosuppression compared to single priming, mass spectrometry was performed. This was to confirm that cells exposed to hypoxia did not upregulate any proteins with immunosuppressive capacity that were missed on PCR or flow cytometry analysis.

Proteins that changed in expression due to hypoxia priming were predominantly mitochondrial proteins that had a role in cellular metabolism. Specifically, proteins involved in oxidative phosphorylation and the citric acid (TCA) cycle were down-regulated, as were mitochondrial ribosomal proteins. When STRING analysis was performed on the list of proteins that changed over 2-fold from hypoxia priming (over control MSCs), it did not associate any proteins with immunomodulation.

Dual primed cells showed similar changes in the metabolic pathways altered by hypoxia alone, although in some instances, a protein was downregulated slightly less than 2-fold such that

there was not 100% overlap in the list of downregulated proteins between hypoxia and dual primed cells **(Table 2).**

Table 2 STRING analysis of pathways altered by hypoxia primed or dual primed MSCs relative to control MSCs.

Hypoxia Primed			
pathway ID	**pathway description**	**protein count**	**false discovery rate**
GO.0032543	mitochondrial translation	18	4.93E-16
GO.0006119	oxidative phosphorylation	16	1.52E-16
GO.0072350	tricarboxylic acid metabolic process	7	2.27E-06
Dual Primed			
pathway ID	**pathway description**	**protein count**	**false discovery rate**
GO.0032543	mitochondrial translation	16	2.79E-07
GO.0006119	oxidative phosphorylation	11	3.08E-05
GO.0072350	tricarboxylic acid metabolic process	7	6.20E-04

3.4 Discussion

Studies from the last decade have revealed that MSCs are not immunosuppressive at baseline but must be induced to adopt this phenotype by environmental cues like inflammatory cytokines. Nevertheless, clinical trials to-date have used naïve MSCs (called "control" MSCs in this paper). In support of this approach, MSCs are often tested for treatment of inflammatory conditions, and they may experience relevant priming cues after they have been injected. However, the down side is that cells experience variable induction based on the specific patient and disease, with a delay in the onset of their therapeutic effect. Given that MSCs are thought to have a short lifespan *in vivo* (hit-and-run hypothesis),[16,19,20] a significant fraction of their therapeutic opportunity may be cut out by having to be primed only after injection, and it may limit their ability to be used preventatively in situations where inflammation has not fully developed.

For the above reasons, our main objective was to better define and characterize an optimal MSC priming regimen *in vitro*. While IFN-γ is a common priming cue, we hypothesized

based on the cancer (i.e. tumor immune escape) and MSC literature that adding hypoxia would lead to even more effective MSCs and sought to compare these two priming cues side-by-side and in combination. Our central findings were that IFN-γ and hypoxia priming led to MSCs that were equally more effective at inhibiting T-cell division than unprimed MSCs, and that using both cues together had an additive effect, with dual-primed MSCs showing twice the improvement in immunosuppressive capacity than single priming alone.

To better understand how MSC priming influenced initial T-cell activation, we measured CD25 expression, which was suppressed in a similar pattern to T-cell division across the different MSC priming groups. When combined with the findings that dual-primed MSC-MLRs were correlated with the largest remaining naïve T-cell population, the lowest Day 1 and 3 pro-inflammatory cytokine levels, and the lowest induction of T-cell GLUT1 expression, this suggests that T-cell division was best impaired in this experimental group because fewer T-cells became activated in the first place.

We next sought to understand the mechanisms through which dual primed MSCs mediated their effects. Initial PCR data suggested that each priming cue upregulated distinct immunosuppressive genes, with IFN-γ primarily inducing IDO and PD-L1, and hypoxia inducing HLA-G and COX-2. However, when we explored these upregulated genes at the protein level, we saw different patterns. Notably, protein level expression of IDO was consistently superior in dual primed cells compared to IFN-γ alone. This contrasted with less induction of IDO in dual vs. IFN-γ primed cells at the mRNA level. Since hypoxia did not upregulate IDO at the protein level, this suggests a synergistic post-transcriptional interaction between IFN-γ and hypoxia signaling that was not predictable from our PCR studies. HLA-G protein also showed the highest induction from dual priming, which was consistent with PCR

data, but curiously, it was better enhanced by IFN-γ alone vs. hypoxia alone, differing from the PCR results. HLA-G upregulation by hypoxia at the mRNA level has been reported previously,[56] as has its extensive post-transcriptional regulation,[85] which may explain the observed mRNA to protein level discrepancy. Of final note, COX-2 protein was similarly induced by the different priming regimens.

The protein level findings presented a problem with our initial mechanistic assumptions. One could attribute the superiority of dual priming to its promotion of the highest expression of immunosuppressive proteins, with similar PD-L1 and COX-2 expression to IFN-γ priming alone, and slightly higher HLA-G and IDO expression. However, these findings do not explain why hypoxia alone, which failed to induce any of these factors more than IFN-γ at the protein level, was equally as efficacious as IFN-γ at producing inhibitory MSCs in our MSC-MLR functional assays.

Referring back to the tumor literature, we were inspired to investigate a possible metabolic mechanism. Solid tumors use aerobic glycolysis for metabolism, which leads to rapid glucose consumption and lactate production.[86] Glucose deprivation itself has been shown to limit T-cell division, as T-cells also use aerobic glycolysis and have high glucose demand.[87] The buildup of local lactate concentrations in tumors (up to 40 mM) can also directly promote anti-inflammatory immune cell phenotypes, limit T-cell cytotoxicity and division, and destroy intra- to extracellular lactate gradients such that the pH of the cell becomes acidic.[88]

We postulated that hypoxia priming of MSCs could lead to similar metabolic-based inhibition pathways. We confirmed that hypoxic exposure shifts MSC metabolism towards glycolysis and that hypoxia and dual primed MSCs rapidly deplete glucose and produce lactate within one day of MSC-MLR co-culture. While media lactate levels appeared to eventually

saturate across the different MSC groups, Day 1 levels were approximately 2-fold higher for hypoxia-primed MSCs and 3-fold higher for dual-primed MSCs compared to MSCs maintained under control conditions. These different concentrations impacted pHi and T-cell division in L-lactic acid titration experiments. Studies by others have shown that L-lactic acid concentrations of 15 mM and 10 mM correspond to a pHi of 6.25 and 6.8, respectively.[88] As with our study, a dose-dependent inhibition of T-cells was found, with greatly impaired division once lactate concentrations exceeded 10 mM. Given that our hypoxia-primed and dual-primed MSCs produced these high lactate concentrations by Day 1 in MSC-MLRs, we propose that the high media lactate immediately influenced T-cell fate, as supported by the lower Day 1 T-cell GLUT1 expression and the higher Day 5 naïve fraction compared to control MSCs.

While the confluence of the PCR, flow cytometry, and metabolic studies lent support to this metabolic hypothesis for hypoxia-induced MSC immunosuppression, we did not exclude the possibility that hypoxia could have upregulated an immunomodulatory protein that we did not analyze at the mRNA or protein level. We thus pursued mass spectrometry to compare the proteome of MSCs exposed to the different priming conditions. In support of our metabolic theory, proteins that changed in expression from hypoxia priming (vs. control MSCs) were not associated with any immune pathways as per STRING analysis. This bioinformatics analysis did, however, demonstrate that most proteins that changed in expression were found in the mitochondria and were involved in metabolism. Specifically, pathways related to aerobic respiration – the TCA cycle and oxidative phosphorylation – were both downregulated, consistent with our previous findings that hypoxia priming shifted metabolism towards glycolysis. Similar pathway findings were also found in dual primed MSCs, likely contributing to their superior immunosuppressive capacity.

Cell-specific metabolic pathways have recently generated excitement as new targets for blocking cancer immune escape, but they could alternatively be opportunities for promoting immune suppression and tolerance. Indeed, one group has already explored using inhibitors of glycolysis to inhibit T-cell mediated allorejection in organ transplantation.[89] We propose that hypoxia and dual primed MSCs could provide a similar function, by outcompeting T-cells for glucose and inhibiting them via high lactate levels.

When MSCs are injected intravenously, they are unlikely to reach the high lactate concentrations seen in our experiments due to buffering by the blood; while tumors can reach levels up to 40 mM, blood levels >4 mM are considered "lactic acidosis". However, MSCs are known to quickly home to inflammatory sites where they could more readily influence the local metabolic environment.[30] This could also be accomplished via local injection of MSCs and MSC spheroids,[90,91] which is being explored for local tissue repair and for protection of co-transplanted allogeneic cells.[92,93] Spheroidal formulation would also have the advantage of potentiating the metabolic shift towards glycolysis, as studies have shown that both the central hypoxic core and signaling from the 3D architecture itself promotes a glycolytic phenotype.[42]

As a final consideration, "oxygen consuming" hydrogels have recently been designed, which maintain a local hypoxic environment for encapsulated cells that could also promote extended glycolytic metabolism.[94] Considering there have been several published reports of IFN-γ containing biomaterials, it seems feasible that our dual priming regimen could thus be formulated for local injection by encapsulating cells in IFN-γ functionalized aggregates or low oxygen hydrogels.[95–98]

While the benefits of our priming regimen need to be tested *in vivo*, we believe that this initial, strictly *in vitro*, assessment is valuable in terms of elucidating how MSCs react to

microenvironmental factors that can enhance their therapeutic capacity. Given that hypoxia and inflammation often occur together in acute trauma and chronic disease, mechanisms described for our dual priming regimen may also better represent the functional changes in MSCs that are introduced into these pathophysiological situations.[99,100]

In summary, we have compared two microenvironmental cues common to known situations of immune escape (e.g. tumors, maternal-fetal interface): IFN-γ and hypoxia, and demonstrated that they elicit distinctly different mechanisms of immune suppression in MSCs. We show that combining these separate pathways by exposure of MSCs to both priming cues leads to additive immunosuppressive effects. While IFN-γ is the most frequently studied MSC priming regimen, we believe that hypoxia is a relatively low cost addition that not only promotes glycolysis but also enhances the IFN-γ induced expression of IDO and HLA-G. Priming MSCs in this manner should lead to a more standardized and efficacious therapy, which could be explored for treatment of dozens of autoimmune and inflammatory disorders.

3.5 Future Directions

While our focus is on the development of MSCs as an immnuosuppressive cell therapy, recent attention has also been paid to the extracellular vesicles they secrete, specifically those with a size <100-150 nm called exosomes.[101,102] Several studies have shown these exosomes have therapeutic benefit for applications such as ischemia-reperfusion injury,[103,104] fracture healing,[105] and graft-vs-host-disease.[106]

An interesting feature about the therapeutic ability of these exosomes is that it does not require priming. While unprimed MSCs become primed when they are injected into a patient with an inflammatory disorder, the exosome fraction of unprimed MSCs is collected before they

have a chance to respond to inflammation. This thesis has shown that unprimed MSCs have low expression of the immunosuppressive proteins implicated in their function as a cell therapy. Thus, the exosomes from unprimed MSCs must work by a separate mechanism.

Nevertheless, it is possible that if priming MSCs leads to a better cell therapy, it may also improve the therapeutic potential of the exosomes they secrete. This led to us conducting some pilot studies to see if exosomes from control, IFN-γ, hypoxia, or dual primed MSCs would be more inhibitory in MLRs. Since our lab does not have an ultracentrifuge, the polymer method was used for exosome isolation.[107] This takes advantage of the ability of polyethylene glycol (branded as ExoQuick TC) to pull large particles out of suspension. Unfortunately, after many experiments with some inconsistent data, we discovered that the polymer also isolated the IFN-γ protein. Hence, pro-inflammatory cytokine was being dosed into MLRs alongside exosomes (which are presumably immunosuppressive). Future attempts at studying the therapeutic potential of exosomes from IFN-γ primed MSCs should use a different method of exosome isolation to prevent co-collection of the cytokine.

Chapter 4

Aim 2: To conduct a global proteomic and metabolomic characterization of single vs. dual IFN-γ/hypoxia primed MSCs

4.1 Overview

Our previous studies demonstrated that hypoxia can enhance the immunomodulatory function of MSCs by altering cell metabolism. Given there have been many papers on hypoxia preconditioning of MSCs, it was somewhat surprising that this mechanism had not been previously described. However, if the paradigm has thus far been that "cytokines license MSCs to be anti-inflammatory" and "hypoxia affects cell survival and angiogenesis", then it is easy to only look for these same patterns in new studies and applications.

Recognizing that in our own study we limited our analysis to the effects of priming on immune modulation, we challenged ourselves to acquire a more global understanding of how these environmental cues affect diverse aspects of MSC behavior. Certainly, the therapeutic capacity of MSCs would also be affected by changes to viability, migration capacity, and so forth. Our second aim was thus to uncover the changes to the proteome and metabolome of MSCs upon exposure to IFN-γ, hypoxia, or both cues together. While our findings should lend insight to how different priming regimens may (or may not) benefit MSCs for treatment of diverse clinical indications, they may also reflect the adaptations unprimed MSCs make upon administration to patients with hypoxic or inflammatory disorders.

4.2 Methods

4.2.1 Mass spectrometry

Protein was collected from MSCs via a methanol-chloroform extraction protocol. MSC plates were washed x 3 with ice-cold PBS to thoroughly remove residual FBS and cytokines. 450 µL of lysis buffer consisting of TBS with 3% SDS and 50 µL protease inhibitors (Sigma # P8340) was applied to each MSC plate. The lysate was collected in a 1.5 mL tube and incubated at 60 °C for 30 minutes. 400 µL of methanol and 100 µL of chloroform were added, and samples were vortexed and centrifuged at 16 000 x g for 1 min. The protein pellet was washed with methanol three times and allowed to air dry before final resuspension in 30 µL of solubilization buffer (100 mM ammonium bicarbonate, 8 M urea, and 0.1 M DTT in Optima water) and snap freezing with liquid N_2 for storage at -80 °C. Immediately prior to analysis, samples were further reduced, alkylated, and trypsin digested, and yeast alcohol dehydrogenase was added as an internal control. Samples were collected from biological triplicates, where each replicate of a given

priming condition came from a separately thawed cryovial of MSCs. Each individual sample was additionally run in duplicate. Mass spectrometry was performed at the Quantitative Proteomics and Metabolomics Center at Columbia University with an UltiMate 3000 RSLCNano ultrapressure liquid chromatograph coupled to a Q Exactive HF (Orbitrap) mass spectrometer (ThermoFisher). More detailed methods can be found in the supplemental information (**SI).**

iPathway Guide (Advaita, 2017) and String v10.5 (string-db.org/) were used to understand the nature of the differentially expressed (DE) proteins, which were defined by a |log2 fold change (log2FC)| > 0.6 and a $p < 0.05$. All proteins are listed by their related gene names, as these are the names used in the iPathway Guide program.

4.2.2 Metabolomics analysis

MSC plates (6-well) were washed three times with ice-cold PBS to thoroughly remove residual FBS and cytokines. 500 µL of chilled 80% methanol containing internal standard (17 µM 4-chlorophenylacetic acid) were then added to each well, and the plates were placed on a shaker for 30 minutes in a cold room. Samples were subsequently collected into 15 mL Falcon tubes, with lysate from two full 6-well plates used for each individual sample. As with the proteomics set up, there were three biological replicates for each priming condition. Samples were stored at -80 °C before analysis at the Quantitative Proteomics and Metabolomics Center at Columbia University, where the metabolomics analysis was performed (detailed methods in **SI**).

4.3 Results

4.3.1 Overview of data

MSCs used for proteomic and metabolomics analyses had a viability of >94%, based on trypan

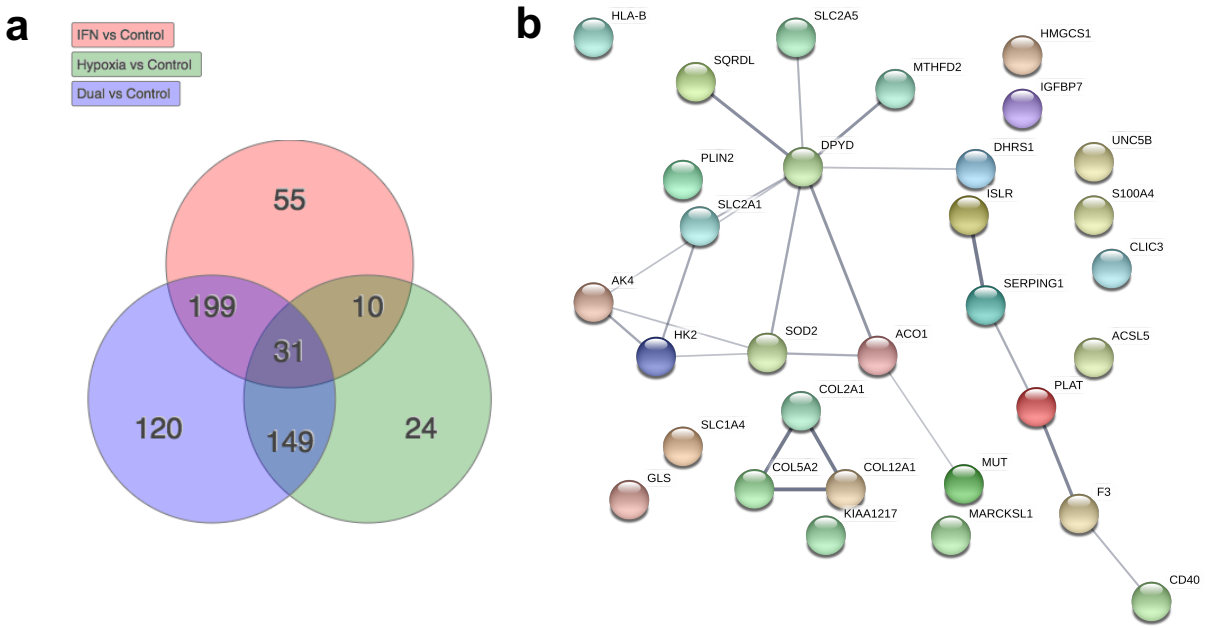

Figure 13 Overview of data. a) The total number, and overlap amongst priming conditions, of proteins that show significant differential expression compared with control MSCs **b)** STRING network of the 31 proteins that are differentially expressed from all priming conditions.

blue exclusion, with no significant differences based on exposure to hypoxia or IFN-γ. While we did not observe a change in morphology indicative of undesired differentiation, exposure to IFN-γ did increase the average cell diameter **(Figure S2)**, as has been observed by others. Our prior studies have also shown minimal changes to MSC surface marker expression, with the exception that IFN-γ leads to expression of HLA-DR, which is not expressed at baseline.

A total of 3,465 proteins were detected, with 2,435 proteins identified by >1 peptide (conservative set). Many proteins identified by only one peptide are accurate results; however, the conservative set will be presented in figures, and tables will indicate when including proteins outside of this set. Our own validation studies can be seen in **Figure S3**, which also serves to validate some of the smaller magnitude (yet significant) findings.

Figure 13a shows the overlap in differential expression (DE) of proteins amongst priming conditions, with the 31 DE proteins from all priming conditions shown in **Figure 13b**.

The most central node is dihydropyrimidine dehydrogenase (DPYD), the rate-limiting-step in pyrimidine metabolism.

Table 3 documents the percentage of the 2,435 proteins that are DE for each priming condition. IFN-γ priming led to a significant change in expression in ~12% of the proteins, hypoxia led to a change in ~9% while dual IFN-γ/hypoxia priming led to a change ~21%. The very neat addition (9+12=21), suggests that IFN-γ and hypoxia alter distinct pathways without much overlap (only 41 proteins as per **Figure 13a**). In further support of this, most proteins with DE following hypoxia were mitochondrial, whereas IFN-γ predominantly affected non-mitochondrial proteins.

Table 3 Overview of the impact of IFN-γ and/or hypoxia on the MSC proteome.

	IFN-γ	Hypoxia	Dual
% of proteins that are DE	12.10%	8.80%	20.50%
% of DE proteins that are in the mitochondria	12.20%	62.60%	29.30%

Metabolomics analysis identified forty-seven intracellular metabolites with strong confidence. The relative abundances of nine metabolites are highlighted in **Table 4**. Priming with IFN-γ resulted in higher increases in β-alanine levels than priming with hypoxia, but both cues acted together to produce the highest amounts of this metabolite in dual-primed cells. Taurine and hypotaurine showed similar trends to β-alanine. While a relative abundance of 1E+99 implies there was no detectable metabolite in the control MSCs, the relative abundance of taurine in IFN-γ primed vs. hypoxia primed cells was 6.06-fold higher (evident

Table 4 Relative metabolite abundance in IFN-γ and hypoxia primed MSCs normalized to the abundance in control MSCs.

	IFN-γ	Hypoxia	Dual
Beta- alanine	6.56	1.63	10.60
hypotaurine	2.27	1.51	3.45
L-kynurenine	1E+99	0.00	1E+99
L-tyrosine	1E+99	0.00	1E+99
D-glucose	1.20	1.45	2.88
O-Phosphoethanolamine	1.15	2.92	2.45
pyruvic acid	0.72	0.44	0.49
L-(+) lactic acid	0.55	1.54	1.83
taurine	1E+99	1E+99	1E+99

from larger data set). There was no significant difference in relative abundance of kynurenine or tyrosine in IFN-γ primed vs. dual primed cells.

Given the above changes in the expression of proteins and metabolites, we analyzed their relevance to four biological settings: metabolism, immune modulation, extracellular matrix (ECM), and cell survival. Of note, these are only tentative boundaries, as one pathway often has a direct influence over another.

4.3.2 Effects on cellular metabolism

Exposure to hypoxia resulted in significant changes in carbon metabolism. MSCs had broad upregulation of proteins involved in glycolysis and a greater capacity for uptake of glucose (GLUT1/SLC2A1) and fructose (GLUT5/SLC2A5), as well as for export of lactate (MCT4/SLC16A3) and hydrogen ions (CA12). By contrast, TCA cycle proteins were mostly downregulated, as were the enzymes involved in fat degradation and transport, amino acid catabolism and transport, and the electron transport chain (ETC). Consistent with the fewer mitochondrial proteins, mitochondrial ribosomal proteins (MRP family) were downregulated. Hypoxia also influenced glycogen turnover, as both glycogen synthase and glycogen phosphorylase L were upregulated.

IFN-γ had a more selective impact on metabolism. While generally not altering any pathway at every step, IFN-γ led to an upregulation of GLUT5 (log2FC = 5.32 vs. only 1.55 from hypoxia), cytoplasmic aconitase (ACO1/IRP1), hexokinase II (HKII), and long chain acyl-CoA synthetase (ACSL5). Curiously, these proteins were also upregulated by hypoxia **(Figure 13b).** Thus, when MSCs were exposed to both hypoxia and IFN-γ (dual priming), they aligned

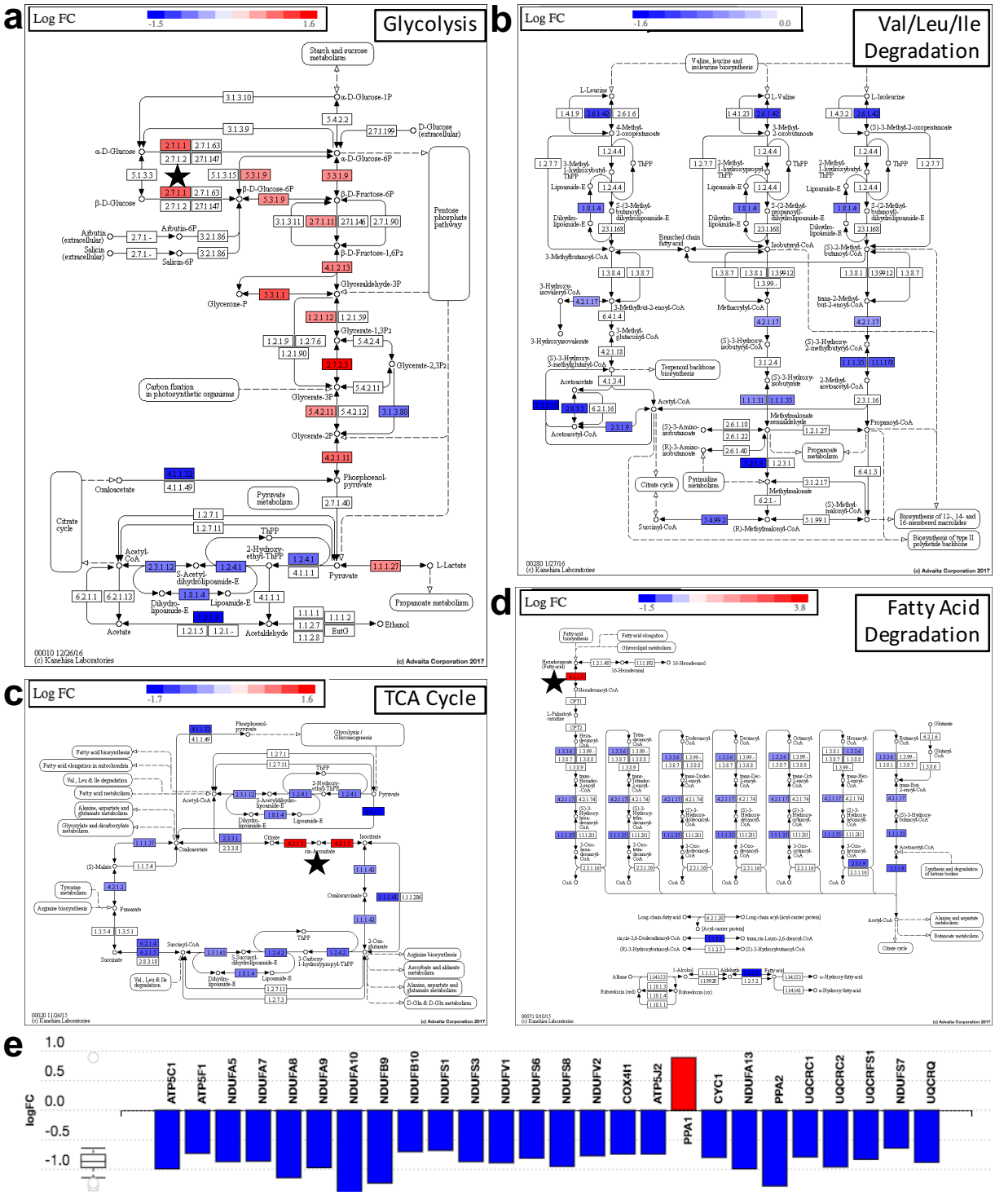

Figure 14 The effect of dual IFN-γ/hypoxia priming a) on glycolysis, **b)** neutral amino acid degradation **c)** the TCA cycle **d)** fat degradation and **e)** the electron transport chain. Note that the trends are similar for hypoxia primed cells, however, co-exposure to IFN-γ reinforced the upregulation of HKII, ACO1, and ACSL5, which are indicated with a black star (★) in panels A, C, and D, respectively. Beyond upregulating these proteins, IFN-γ had an unremarkable impact on the above pathways.

closer to the metabolic changes observed with hypoxia, but with an even greater induction of the four proteins mentioned. These trends can be seen in **Figure 14a-e**, which demonstrates the combined changes in metabolism for dual primed MSCs. Only dual primed cells significantly upregulated proteins involved in gluconeogenesis (**Figure S4**).

4.3.3 Effects on immune modulation

The immune regulatory function of MSCs is thought to be one of their most important qualities and highly responsive to microenvironmental cues. Curiosly, hypoxia did not lead to DE of proteins implicated in traditional immune pathways. By contrast, IFN-γ had a large impact. For example, IFN-γ induced expression of proteins associated with antigen presentation **(Figure S5)**, the defense against viral and microbial pathogens (IFIT, TRIM, NOD, and CXCL families; **Supp. File 1**), and chemotaxis (CXCL9-CXCL11, CD47, CD97).

Table 5 Differential expression (log2 FC relative to control MSCs) of proteins related to the complement cascade, immune tolerance, and leukocyte migration. * identified by only 1 peptide.

	IFN-γ	Hypoxia	Dual	Function
C1QBP	-0.12	**-1.2**	**-1.13**	inhibits complement factor 1
C1R	**2.55**	-0.51	**2.66**	forms complement factor 1
C1S*	**2.01**	-0.07	**1.94**	forms complement factor 1
CD47	**1.24**	0.01	**1.19**	protection from phagocytosis; transendothelial migration
CD97	**1.39**	0.17	**1.23**	chemotaxis
CFH*	**6.8**	0.49	**7.38**	helps direct complement to pathogens vs. host cells
CSF1	**3.41**	-0.28	**3.18**	monocyte maturation
CXCL9	**6.51**	0.03	**6.8**	chemotaxis; antimicrobial
CXCL10*	**2.04**	0.12	**1.96**	chemotaxis; antimicrobial
CXCL11*	**2.44**	-0.13	**2.38**	chemotaxis; antimicrobial
HLA-E	**3.01**	-0.03	**3.47**	protects cells from NK cells
HLA-F*	**7.16**	0.16	**6.97**	possibly immune tolerance
IDO1	**6.64**	0.19	**6.51**	immune tolerance
LGALS3BP	**1.54**	-0.22	**1.32**	galectin 3 binding protein
LGALS9B*	**4.76**	**-0.88**	**4.11**	analog of galectin 9
LRRC32	0.3	0.35	**0.89**	promotes surface expression of TGF-β on T-regs
SERPING1	**3.61**	0.81	**3.7**	inhibits complement factor 1
PDL1*	**6.38**	-0.2	**6.27**	immune tolerance
WARS	**3.88**	-0.08	**3.78**	trytophan production

IFN-γ exposure also resulted in upregulation of factors that promote the complement cascade (C1QBP, C1R, C1S). While these factors could put MSCs at greater risk for

complement-related cell death and clearance, it is notable that SERPING1 and complement factor H (CFH) were highly induced (**Table 5)**, which could provide protection.

Other factors that could protect MSCs from immune mediated clearance were upregulated, such as CD47, HLA-E, PD-L1, as well as the tryptophan catabolizing enzyme indoleamine-2,3-dioxygenase (IDO1). TGF-β1 had the highest induction in dual primed cells but at a low level (log2FC = 0.58). However, a related protein, LRRC32, was significantly induced in dual primed cells. Several proteins associated with MSC immune modulation by others - HLA-G, HGF, LIF, NOS2/iNOS, and TSG-6 - were not detected in any MSC groups.[98]

Table 6 Differential expression (relative to control MSCs) of proteins related to the ECM. log2 FC is shown. *proteins identified by only 1 peptide.

	IFN-γ	Hypoxia	Dual
AGRN*	**4.35**	**1.47**	**6.16**
COL1A1	**-1.37**	-0.57	**-2.22**
COL1A2	**-1.03**	-0.48	**-1.61**
COL2A1	**-1.42**	**-0.64**	**-2.67**
COL3A1	**-1.05**	0.13	**-1.16**
COL4A1	**0.65**	0.46	**1.21**
COL4A2	0.51	0.54	**4.18**
COL5A1	**-0.75**	-0.14	**-0.92**
COL5A2	**-0.9**	**-0.74**	**-2.27**
COL6A2	0.18	**0.61**	**0.89**
COL6A3	0.1	**0.63**	**0.76**
COL12A1	**-0.97**	**-0.96**	**-2.59**
COL15A1	**-1.06**	-0.56	**-1.77**
COL16A1	**-0.71**	-0.2	**-0.67**
ELN	**-1.27**	-0.26	**-1.36**
FBLN1	**-0.73**	-0.45	-0.17
FBN1	-0.02	0.26	**0.91**
LAMA2*	**0.67**	-0.15	**1.34**
LAMA4	**1.67**	0.27	**1.83**
LAMB1	**-1.03**	-0.37	**-1.11**
LAMC1	**-0.67**	0.05	-0.38
LOX	-0.43	**1.05**	**0.96**
LOXL1*	0.22	**0.72**	**2.11**
LOXL2	**-0.79**	**0.99**	0.27
LOXL3*	**0.65**	**2.72**	**4.21**
PLOD1	0.08	**0.68**	0.49
PLOD2	0.27	**1.74**	**1.9**
SPARC	**-1.56**	0.21	**-1.13**
THBS1	**-1.25**	0.13	**-0.76**
THBS2	**-1.62**	0.16	**-1.04**
TIMP1	0.38	**0.91**	**0.89**
TIMP3	-0.56	0.37	**-0.86**
TNC	0.03	0.01	**0.62**

4.3.4 Effects on extracellular matrix

Both IFN-γ and hypoxia had large impact on the ECM (**Table 6**). IFN-γ predominantly affected the production of collagen components, with significant downregulation of collagens 1-3, 5, 12, 15 and 16, and upregulation of collagen 4. IFN-γ also increased laminin alpha chains and agrin, while downregulating elastin and fibulin. Hypoxia upregulated collagen 6 and had many effects similar to IFN-γ. Consequently, the DE patterns of dual primed cells were often suggestive of synergistic influences of the two

cues, with the most dramatic example being COL4A2, where IFN-γ or hypoxia conditioning resulted in log2FC = 0.5, while dual priming resulted in log2FC = 4.18.

These cues also affected regulators of ECM metabolism and angiogenesis. Hypoxia had a large effect on collagen crosslinking, as it upregulated several lysyl oxidases (LOX, LOXL1-3) and lysyl hydroxylases (PLOD1&2). When MSCs were dual primed, induction of LOXL1 and LOXL3 was bolstered even further, suggesting another area of synergy. Dual priming also affected expression of TIMP1 and TIMP3, which were upregulated and downregulated, respectively, and led to unique induction of tenascin-C. Lastly, IFN-γ and dual primed cells downregulated thrombospondins 1&2, which act to inhibit angiogenesis.

4.3.5 Effects on cell survival

When cultured in monolayers at basal culture conditions, MSCs experience cues that maintain cell survival. Once injected into patients, however, the MSCs lose their attachment sites and experience stressful signals such as hypoxia and inflammation. We therefore investigated how these cues affect the pathways directly related to cell survival: anoikis, apoptosis, and autophagy.

Several anoikis-resistance factors were upregulated following hypoxia and IFN-γ exposure **(Figure 15)**. S100A4 was upregulated by both IFN-γ and hypoxia (log2FC = 0.75 and 0.64, respectively), while the greatest induction came from dual priming (log2FC =1.59). Dual primed cells also showed the greatest upregulation of ANGPTL4 (log2FC = 2.56 vs. 2.05 from hypoxia alone), induction of both PDGFRA and PDGFRB, and unique upregulation of integrin alpha chain V (ITGA5).

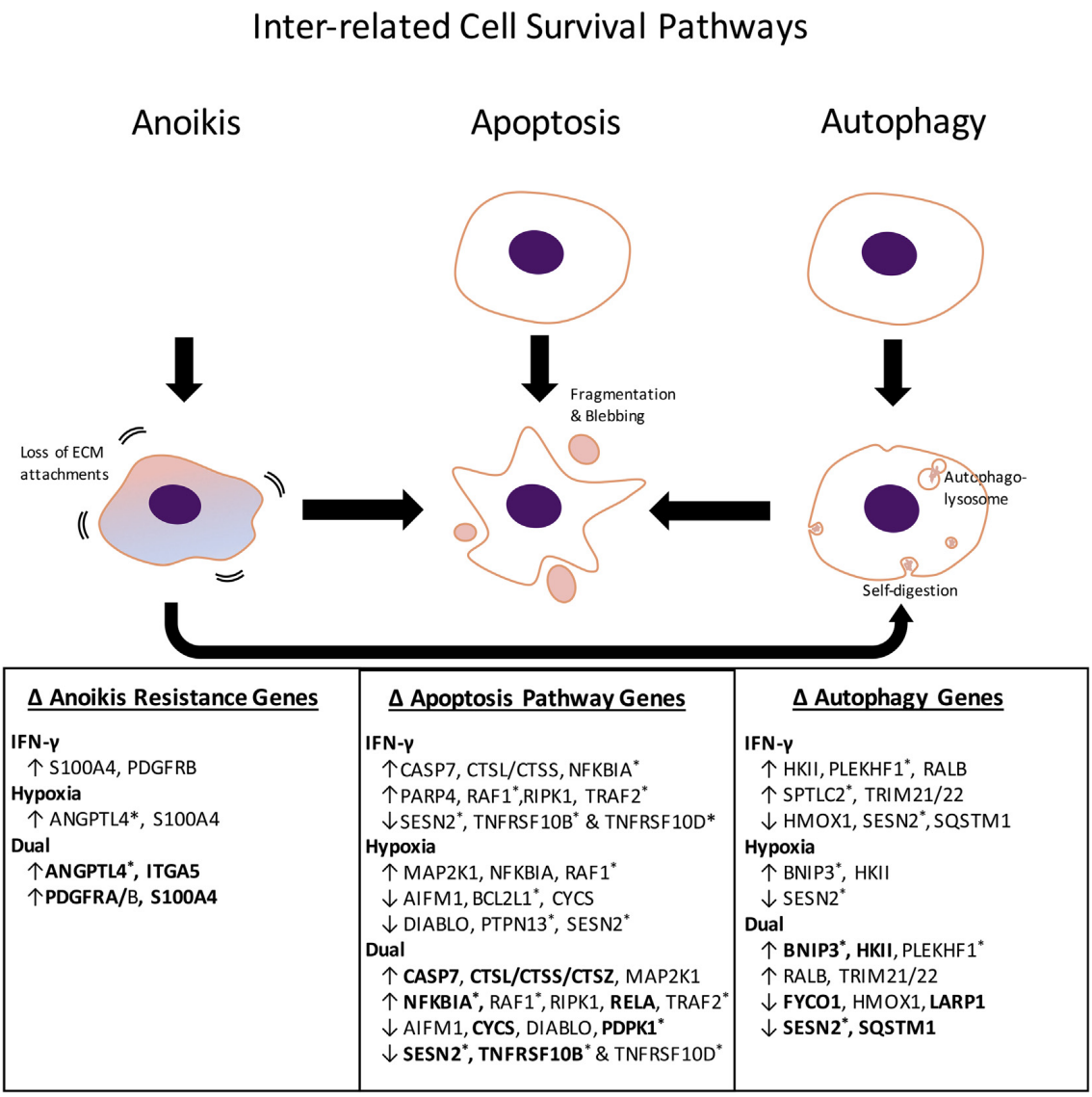

Figure 15 Interrelation of anoikis, apoptosis, and autophagy. * proteins that were identified by a single peptide. Bold type indicates significant effects of dual priming when compared to single priming. Proteins listed for apoptosis and autophagy were identified using pathways on iPathway Guide, and those related to survival from anoikis were determined from literature.[108–112]

The changes to apoptosis-related genes were suggestive of both promotion and inhibition of this process. The promotion of apoptosis was evidenced by the increases in expression of cathepsins, caspase 7 and NFKBIA, and decreases in expression of BCL2L1 and PDPK1. The inhibition of apoptosis was evidenced by increased expression of MAP2K1, RAF1 and RELA, and decreased expression of AIFM1, CYCS, DIABLO, SESN2, and TNFR10B & D (TRAIL

receptors). Other proteins listed in **Figure 15** have variable, context-specific effects. Overall, IFN-γ and hypoxia seemed to have mixed effects on apoptosis, which was also seen with dual priming.

All proteins listed under autophagy serve to facilitate that pathway (**Figure 15**). As with apoptosis, there were changes that both promote and inhibit this process. IFN-γ upregulated TRIM21 and TRIM22, whereas hypoxia highly induced BNIP3 (log2FC = 3.47), and both factors induced HKII. BNIP3 and HKII had an even greater induction from dual priming, while SESN2 was synergistically downregulated (the most downregulated protein in the whole data set). Since SESN2 is also pro-apoptotic, its downregulation may have consequences for both autophagy and apoptosis.

Beyond the pathways listed above, some additional metabolomics changes described in **Table 4** are worth highlighting. For example, taurine has many anti-oxidant and cytoprotective properties,[113–115] and this metabolite was found in all primed cells but was undetected in control MSCs. β-alanine was also upregulated in all priming conditions. This amino acid is the precursor to the anti-oxidant carnosine, which has shown cytoprotective properties in similar situations to taurine.[116,117] From a biological standpoint, β-alanine is made from pyrimidine metabolism, and its accumulation in primed cells is consistent with their upregulation of DPYD – the first enzyme in this pathway.

4.4 Discussion

Several meritorious studies have been dedicated to identifying the protein expression profile of MSCs derived from different tissue sources.[118,119] Regardless of tissue source, when MSCs are kept in basic culture conditions, their baseline behavior does not represent the many adaptations

they make in the setting of injury and disease. Since inflammation and hypoxia are common to many pathological environments, we sought to better understand the biology of therapeutic MSCs via simulating these signals with 1% O_2 and IFN-γ. Our goal was to get insight into the proteomic and metabolomic changes of MSCs co-exposed to these cues for 48h, and to parse out the relative contribution of each factor and identify synergies. The major themes we uncovered are that IFN-γ induces MSCs to contain an injury by limiting damage from infection, inflammation and fibrosis, while hypoxia promotes adaptation to low oxygen via increasing proteins involved in anaerobic metabolism, angiogenesis, autophagy, and cell migration. Combining these cues roughly combines their individual effects, with additional synergies.

As expected, IFN-γ had a strong impact on MSC immune modulation. Our study confirmed some well-known downstream effects of interferons, such as upregulation of HLA proteins, anti-microbial and anti-viral factors, and the immunosuppressive proteins IDO and PD-L1.[23] However, we also uncovered some less described proteins and metabolites that could confer MSC protection. For example, IDO is known to inhibit T-cells via metabolizing tryptophan to kynurenine (supported by our metabolomics data). This tryptophan depletion could also be harmful to MSCs. Thus, it is interesting that IFN-γ upregulates tryptophanyl tRNA-synthetase (a.k.a. WARS), which could serve as a MSC-protective method by replenishing intracellular tryptophan stores.[120]

IFN-γ also led to a mild induction of CD47, which binds to the SIRPα receptor on macrophages and has been described as a "don't eat me" signal (blocks phagocytosis) that may also promote peripheral tolerance.[121] This pathway has been implicated as a mechanism for tumor immune escape, and could be an interesting lead to pursue for MSC immunomodulation.[122] We also noted strong induction of the complement inhibitory factor –

CFH. MSCs, particularly the cryopreserved products used in industry-sponsored clinical trials, have been shown to activate the complement cascade, expediting MSC lysis and clearance.[123] Since the therapeutic utility of MSCs would presumably be better if they had a longer half-life, one group coated the cell surface with CFH to prevent this type of clearance.[124] Our data indicate a similar effect may result from simply exposing MSCs to IFN-γ. Lastly, we observed induction of the cell-protective metabolites, taurine and β-alanine, the latter of which is protective upon conversion to carnosine.[114–117]

Beyond immune modulation, IFN-γ produces an anti-fibrotic MSC phenotype**.** Except for collagen IV and agrin, IFN-γ downregulates all other structural ECM proteins. Agrin is an ECM proteoglycan part of the basement membrane, so its upregulation with collagen IV is consistent with preserving basement membrane formation. However, agrin has also been implicated as part of the immune synapse, and so its upregulation may be related to that function.[125] The otherwise widespread decrease in structural proteins is significant, because tissue fibrosis from excessive deposition of ECM is a common consequence of unchecked inflammation and is detrimental to having functional tissues.[126] Thus, IFN-γ priming of MSCs may help prevent pathological fibrosis by both inhibiting inflammation and decreasing ECM secretion. This anti-fibrotic effect has clinical relevance. In one study, patients treated with recombinant IFN-γ significantly reduced the development of liver fibrosis in the setting of chronic hepatitis B.[127]

While IFN-γ instructs MSCs to resolve tissue injury, hypoxia leads to many survival adaptations. First, hypoxia shifts cell metabolism towards non-oxygen dependent strategies – namely glycolysis and glycogenolysis. To facilitate the reliance on these pathways, cells increase lactate dehydrogenase, lactate transporters, glucose and fructose transporters, and carbonic anhydrase (to assist with pH balance)[128]. Degradation and transport of amino acids and fatty

acids, which generally feed into the TCA cycle and ETC (oxygen dependent), are downregulated, as is mitochondrial protein expression in general.

A second approach to survival is through conservation of energy stores via autophagy. We observed significant induction of the pro-autophagic BNIP3, which is consistent with studies by others.[110] Lastly, MSCs can attempt to restore a physoxic environment by promoting angiogenesis or migrating away from the low oxygen region. Consistent with reports by others, we found that hypoxia upregulates the entire family of lysyl oxidase (LOX, LOXL1-3) and lysyl hydroxylase (PLOD1&2) enzymes, which serve to cross-link collagen and elastin. These proteins are associated with promoting angiogenesis[129] and cell migration.[130,131] The additional upregulation of anoikis-resistance proteins like ANGPTL4 and S100A4, may facilitate survival during this process.[10,109,110]

The collective adaptations to hypoxia may inadvertently make MSCs a better cell therapy. Several animal studies have shown that hypoxic preconditioning of MSCs before administration enables them to better survive in the clinical setting of ischemia. Upregulation of autophagy has been directly shown to contribute. In one study, preconditioning MSCs with hypoxia improved their ability to repair infarcted hearts; however, this difference was partially abolished by an autophagy inhibitor. The changes in metabolism could also influence the immune modulatory function of MSCs. As has been described in the tumor literature, when cells (like MSCs) prioritize glycolysis for their own survival, they inhibit inflammatory immune cells in the nearby environment through glucose competition and lactate signaling.[132–134] This would explain why hypoxia preconditioned cells have a better ability to suppress T-cells *in vitro* without superior upregulation of immunosuppressive proteins like IDO.[73]

Clearly the response of MSC to IFN-γ and hypoxia are very different, and it makes sense that combining these cues results in additive effects. Indeed, dual primed cells demonstrate the metabolic changes of hypoxia, the immunomodulatory changes of IFN-γ, and the ECM and survival changes of both cues. Nevertheless, there were many points of synergy.

While hypoxia alone did not upregulate any immunosuppressive factors, dual IFN-γ/hypoxia exposure led to synergistic upregulation of LRRC32 (a.k.a. GARP), which is known to tether TGF-β1 (also most abundant in dual primed cells) to regulatory T-cells and megakaryocytes and play a role in the immunosuppressive function of MSCs.[135,136] Dual priming also downregulates structural ECM proteins and upregulates basement membrane proteins beyond IFN-γ alone, and upregulates LOXL enzymes more than hypoxia alone. The LOXL family has been shown to cross-link ECM proteins to attract anti-inflammatory macrophages, promote angiogenesis, and mobilize cells to migrate to distal organs.[130,131,137,138] Survival in this "metastatis-like" scenario is consistent with dual primed cells having the highest expression of ACSL5, ANGPTL4, BNIP3, HKII, PDGFRA, S100A4, as well as taurine and β-alanine (precursor to carnosine).

While we have attempted to profile how MSCs respond to a diseased microenvironment, several limitations should be considered. Clearly, more than hypoxia and IFN-γ are present *in vivo*, as there are many other paracrine factors and immune cells that will affect MSC behavior. Our analysis is meant to isolate the effect of at least two of these factors to help us understand how they contribute to the whole. In doing so, we also gain insight towards the many ways by which priming MSCs with these cues beforehand could enhance their therapeutic capacity (immune modulation, pro-survival etc.).[70,139]

A second limitation is that the samples comprised of adherent cells that were healthy from ~10 days in cell culture. MSCs used in industry sponsored clinical trials are cryopreserved, thawed, and injected within a few hours. Loss of attachment can be expected to affect cell viability, and cryopreservation is known to affect MSC metabolism, viability, and responsiveness to IFN-γ.[140–142] Our data thus represent the best-case-scenario, as the proteome and metabolome of recently thawed cells may be less malleable.

Finally, there are three outstanding questions: 1) What is the role of ACO1/IRP1 upregulation from IFN-γ and hypoxia? 2) What is the function of GLUT5 upregulation when blood fructose levels are low? Given that IFN-γ upregulates ASCL5 and SLC27A3, does IFN-γ have a meaningful effect on long chain lipid metabolism?

4.5 Future Directions

The mass spectrometry and metabolomics findings revealed many interesting changes, which have yet to be fully characterized. For example, two potentially self-protective proteins upregulated by IFN-γ were CD47 and CFH, and it would be interesting to explore how clinically relevant these proteins are (or could be, if further overexpressed) in terms of facilitating MSC survival and function *in vivo*. Hypoxia also had a profound impact on ECM modification, which has been described in the cancer literature, but the functional relevance to clinical MSC therapies has yet to be explored. Further studies could help discern if these ECM changes make the MSCs well-suited for specific clinical indications where those changes facilitate better healing.

Chapter 5

Aim 3: To compare the ability of dual IFN-γ/hypoxia primed vs. unprimed MSCs to prevent disease progression in models of acute GvHD

5.1 Overview

Since the mid-2000s, there have been hundreds of clinical trials registered for assessing the utility of MSCs in treating immune disorders. One of the most well-studied indications has been acute GvHD.[143–146] GvHD is a common complication of foreign donor hematopoietic stem cell transplantation (allo-HCT; a.k.a. bone marrow transplant), whereby immune cells in the graft attack the patients' tissues, particularly the skin, gastrointestinal tract, and liver, which can lead to organ failure and death. Steroids are the first line treatment but only provide a complete response in 25-40% of patients.[145] Second-line treatments do not fare much better and increase

the risk of deadly opportunistic infection. The failure of multiple immunosuppressive drugs to provide a safe and effective therapy suggests a new category of therapy is warranted.

MSCs have been evaluated in many case reports and clinical trials for acute GvHD[145,147]. Unlike other immunosuppressive drugs, few side effects have been described, conferring a clear safety benefit. However, the efficacy of these MSCs has been unconvincing. While they have shown promise in case reports and in Phase II clinical trials, a Phase III trial testing a commercial MSC product (Prochymal) failed to meet its primary endpoint,[52] and MSC therapies have yet to gain FDA approval.

Based on the functional and proteomic characterization of dual IFN-γ/hypoxia primed MSCs, we believe they may be better able to prevent the progression of GvHD than their unprimed counterparts. To test this, we evaluated them in a commonly used xenogeneic mouse model of GvHD.[148] This model has the advantage of pairing human immune cells (the disease-causing HCT) with human MSCs (the therapeutic cells), although it is still a partially xenogeneic model, since the human immune cells attack mouse tissues.

Given that animal studies do not always predict clinical efficacy, we also sought to leverage our lab's experience in engineering human tissue models of disease from stem cells.[149,150] There are no published reports of a tissue engineered GvHD model; however, a study from 1988 describes an *ex vivo* system of skin GvHD whereby immune cells from the HCT donor are initially co-cultured with APCs from the putative patient and are then added to a biopsy punch of the patient's skin.[151] The severity of skin GvHD that developed (histological grade) in this model was predictive of the severity that developed after the patient underwent HCT. To have more control over system components, we have been re-creating this model but with tissue engineered skin. Our progress is ongoing, but we anticipate this could be a

complementary model to mouse studies for testing potential new GvHD therapeutics.

5.2 Methods

5.2.1 Induction of GvHD in a xenogeneic mouse model

NOD.Cg-*Prkdc*^{scid}*Il2rg*^{tm1Wjl}*/SzJ (*NOD-*scid IL2r*γ^{null} abbreviated as NSG) mice were purchased from Jackson Laboratories, (Bar Harbor, ME). Mice were used in experiments at 8-12 weeks of age and housed in a specific pathogen-free microisolator environment. All protocols were approved by the Columbia University Institutional Animal Care and Use Committee (IACUC). NSG mice were conditioned with sublethal total-body irradiation (TBI; RS 2000 X-ray Irradiator, Rad Source Technologies, Inc. (Buford, GA, USA)) followed by next-day intravenous injection of fresh PBMCs into the mouse tail vein. Mouse survival was checked every day, and body weight was measured every 3-4 days.

5.2.2 Administration of therapeutic MSCs to mice

Control (unprimed) human MSCs or dual IFN-γ/hypoxia primed MSCs (0.75×10^6) were intravenously injected into the mouse tail vein on the same day as human PBMCs. Prior to injection, the MSCs were washed x3 in PBS to eliminate FBS and cytokines, and were resuspended in BMM for delivery. To prevent mouse death from MSC emboli to the pulmonary vasculature, cells were filtered through a 30 μm mesh immediately before delivery, reducing MSCs to single-cell suspension. They were also injected in a total volume of 500 μL, via two slow pushes of 250 μL. This led to a >95% immediate survival rate. While all MSC lines were tested negative for mycoplasma and looked sterile prior to injection, mice were still provided

with medicated water that contained trimethoprim and sulfamethoxazole (Hi-Tech Pharmacal. Co. Inc., (Amityville, NY)).

5.2.3 Engineering an immunocompetent full skin equivalent (FSE) to model GvHD

To emulate the 1988 explant model of skin GvHD but using tissue engineered skin, it was necessary to develop a method for acquiring blood cells that were autologous to pluripotent stem cells. Our collaborators in the Christiano lab have experience with engineering full skin equivalents (FSE) from induced-pluripotent stem cells (iPSC).[152] However, when these cell lines are purchased from commercial vendors or acquired by material transfer agreements from other universities, it is impossible to acquire blood cells that are autologous to the iPSC line. An obvious solution would be to try to differentiate the iPSC line to different blood cell lineages. While this has been done to a certain extent for macrophages,[153] it is more challenging for other lineages (e.g. T-cells that need clonal diversity, APC subsets), and thus it would be easier to simply use matched blood samples. We thus co-developed an IRB protocol with the Center for Advanced Laboratory Medicine (CALM) that enables repeat blood collections from local, anonymous donors, where the first donation is also used to generate an iPSC line. Since the donors can be called back for future donations, there is a consistent source of blood cells, which have a normal biologic ratio amongst subsets, and they can be used fresh or cryopreserved for future use. The general concept is schematized in **Figure 16**.

5.2.4 Generation and characterization of iPSC lines

Blood-derived iPSC lines were generated in line with the CUMC institutional ethics review board. Small (8 mL) blood samples were collected by the CALM and immediately brought to the

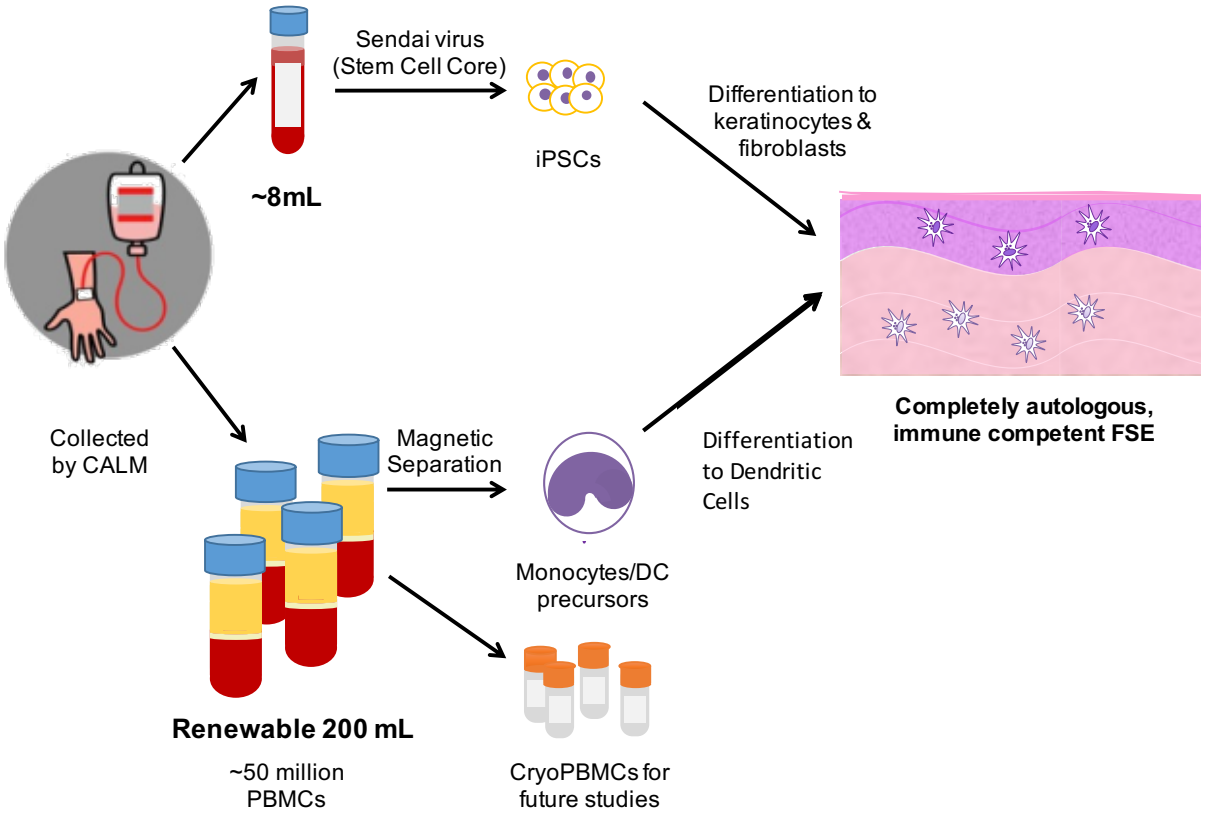

Figure 16 Schematic of our approach to producing fully autologous, immune competent tissues, such as full skin equivalents (FSEs) containing autologous dendritic cells (DCs).

Columbia Stem Cell Core for reprogramming of T-cells into iPSCs using the Sendai virus method.[154] Blood donations came from healthy individuals with the provision that future, larger donations could be arranged for having autologous immune cells to iPSC-derived tissues. The line "BS1" was used for all subsequent experiments.

Colonies of iPSCs were picked and cryopreserved, and expanded cells were evaluated by numerous means. These included flow cytometry for the pluripotency markers: Oct4, Nanog, Tra-1-60, and SSEA4 (performed by Columbia Stem Cell Core), karyotype analysis (outsourced to Cell Line Genetics), and tri-lineage differentiation (performed at Columbia Stem Cell Core using the R&D Human Pluripotent Stem Cell Functional Identification Kit). Cells were also tested for their differentiation potential to cardiomyocytes to evaluate how well standard laboratory differentiation protocols stood up to this new source of iPSCs (data not shown).

5.2.5 Engineering FSEs using iPSC-derived keratinocytes and fibroblasts

Fibroblasts were made from iPSCs as previously published by the Christiano lab, but with the new BS1 blood-derived iPSC line.[155] Briefly, iPSCs were aggregated into embryoid bodies in iPSC media (-FGF, +0.3 mM ascorbic acid (Sigma), 10 ng/mL TGFβ2 (R&D), +ITS-A supplement) on low attachment plates. These were moved to gelatin-coated plates to induce cell outgrowth and switched to high glucose DMEM (+ascorbic acid, +20% FBS) for 10 days. Cells that demonstrated outgrowth were repeatedly passaged to obtain spindle-shaped cells.

Keratinocyte (KC) differentiation was performed by modifications of the protocol described by Itoh *et al*. To make 3-D skin equivalents, type I collagen containing iPSC-derived fibroblasts was polymerized onto polyethylene terephthalate membranes for 5-7 days, as previously published.[155] iPSC-KCs were then seeded onto the matrix and incubated for 6 days, after which the whole FSE was moved to the air-liquid interface to induce cornification of the epidermis for 7 days.

5.2.6 Creating autologous dendritic cells

The BS1 donor was asked to donate blood on several occasions. This was collected in CPT tubes (Becton Dickinson), which have a Ficoll layer imbedded such that spinning the tubes automatically separates out the PBMC layer. Some PBMCs were collected and cryopreserved as a source of autologous PBMCs for future studies. However, when dendritic cells were required, fresh BS1 PBMCs were magnetically sorted using CD14+ positive selection beads (Miltenyi) to first obtain the monocytes, which were differentiated to dendritic cells (DCs) using 50 ng/mL GM-CSF and 100 ng/mL IL-4 (Peprotech) for 5 days. Immature DCs were characterized by flow cytometry, using previously described methods and antibodies shown in **Table S7.**

5.2.7 Simulation of the GvH response

To simulate the GvH response, BS1 DCs were co-cultured with either autologous or allogeneic PBMCs, as with previous MLR experiments. After 3 days of co-culture, some PBMCs were collected, seeded onto a collagen gel, and left overnight. Skin constructs were then transferred on top of the PBMC-containing gel (PBMC adjacent to dermis), and after four days of culture, the engineered skin was fixed and analyzed by H&E staining (JungU Shin). Other PBMCs in co-culture with auto- or allogeneic DCs were left to react for 6 days to assess the T-cell division via flow cytometry as per previous MLR experiments.

5.3 Results

5.3.1 Optimizing GvHD disease induction

Initially, several different GvHD induction regimens were evaluated, which are shown in **Figure 17**. Combining the highest cell and radiation dose (10^7 PBMCs, 1.5 Gy TBI) led to rapid disease progression. While mice in other groups maintained body weight until ~Day 15 post-transplant, mice that received the more aggressive regimen had all died by then. Indeed, the rate of mouse death was twice as rapid in this group compared with those that received a cell or radiation dose that was 25-33% lower. This aggressive induction regimen was chosen for future studies.

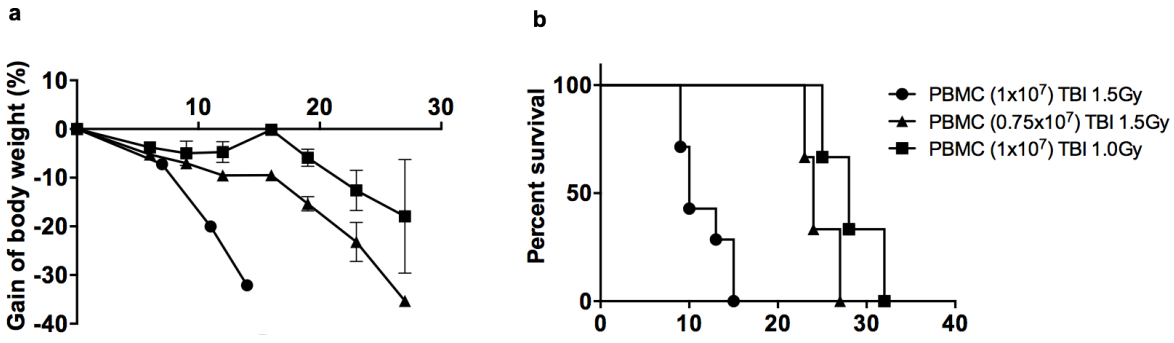

Figure 17 Titration of different GvHD induction regimens. (a) Weight loss over time from 3 different induction regimens **(b)** Mouse survival over time from 3 different induction regimens.

5.3.2 Inhibition of xeno-GVHD via primed MSCs (pMSCs)

In the next study, control (unprimed) or dual primed MSCs (pMSCs) were administered on Day 0 along with the PBMCs. Mice in all groups showed a small initial drop in body weight due to the radiation; however, all groups were able to recover from this before the GvHD set in. While the same aggressive induction regimen was used as the dose-titration experiment (**Figure 17**), untreated mice in this study did not start to die until Day 12 (**Figure 18b**).

The body weight and survival curves for the mice treated with control MSCs were not significantly different from the completely untreated group. Dual primed MSCs, by contrast, showed a relatively prolonged course for loss of body weight (**Figure 18a)**, and survived significantly longer than untreated mice (**Figure 18b**).

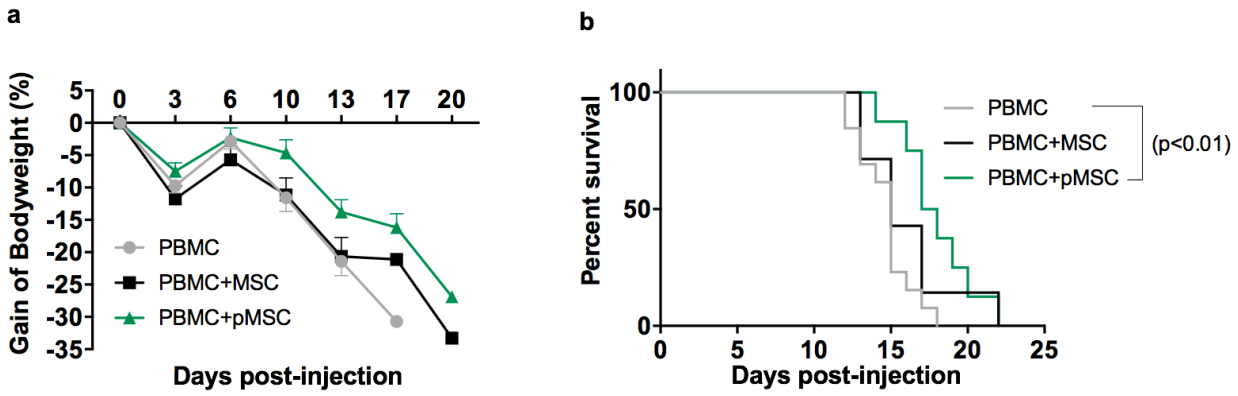

Figure 18 Effect of Control vs. Dual Primed MSCs on GvHD progression. (a) Weight loss over time. **(b)** Mouse survival over time. n = 8-13 per group.

5.3.3 Blood-derived iPSC lines demonstrate pluripotency

In parallel to *in vivo* studies, steps were taken towards developing an *ex vivo*, tissue-engineered skin GvHD model. The first step of this was to derive a blood-derived iPSC line, which was called BS1. This line was demonstrated to have differentiation capacity into endoderm, mesoderm, and ectoderm when induced with germline specific cues **(Figure 19a)**.

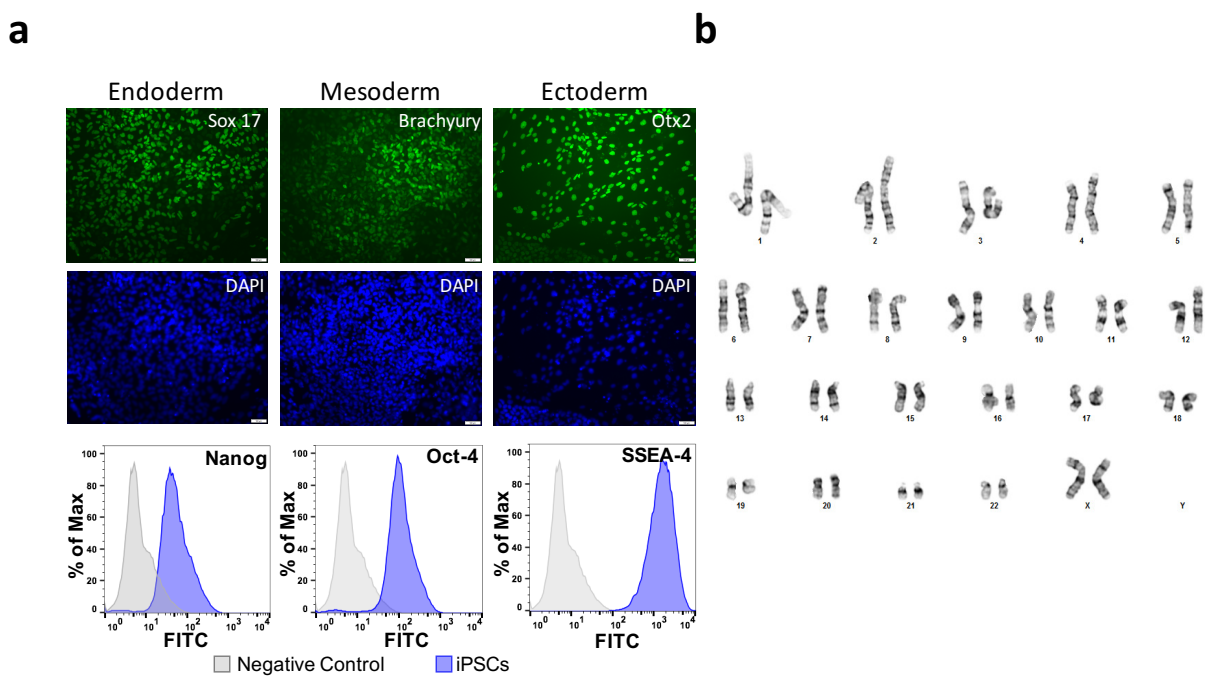

Figure 19 (a) Demonstration of BS1 iPSC line pluripotency by germline differentiation and flow cytometry**. (b)** Karyotype demonstrates no chromosomal abnormalities.

Furthermore, the majority of these cells stained positive for the pluripotency markers Nanog, Oct4, and SSEA-4. Karyotype analysis of cells at a low passage number (<20) demonstrated no chromosomal abnormalities **(Figure 19b)**.

5.3.4 Extended differentiation of iPSCs leads to cells phenotypically similar to primary human KCs

Extending KC differentiation protocols to 60 days led to a marked change in expression of key ECM proteins **(Figure 20)**. Primary human KC have a very distinct bimodal expression pattern of Keratin-14 on flow cytometry analysis. iPSC differentiation protocols for 12 and 30 days looked identical to each other with a single Keratin-14 peak that was dimmer than that of primary cells. However, extending the differentiation to 60 days led to a bright, bimodal expression pattern identical to that of the primary human KCs.

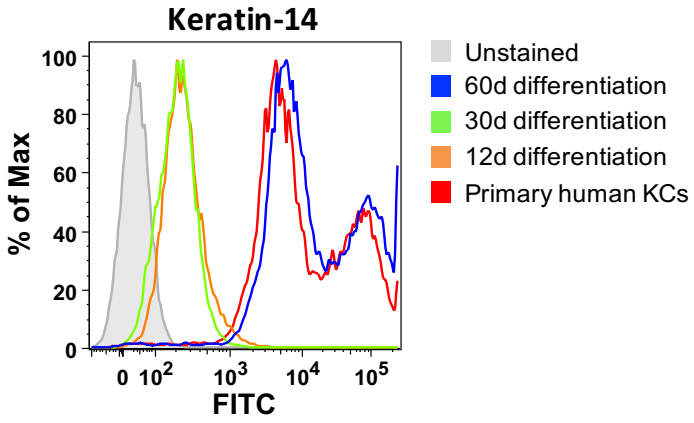

Figure 20 Optimizing iPSC→KC differntiation. iPSCs were exposed to different durations of differentiation and then stained for the maturation marker Keratin-14

5.3.5 Monocyte-derived DCs express expected DC markers

Monocytes directed towards an immature DC phenotype were assessed by flow cytometry **(Figure 21)**. As expected, DCs minimally expressed CD14 but highly expressed CD11c. Dermal DC markers (CD36 and DC-SIGN) were more highly expressed than epidermal DC markers (Langerin and E-cadherin). HLA-DR exhibited moderate signal, whereas CD80 was not expressed.

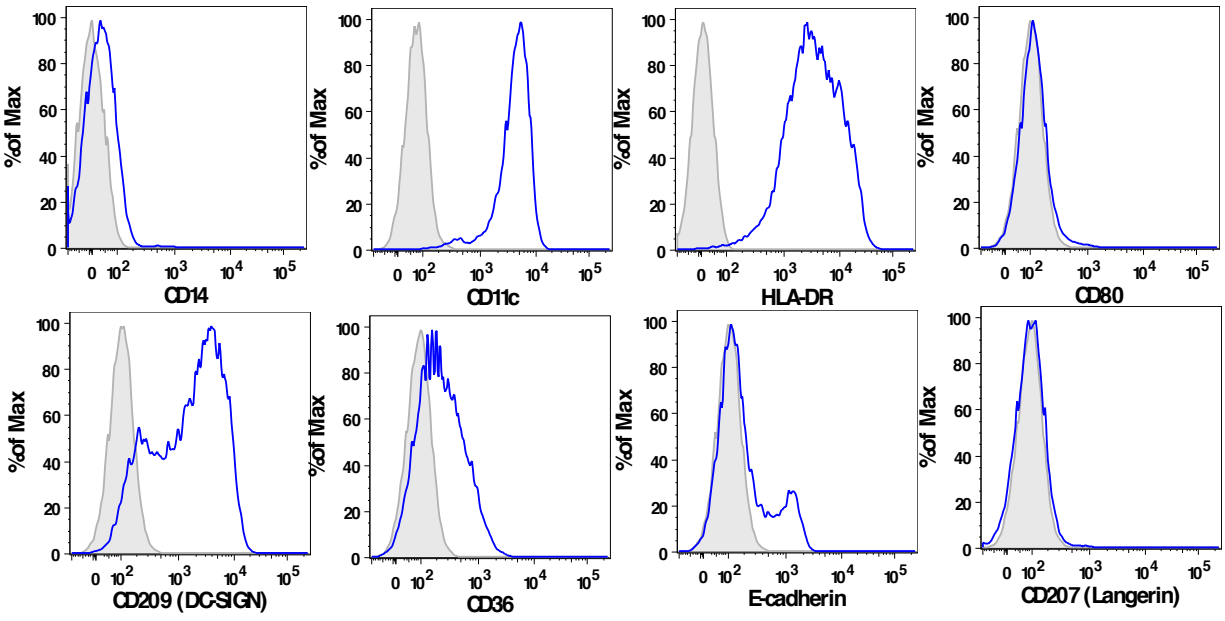

Figure 21 Evaluation of monocyte-derived DC surface marker expression by flow cytometry.

5.3.6 T-cells co-cultured with allogeneic DCs show greater activation and migration into FSE than those co-cultured with autologous DCs

Violet-labelled PBMCs were co-cultured with DCs that were either autologous or allogeneic. After 6-days of co-culture, some cells were analyzed by flow cytometry **(Figure 22)**. This revealed a small amount of T-cell division in the autologous case (14.9% of cells divided); however, division was much more significant for the allogeneic condition (65.7% of cells divided).

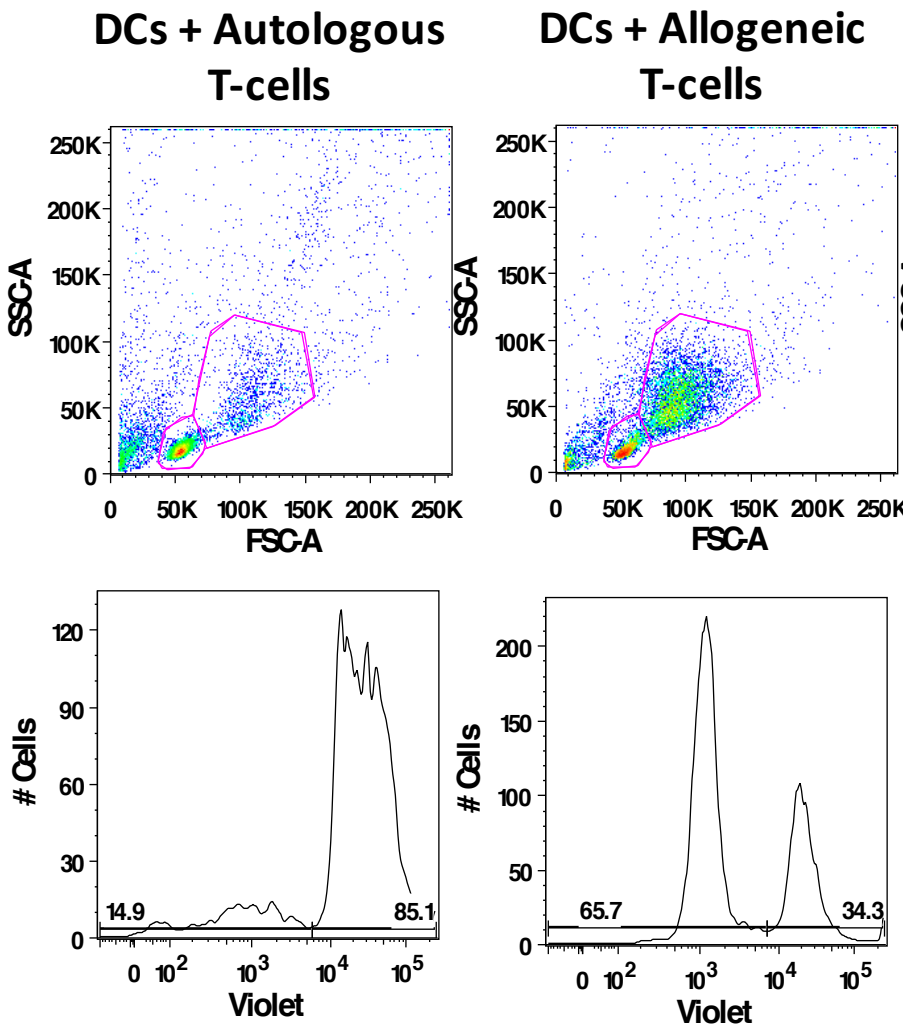

Figure 22 Mixed lymphocyte reaction using autologous (left) vs. allogeneic (right) using DCs as stimulators and either autologous or allogeneic PBMCs as responders. Flow cytometry conducted after 6-days of co-culture.

Some PBMCs were instead transferred to FSEs after only 3 days of co-culture with DCs **(Figure 23).** While PBMCs did not penetrate the dermis when they came from the autologous co-culture, a small percentage of cells showed migration when they had been previously in allogeneic co-culture.

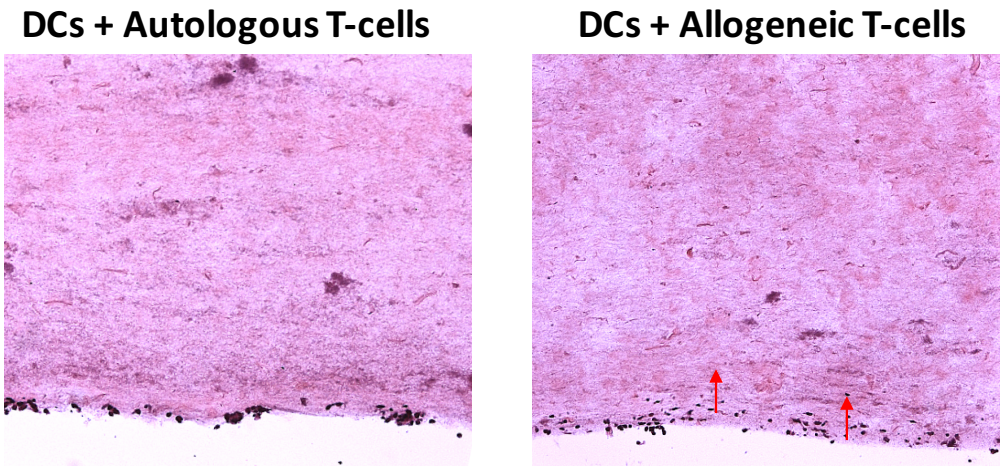

Figure 23 PBMCs either autologous or allogeneic to DCs were co-cultured for 3-days before being transferred to FSEs.

5.4 Discussion

The severity of GvHD that develops is sensitive to many factors, including the PBMC dose, the radiation dose, as well as less controllable variables such as the microbiome a mouse adopts within a given barrier facility.[156] We initially tested different doses of PBMCs and TBI to determine which induction regimen we should continue with for our MSC studies.

The definition for a complete response in clinical trials that have used MSCs in steroid-refractory GvHD patients has been "disease free survival by 28 days". This might suggest that the two lower dose induction regimens we tested would be more appropriate, since they have a 1-month disease progression. However, there are two factors to keep in mind. The first is that we are evaluating our MSCs as a preventative strategy and not in mice that already have late-stage, steroid-refractory disease. The second is that the human clinical trials dosed the MSCs twice a

week for every week in that month, whereas we are only doing a single injection at the beginning.[140] Multiple injections in a mouse model would increase the loss of mice from MSC pulmonary emboli. Thus, we decided to use the aggressive GvHD model, as that would maximize the ratio of time MSCs from our single injection would be in contact with the GvHD inducing immune cells.

Having decided upon this aggressive induction regimen, we assessed the ability of a low dose (750,000 MSCs) of control vs. dual primed MSCs to slow disease progression. Dual primed cells clearly provided benefit over untreated mice based on the weight loss and survival curves, while control MSCs did not. Mice that received dual primed MSCs also had slower disease progression than those that received control MSCs; however, one mouse in the control MSC group survived to day 22, which was anomalous (all others had died by day 17) and prevented there being a statistically significant difference between these two experimental groups based on survival. Nevertheless, the data are encouraging.

While we initially chose a relatively low dose of cells to prevent "over-dosing the mice", based on the data obtained, doubling this cell dose will likely lead to better treatment of the aggressive GvHD that develops and may help to accentuate group differences. In summary, we have shown initial evidence that dual primed can significantly slow the progression of severe GvHD, whereas unprimed MSCs cannot.

5.5 Future Directions

We plan to continue performing xeno-GvHD mouse studies with larger sample sizes, as well as mid-point pathology, as the latter will permit the evaluation of disease progression by additional metrics such as tissue histology. From there, we may follow-up with a study in which MSCs are

administered 1-week into disease progression, which will test their ability to treat (not prevent) GvHD that has already developed.

While much progress has been made with our *ex vivo* tissue platform of GvHD, our initial focus will be to simply characterize and fully develop this as a disease model. Future students may test different therapeutics on this model or similar immune-competent engineered tissue models that could be developed with the tools we have created for modeling GvHD.

Chapter 6

Conclusions

Decades of research have been devoted to understanding the biology and therapeutic potential of MSCs. This includes biochemical and animal studies, as well as hundreds of industry and academia-sponsored clinical trials.

The safety of using both autologous and allogenic MSCs is well-established, and the FDA has recently developed numerous strategies to facilitate the approval of novel cell and gene therapies, such as through the "regenerative medicine advanced therapy" (RMAT) designation that was provided by the 21st Century Cures Act. It appears that we are finally at the moment in history when regenerative medicine therapeutics could start to be FDA approved and reach patients in the United States.

Nevertheless, if MSCs continue to be tested in clinical trials without approaching their production differently, there is no reason to expect that the outcome should be any more favorable than it has been in previous clinical trials. Given the multipotent nature of these cells,

and their sensitivity to microenvironmental cues, injecting naïve, unprimed MSCs lends itself to wide variability in therapeutic activity, since the cells may adopt different behaviors based on each patients' internal environment.

Our focus has been on developing MSCs as cell therapies to treat inflammatory conditions. To help create a uniform population of immunosuppressive cells, and reduce patient-specific variability in MSC phenotype, our objective was to develop a brief *in vitro* priming regimen that the cells would undergo after they had been expanded to therapeutic cell numbers. We chose to perform an in-depth evaluation of two priming cues – hypoxia and IFN-γ - that had previously been cited to serve complementary purposes in the literature. Hypoxia was known to promote cell survival and IFN-γ was known to induce an immunosuppressive phenotype in MSCs.

In vitro studies uncovered that, indeed, both cues could instruct MSCs towards a more anti-inflammatory state. IFN-γ accomplished this via promoting the upregulation of immune-regulatory proteins: HLA-G, HLA-E, IDO, PD-L1, and hypoxia accomplished this by altering MSC metabolism towards a glycolytic state that challenged T-cells in the environment, which are also dependent on glycolysis and sensitive to local lactate concentration. As these are distinct mechanisms of action, it was not surprising that dual priming MSCs with both cues led to twice the improvement in immunosuppressive capacity over either cue alone.

To more fully understand how priming with hypoxia, IFN-γ, and their combination affected MSC behavior, we followed up our *in vitro* immune suppression studies with a global proteomic and metabolic analysis. This revealed two distinct patterns of adaptations that MSCs make to each cue.

MSCs respond to IFN-γ in a manner that makes sense in the context of wound healing. The cells upregulate their anti-pathogen response to eliminate foreign invaders, upregulate several immunosuppressive proteins to prevent pathological inflammation, and increase their expression of factors that promote their own survival from immune mediated clearance. Additionally, cells decrease ECM deposition, which serves as an anti-fibrotic mechanism. The response to hypoxia serves an entirely different purpose, which is to engage pathways that permit cell survival in a low oxygen setting.

Hypoxia primed MSCs switch to glycolysis for energy and down regulate oxygen-dependent mechanisms of metabolism. They also increase proteins involved in autophagy and cell migration. As with our earlier studies, we found these changes were additive for dual primed MSCs, although there were many synergies, particularly when it came to ECM deposition and modification. These studies lent much insight (including some novel mechanisms) to our understanding of MSC biology, and they suggested how using IFN-γ and hypoxia together could confer many benefits to MSCs used clinically.

To evaluate the primed cells in the setting of disease, we turned to a xenogeneic mouse model of GvHD and started to develop an engineered tissue model of skin GvHD as a parallel testing platform. Our preliminary mouse model findings support that priming enables MSCs to better prevent GvHD, and we are optimistic about the confirmatory studies that are planned for the next several months. The hope is that the science of priming MSCs, which we have advanced in this thesis, can ultimately lead to more consistently effective MSC therapies in humans.

REFERENCES

1. Dominici, M. *et al.* Minimal criteria for defining multipotent mesenchymal stromal cells. The International Society for Cellular Therapy position statement. *Cytotherapy* **8,** 315–317 (2006).
2. Kobolak, J., Dinnyes, A., Memic, A., Khademhosseini, A. & Mobasheri, A. Mesenchymal stem cells: Identification, phenotypic characterization, biological properties and potential for regenerative medicine through biomaterial micro-engineering of their niche. *Methods* **99,** 62–68 (2015).
3. Gadkari, R., Zhao, L., Teklemariam, T. & Hantash, B. M. Human embryonic stem cell derived-mesenchymal stem cells: an alternative mesenchymal stem cell source for regenerative medicine therapy. *Regen. Med.* **9,** 453–465 (2014).
4. Yun, Y. I. *et al.* Comparison of the anti-inflammatory effects of induced pluripotent stem cell–derived and bone marrow–derived mesenchymal stromal cells in a murine model of corneal injury. *Cytotherapy* **19,** 28–35 (2017).
5. DiMarino, A. M., Caplan, A. I. & Bonfield, T. L. Mesenchymal stem cells in tissue repair. *Front. Immunol.* **4,** 1–9 (2013).
6. Fahy, N., Alini, M. & Stoddart, M. J. Mechanical stimulation of mesenchymal stem cells: Implications for cartilage tissue engineering. *J. Orthop. Res.* (2017). doi:10.1002/jor.23670
7. Anitha, A. *et al.* Bioinspired Composite Matrix Containing Hydroxyapatite-Silica Core-Shell Nanorods for Bone Tissue Engineering. *ACS Appl. Mater. Interfaces* **9,** 26707–26718 (2017).

8. Jang, S., Cho, H., Cho, Y., Park, J. & Jeong, H. Functional neural differentiation of human adipose tissue-derived stem cells using bFGF and forskolin. *BMC Cell Biol.* **10,** 25 (2010).

9. Dadon-Nachum, M., Sadan, O., Srugo, I., Melamed, E. & Offen, D. Differentiated Mesenchymal Stem Cells for Sciatic Nerve Injury. *Stem Cell Rev. Reports* **7,** 664–671 (2011).

10. Wang, F.-W. *et al.* Protective effect of melatonin on bone marrow mesenchymal stem cells against hydrogen peroxide-induced apoptosis in vitro. *J. Cell. Biochem.* **114,** 2346–55 (2013).

11. Yoon, Y., Lee, N. & Scadova, H. Myocardial regeneration with bone-marrow-derived stem cells. **97,** 253–263 (2005).

12. Caplan, A. I. & Correa, D. The MSC: An injury drugstore. *Cell Stem Cell* **9,** 11–15 (2011).

13. Phinney, D. G. & Prockop, D. J. Concise review: mesenchymal stem/multipotent stromal cells: the state of transdifferentiation and modes of tissue repair--current views. *Stem Cells* **25,** 2896–2902 (2007).

14. Tögel, F. *et al.* Vasculotropic, paracrine actions of infused mesenchymal stem cells are important to the recovery from acute kidney injury. *Am. J. Physiol. Renal Physiol.* **292,** F1626–F1635 (2007).

15. Lee, R. H. *et al.* Intravenous hMSCs Improve Myocardial Infarction in Mice because Cells Embolized in Lung Are Activated to Secrete the Anti-inflammatory Protein TSG-6. *Cell Stem Cell* **5,** 54–63 (2009).

16. Ankrum, J. a, Ong, J. F. & Karp, J. M. Mesenchymal stem cells: immune evasive, not immune privileged. *Nat. Biotechnol.* **32,** 252–60 (2014).

17. Gao, F. *et al.* Mesenchymal stem cells and immunomodulation: current status and future prospects. *Cell Death Dis.* **7,** e2062 (2016).

18. Liechty, K. W. *et al.* Human mesenchymal stem cells engraft and demonstrate site-specific differentiation after in utero transplantation in sheep. *Nat. Med.* **6,** 1282–1286 (2000).

19. Von Bahr, L. *et al.* Analysis of tissues following mesenchymal stromal cell therapy in humans indicates limited long-term engraftment and no ectopic tissue formation. *Stem Cells* **30,** 1575–1578 (2012).

20. Ng, K. S., Kuncewicz, T. M. & Karp, J. M. Beyond Hit-and-Run: Stem Cells Leave a Lasting Memory. *Cell Metab.* **22,** 541–543 (2015).

21. Chinnadurai, R., Ian B. Copland, Seema R. Patel & Jacques Galipeau. IDO-Independent Suppression of T Cell Effector Function by IFN- γ − Licensed Human Mesenchymal Stromal Cells. *J Immunol* **192,** 1491–1501 (2014).

22. DelaRosa, O. *et al.* Requirement of IFN-gamma-mediated indoleamine 2,3-dioxygenase expression in the modulation of lymphocyte proliferation by human adipose-derived stem cells. *Tissue Eng. Part A* **15,** 2795–2806 (2009).

23. Krampera, M., Galipeau, J., Shi, Y., Tarte, K. & Sensebe, L. Immunological characterization of multipotent mesenchymal stromal cells-The international society for cellular therapy (ISCT) working proposal. *Cytotherapy* **15,** 1054–1061 (2013).

24. Nasef, A. *et al.* Immunosuppressive effects of mesenchymal stem cells: involvement of HLA-G. *Transplantation* **84,** 231–7 (2007).

25. Ding, D.-C., Chang, Y.-H., Shyu, W.-C. & Lin, S.-Z. Human umbilical cord mesenchymal stem cells: a new era for stem cell therapy. *Cell Transplant.* **24,** 339–47 (2015).

26. Ma, S. *et al.* Immunobiology of mesenchymal stem cells. *Cell Death Differ.* **21,** 216–225 (2014).

27. Chang, H.-K. *et al.* Inducible HGF-secreting Human Umbilical Cord Blood-derived MSCs Produced via TALEN-mediated Genome Editing Promoted Angiogenesis. *Mol. Ther.* **24,** 1–11 (2016).

28. Nasef, A. *et al.* Leukemia inhibitory factor: Role in human mesenchymal stem cells mediated immunosuppression. *Cell. Immunol.* **253,** 16–22 (2008).

29. Moll, G. *et al.* Mesenchymal stromal cells engage complement and complement receptor bearing innate effector cells to modulate immune responses. *PLoS One* **6,** (2011).

30. Eseonu, O. I. & De Bari, C. Homing of mesenchymal stem cells: mechanistic or stochastic? Implications for targeted delivery in arthritis. *Rheumatology* **54,** 210–218 (2015).

31. Han, S. *et al.* A versatile assay for monitoring in vivo-like transendothelial migration of neutrophils. *Lab Chip* **12,** 3861 (2012).

32. Karp, J. M. & Leng Teo, G. S. Mesenchymal stem cell homing: the devil is in the details. *Cell Stem Cell* **4,** 206–216 (2009).

33. Becker, A. De & Riet, I. Van. Homing and migration of mesenchymal stromal cells: How to improve the efficacy of cell therapy? *World J. Stem Cells* **8,** 73 (2016).

34. Cheng, Z. *et al.* Targeted Migration of Mesenchymal Stem Cells Modified With CXCR4 Gene to Infarcted Myocardium Improves Cardiac Performance. *Mol. Ther.* **16,** 571–579 (2008).

35. Wei, J.-N. *et al.* Transplantation of CXCR4 Overexpressed Mesenchymal Stem Cells Augments Regeneration in Degenerated Intervertebral Discs. *DNA Cell Biol.* **35,** 241–248

(2016).

36. Li, H. *et al.* CCR7 expressing mesenchymal stem cells potently inhibit graft-versus-host disease by spoiling the fourth supplemental Billingham's tenet. *PLoS One* **9,** 1–16 (2014).

37. Miller, A. H. & Raison, C. L. The role of inflammation in depression: from evolutionary imperative to modern treatment target. *Nat Rev Immunol* **16,** 22–34 (2017).

38. Bailey, K. A., Haj, F. G., Simon, S. I. & Passerini, A. G. Atherosusceptible Shear Stress Activates Endoplasmic Reticulum Stress to Promote Endothelial Inflammation. *Sci. Rep.* **7,** 8196 (2017).

39. Toyserkani, Navid, M. *et al.* Concise Review: A Safety Assessment of Adipose- Derived Cell Therapy in Clinical Trials: A Systematic Review of Reported Adverse Events. *Stem Cells Transl. Med.* **6,** 1786–1794 (2017).

40. Squillaro, T., Peluso, G. & Galderisi, U. Review Clinical Trials With Mesenchymal Stem Cells : An Update. **25,** 829–848 (2016).

41. Cras, A. *et al.* Update on mesenchymal stem cell-based therapy in lupus and scleroderma. *Arthritis Res. Ther.* **17,** 301 (2015).

42. Houtgraaf, J. H. *et al.* Intracoronary infusion of allogeneic mesenchymal precursor cells directly after experimental acute myocardial infarction reduces infarct size, abrogates adverse remodeling, and improves cardiac function. *Circ. Res.* **113,** 153–166 (2013).

43. Hamamoto, H. *et al.* Allogeneic Mesenchymal Precursor Cell Therapy to Limit Remodeling After Myocardial Infarction: The Effect of Cell Dosage. *Ann. Thorac. Surg.* **87,** 794–801 (2009).

44. Amado, L. C. *et al.* Cardiac repair with intramyocardial injection of allogeneic mesenchymal stem cells after myocardial infarction. *Proc. Natl. Acad. Sci.* **102,** 11474–

11479 (2005).

45. Shake, J. G. *et al.* Mesenchymal stem cell implantation in a swine myocardial infarct model: Engraftment and functional effects. *Ann. Thorac. Surg.* **73,** 1919–1926 (2002).

46. Quevedo, H. C. *et al.* Allogeneic mesenchymal stem cells restore cardiac function in chronic ischemic cardiomyopathy via trilineage differentiating capacity. *Proc. Natl. Acad. Sci. U. S. A.* **106,** 14022–7 (2009).

47. Hare, J. M., Fishman, J. E., Gerstenblith, G. & Al, E. Comparison of Allogeneic vs Autologous Bone Marrow–Derived Mesenchymal Stem Cells Delivered by Transendocardial Injection in Patients With Ischemic …. *JAMA J. ...* **308,** 2369–2379 (2012).

48. Heldman, A. W. *et al.* Transendocardial mesenchymal stem cells and mononuclear bone marrow cells for ischemic cardiomyopathy: the TAC-HFT randomized trial. *Jama* **311,** 62–73 (2014).

49. Karantalis, V. *et al.* Autologous mesenchymal stem cells produce concordant improvements in regional function, tissue perfusion, and fibrotic burden when administered to patients undergoing coronary artery bypass grafting: The Prospective Randomized Study of Mesenchymal Stem Ce. *Circ. Res.* **114,** 1302–10 (2014).

50. Schaefer, A. *et al.* Long-term effects of intracoronary bone marrow cell transfer on diastolic function in patients after acute myocardial infarction : 5-year results from the randomized-controlled BOOST trial — an echocardiographic study. 165–171 (2010). doi:10.1093/ejechocard/jep191

51. Ankrum, J. & Karp, J. M. Mesenchymal stem cell therapy: Two steps forward, one step back. *Trends Mol. Med.* **16,** 203–209 (2010).

52. Galipeau, J. The mesenchymal stromal cells dilemma-does a negative phase III trial of random donor mesenchymal stromal cells in steroid-resistant graft-versus-host disease represent a death knell or a bump in the road? *Cytotherapy* **15,** 2–8 (2013).

53. Klinker, M. W., Marklein, R. A., Lo Surdo, J. L., Wei, C.-H. & Bauer, S. R. Morphological features of IFN-γ-stimulated mesenchymal stromal cells predict overall immunosuppressive capacity. *Proc. Natl. Acad. Sci. U. S. A.* **114,** E2598–E2607 (2017).

54. Mendicino, M., Bailey, A. M., Wonnacott, K., Puri, R. K. & Bauer, S. R. MSC-based product characterization for clinical trials: An FDA perspective. *Cell Stem Cell* **14,** 141–145 (2014).

55. Chinnadurai, R. *et al.* Immune dysfunctionality of replicative senescent mesenchymal stromal cells is corrected by IFNγ priming. *Blood Adv.* **1,** 628–643 (2017).

56. Mouillot, G. *et al.* Hypoxia modulates HLA-G gene expression in tumor cells. *Hum Immunol* **68,** 277–285 (2007).

57. Barsoum, I. B., Koti, M., Siemens, D. R. & Graham, C. H. Mechanisms of hypoxia-mediated immune escape in cancer. *Cancer Res.* **74,** 7185–7190 (2014).

58. Grivennikov, S. I., Greten, F. R. & Karin, M. Immunity, Inflammation, and Cancer. *Cell* **140,** 883–899 (2011).

59. Tong, C. *et al.* Hypoxia pretreatment of bone marrow - Derived mesenchymal stem cells seeded in a collagen-chitosan sponge scaffold promotes skin wound healing in diabetic rats with hindlimb ischemia. *Wound Repair Regen.* **24,** 45–56 (2016).

60. Ospedaliero, I., Surgery, S. & Road, L. H. Should Hypoxia Preconditioning Become the Standardized Procedure for Bone Marrow MSCs Preparation for Clinical Use ? 1992–1993 (2016). doi:10.1002/stem.2389

61. Tobin, L. M., Healy, M. E., English, K. & Mahon, B. P. Human mesenchymal stem cells suppress donor CD4+ T cell proliferation and reduce pathology in a humanized mouse model of acute graft-versus-host disease. *Clin. Exp. Immunol.* **172,** 333–348 (2013).

62. Liu, J. *et al.* Hypoxia pretreatment of bone marrow mesenchymal stem cells facilitates angiogenesis by improving the function of endothelial cells in diabetic rats with lower ischemia. *PLoS One* **10,** 1–18 (2015).

63. Cerrada, I. *et al.* Hypoxia-Inducible Factor 1 Alpha Contributes to Cardiac Healing in Mesenchymal Stem Cells-Mediated Cardiac Repair. *Stem Cells Dev.* **0,** 120914060720002 (2012).

64. Haque, N., Rahman, M. T., KAsim, N. H. A. & Alabsi, A. M. Review Article Hypoxic Culture Conditions as a Solution for Mesenchymal Stem Cell Based Regenerative Therapy. *Sci. World J.* **2013,** (2013).

65. Xie, L. *et al.* In vitro mesenchymal trilineage differentiation and extracellular matrix production by adipose and bone marrow derived adult equine multipotent stromal cells on a collagen scaffold. *Stem Cell Rev. Reports* **9,** 858–872 (2013).

66. Gray, A., Maguire, T., Schloss, R. & Yarmush, M. L. Identification of IL-1β and LPS as optimal activators of monolayer and alginate-encapsulated mesenchymal stromal cell immunomodulation using design of experiments and statistical methods. *Biotechnol. Prog.* **31,** 1058–70 (2015).

67. A., D. *et al.* Human mesenchymal stromal cell-mediated immunoregulation: Mechanisms of action and clinical applications. *Bone Marrow Res.* **2013,** (2013).

68. Mohammadpour, H., Akbar, A., Nikougoftar, M. & Taher, M. International Immunopharmacology TNF- α modulates the immunosuppressive effects of MSCs on

dendritic cells and T cells. *Int. Immunopharmacol.* **28,** 1009–1017 (2015).

69. Liu, Y., Munoz, N., Tsai, A.-C., Logan, T. & Ma, T. Metabolic Reconfiguration Supports Reacquisi - tion of Primitive Phenotype in Human Mesen - chymal Stem Cell Aggregates. *Stem Cells* **35,** 398–410 (2016).

70. Baer, P. C., Overath, J. M., Urbschat, A., Schubert, R. & Geiger, H. Preconditioning of Human Adipose-derived Stromal/Stem Cells: Evaluation of Short-term Preincubation Regimens to Enhance their Regenerative Potential. *J. Stem Cell Res. Ther.* **6,** (2016).

71. Theus, M. H. *et al.* In vitro hypoxic preconditioning of embryonic stem cells as a strategy of promoting cell survival and functional benefits after transplantation into the ischemic rat brain. *Exp. Neurol.* **210,** 656–670 (2008).

72. Andreeva, E. R. *et al.* IFN-gamma priming of adipose-derived stromal cells at 'physiological' hypoxia and under acute hypoxic stress. *J. Cell. Physiol.* (2017). doi:10.1002/jcp.26046

73. Roemeling-Van Rhijn, M. *et al.* Effects of hypoxia on the immunomodulatory properties of adipose tissue-derived mesenchymal stem cells. *Front. Immunol.* **4,** 1–8 (2013).

74. Holtan, S. G., Creedon, D. J., Haluska, P. & Markovic, S. N. Cancer and Pregnancy: Parallels in Growth, Invasion, and Immune Modulation and Implications for Cancer Therapeutic Agents. *Mayo Clin. Proc.* **84,** 985–1000 (2009).

75. Scharping, N. E. *et al.* The Tumor Microenvironment Represses T Cell Mitochondrial Biogenesis to Drive Intratumoral T Cell Metabolic Insufficiency and Dysfunction The Tumor Microenvironment Represses T Cell Mitochondrial Biogenesis to Drive Intratumoral T Cell Metabolic Insuffici. *Immunity* **45,** 374–388 (2016).

76. Mori, A. *et al.* HLA-G expression is regulated by miR-365 in trophoblasts under hypoxic

conditions. *Placenta* **45,** 37–41 (2016).

77. Leblond, M. M. *et al.* Hypoxia induces macrophage polarization and re-education toward an M2 phenotype in U87 and U251 glioblastoma models. *Oncoimmunology* **5,** 1–13 (2016).

78. Madrigal, M., Rao, K. S. & Riordan, N. H. A review of therapeutic effects of mesenchymal stem cell secretions and induction of secretory modification by different culture methods. *J. Transl. Med.* **12,** 260 (2014).

79. Gao, Q. *et al.* Galectin-3 Enhances Migration of Minature Pig Bone Marrow Mesenchymal Stem Cells Through Inhibition of RhoA-GTP Activity. *Sci. Rep.* **6,** 26577 (2016).

80. Liu, G. Y. *et al.* Secreted galectin-3 as a possible biomarker for the immunomodulatory potential of human umbilical cord mesenchymal stromal cells. *Cytotherapy* **15,** 1208–1217 (2013).

81. Gieseke, F. *et al.* Human multipotent mesenchymal stromal cells use galectin-1 to inhibit immune effector cells. *Blood* **116,** 3770–3779 (2010).

82. Giallongo, C. *et al.* Mesenchymal Stem Cells (MSC) Regulate Activation of Granulocyte-Like Myeloid Derived Suppressor Cells (G-MDSC) in Chronic Myeloid Leukemia Patients. *PLoS One* **11,** e0158392 (2016).

83. Reading, J. L. *et al.* Suppression of IL-7-dependent Effector T-cell Expansion by Multipotent Adult Progenitor Cells and PGE2. *Mol. Ther.* **23,** 1783–1793 (2015).

84. Ragni, E., Viganò, M., Rebulla, P., Giordano, R. & Lazzari, L. What is beyond a qRT-PCR study on mesenchymal stem cell differentiation properties: How to choose the most reliable housekeeping genes. *J. Cell. Mol. Med.* **17,** 168–180 (2013).

85. Moreau, P., Flajollet, S. & Carosella, E. D. Non-classical transcriptional regulation of HLA-G: An update. *J. Cell. Mol. Med.* **13,** 2973–2989 (2009).

86. Doherty, J. & Cleveland, J. Targeting lactate metabolism for cancer therapeutics. *J. Clin. Invest.* **123,** 3685–3692 (2013).

87. Jacobs, S. R. *et al.* Glucose Uptake Is Limiting in T Cell Activation and Requires CD28-Mediated Akt-Dependent and Independent Pathways. *J. Immunol.* **180,** 4476–4486 (2008).

88. Fischer, K. *et al.* Inhibitory Effect of Tumor Cell-Derived Lactic Acid on Human T Cells. *Blood* **109,** 3812–3820 (2007).

89. Lee, C. F. *et al.* Preventing Allograft Rejection by Targeting Immune Metabolism. *Cell Rep.* **13,** 760–770 (2015).

90. Cesarz, Z. & Tamama, K. Spheroid Culture of Mesenchymal Stem Cells. *Stem Cells Int.* Article ID 837126 (2015). doi:10.1155/2016/9176357

91. Dorrello, N. V. *et al.* Functional vascularized lung grafts for lung bioengineering. (2017).

92. Chandravanshi, B. & Bhonde, R. R. Shielding Engineered Islets With Mesenchymal Stem Cells Enhance Survival Under Hypoxia. *J. Cell. Biochem.* **118,** 2672–2683 (2017).

93. Wobma, H. & Vunjak-Novakovic, G. Tissue Engineering and Regenerative Medicine 2015: A Year in Review. *Tissue Eng. Part B Rev.* **22,** 101–113 (2016).

94. Blatchley, M., Park, K. M. & Gerecht, S. Designer Hydrogels for Precision Control of Oxygen Tension and Mechanical Properties. *J. Mater. Chem. B* **3,** 7939–7949 (2015).

95. Zimmermann, J. A. & Mcdevitt, T. C. Pre-conditioning mesenchymal stromal cell spheroids for immunomodulatory paracrine factor secretion. *Cytotherapy* **16,** 331–345 (2014).

96. Zimmermann, J., Hettiaratchi, M. & McDevitt, T. Enhanced Immunosuppression of T

Cells by Sustained Presentation of Bioactive Interferon-y Within Three- Dimensional Mesenchymal Stem Cell Constructs. *Stem Cells Transl. Med.* (2016). doi:10.5966/sctm.2016-0044

97. Reeves, A. R. D., Spiller, K. L., Freytes, D. O., Vunjak-Novakovic, G. & Kaplan, D. L. Controlled release of cytokines using silk-biomaterials for macrophage polarization. *Biomaterials* **73,** 272–283 (2015).

98. Wobma, H. M., Liu, D. & Vunjak-Novakovic, G. Paracrine Effects of Mesenchymal Stromal Cells Cultured in Three-Dimensional Settings on Tissue Repair. *ACS Biomater. Sci. Eng.* acsbiomaterials.7b00005 (2017). doi:10.1021/acsbiomaterials.7b00005

99. Bartels, K., Grenz, A. & Eltzschig, H. K. Hypoxia and inflammation are two sides of the same coin. *Proc. Natl. Acad. Sci. U. S. A.* **110,** 18351–2 (2013).

100. Eming, S., Wynn, T. A. & Martin, P. Inflammation and metabolism in tissue repair and regeneration. *Science (80-.).* **356,** 1026–1030 (2017).

101. Mateescu, B. *et al.* Obstacles and opportunities in the functional analysis of extracellular vesicle RNA - An ISEV position paper. *J. Extracell. Vesicles* **6,** (2017).

102. Witwer, K. W. *et al.* Standardization of sample collection , isolation and analysis methods in extracellular vesicle research Need for standardization ISEV 2012 workshop on evRNA. **2,** 20360 (2014).

103. Arslan, F. *et al.* Mesenchymal stem cell-derived exosomes increase ATP levels, decrease oxidative stress and activate PI3K/Akt pathway to enhance myocardial viability and prevent adverse remodeling after myocardial ischemia/reperfusion injury. *Stem Cell Res.* **10,** 301–312 (2013).

104. Lai, R. C. *et al.* Exosome secreted by MSC reduces myocardial ischemia/reperfusion

injury. *Stem Cell Res.* **4,** 214–222 (2010).

105. Furuta, T. *et al.* Mesenchymal Stem Cell-Derived Exosomes Promote Fracture Healing in a Mouse Model. *Stem Cells Transl. Med.* **5,** 1620–1630 (2016).

106. Kordelas, L. *et al.* MSC-derived exosomes: a novel tool to treat therapy-refractory graft-versus-host disease. *Leukemia* 970–973 (2014). doi:10.1038/leu.2014.41

107. Momen-Heravi, F. *et al.* Current methods for the isolation of extracellular vesicles. *Biol. Chem.* **394,** 1253–1262 (2013).

108. Mashima, T. *et al.* Acyl-CoA synthetase as a cancer survival factor: Its inhibition enhances the efficacy of etoposide. *Cancer Sci.* **100,** 1556–1562 (2009).

109. Shen, W. *et al.* S100A4 protects gastric cancer cells from anoikis through regulation of αv and α5 integrin. *Cancer Sci.* **102,** 1014–1018 (2011).

110. Paoli, P., Giannoni, E. & Chiarugi, P. Anoikis molecular pathways and its role in cancer progression. *Biochim. Biophys. Acta - Mol. Cell Res.* **1833,** 3481–3498 (2013).

111. Guadamillas, M. C., Cerezo, A. & del Pozo, M. A. Overcoming anoikis - pathways to anchorage-independent growth in cancer. *J. Cell Sci.* **124,** 3189–3197 (2011).

112. Liao, Y.-H. *et al.* Epidermal growth factor-induced ANGPTL4 enhances anoikis resistance and tumour metastasis in head and neck squamous cell carcinoma. *Oncogene* **36,** 2228–2242 (2017).

113. Zhang, B., Yang, X. & Gao, X. Taurine protects against bilirubin-induced neurotoxicity in vitro. *Brain Res.* **1320,** 159–167 (2010).

114. Zhang, Z. *et al.* Taurine supplementation reduces oxidative stress and protects the liver in an iron-overload murine model. *Mol. Med. Rep.* **10,** 2255–2262 (2014).

115. Chowdhury, S., Sinha, K., Banerjee, S. & Sil, P. C. Taurine protects cisplatin induced

cardiotoxicity by modulating inflammatory and endoplasmic reticulum stress responses. *BioFactors* **42,** 647–664 (2016).

116. Caruso, G. *et al.* Carnosine modulates nitric oxide in stimulated murine RAW 264.7 macrophages. *Mol. Cell. Biochem.* **431,** 197–210 (2017).

117. Naghshvar, F., Abianeh, S. M., Ahmadashrafi, S. & Hosseinimehr, S. J. Chemoprotective effects of carnosine against genotoxicity induced by cyclophosphamide in mice bone marrow cells. *Cell Biochem. Funct.* **30,** 569–573 (2012).

118. Tachida, Y., Sakurai, H. & Okutsu, J. Proteomic Comparison of the Secreted Factors of Mesenchymal Stem Cells from Bone Marrow, Adipose Tissue and Dental Pulp. *J. Proteomics Bioinform.* **8,** 266–273 (2015).

119. Rolandsson Enes, S. *et al.* Quantitative proteomic characterization of lung-MSC and bone marrow-MSC using DIA-mass spectrometry. *Sci. Rep.* **7,** 9316 (2017).

120. Mcgaha, T. L. *et al.* Amino acid catabolism: A pivotal regulator of innate and adaptive immunity. *Immunol. Rev.* **249,** 135–157 (2012).

121. Toledano, N., Gur-Wahnon, D., Ben-Yehuda, A. & Rachmilewitz, J. Novel CD47: SIRPa Dependent Mechanism for the Activation of STAT3 in Antigen-Presenting Cell. *PLoS One* **8,** (2013).

122. Liu, X., Kwon, H., Li, Z. & Fu, Y. Is CD47 an innate immune checkpoint for tumor evasion? *J. Hematol. Oncol.* **10,** 12 (2017).

123. Moll, G. *et al.* Do Cryopreserved Mesenchymal Stromal Cells Display Impaired Immunomodulatory and Therapeutic Properties? *Stem Cells* **32,** 2430–2442 (2014).

124. Li, Y., Qiu, W., Zhang, L., Fung, J. & Lin, F. Painting factor H onto mesenchymal stem cells protects the cells from complement- and neutrophil-mediated damage. *Biomaterials*

102, 209–219 (2016).

125. Kabouridis, P. S. *et al.* Distinct localization of T cell Agrin during antigen presentation - Evidence for the expression of Agrin receptor(s) in antigen-presenting cells. *FEBS J.* **279,** 2368–2380 (2012).

126. Wynn, T. a, Yugandhar, V. G. & Clark, M. a. Cellular and molecular mechanisms of fibrosis. *J Pathol* **46,** 26–32 (2013).

127. Mertens, P. R., Wei–min Cai, ţ & Dooley, S. Effect of Interferon-Gamma on Hepatic Fibrosis in Chronic Hepatitis B Virus Infection: A Randomized Controlled Study. **3565,** 819–828 (2005).

128. Chiche, J. *et al.* Hypoxia-inducible carbonic anhydrase IX and XII promote tumor cell growth by counteracting acidosis through the regulation of the intracellular pH. *Cancer Res.* **69,** 358–368 (2009).

129. Baker, A. *et al.* Lysyl oxidase plays a critical role in endothelial cell stimulation to drive tumor angiogenesis. **73,** 583–594 (2013).

130. El-Haibi, C. P. *et al.* Critical role for lysyl oxidase in mesenchymal stem cell-driven breast cancer malignancy. *Proc. Natl. Acad. Sci.* **109,** 17460–17465 (2012).

131. Xie, Q. *et al.* Hypoxia triggers angiogenesis by increasing expression of LOX genes in 3-D culture of ASCs and ECs. *Exp. Cell Res.* **352,** 157–163 (2017).

132. Romero-Garcia, S., Moreno-Altamirano, M. M. B., Prado-Garcia, H. & Sánchez-García, F. J. Lactate Contribution to the Tumor Microenvironment: Mechanisms, Effects on Immune Cells and Therapeutic Relevance. *Front. Immunol.* **7,** 52 (2016).

133. Mockler, M. B., Conroy, M. J. & Lysaght, J. Targeting T cell immunometabolism for cancer immunotherapy; understanding the impact of the tumor microenvironment. *Front.*

Oncol. **4,** 107 (2014).

134. Chang, C. H. *et al.* Metabolic Competition in the Tumor Microenvironment Is a Driver of Cancer Progression. *Cell* **162,** 1229–1241 (2015).

135. Tran, D. Q. *et al.* GARP (LRRC32) is essential for the surface expression of latent TGF- on platelets and activated FOXP3+ regulatory T cells. *Proc. Natl. Acad. Sci.* **106,** 13445–13450 (2009).

136. Carrillo-Galvez, a. B. *et al.* Mesenchymal stromal cells express GARP / LRRC32 on their surface: Effects on their biology and immunomodulatory capacity. *Stem Cells* **33,** 183–95 (2015).

137. Chanmee, T., Ontong, P., Konno, K. & Itano, N. Tumor-associated macrophages as major players in the tumor microenvironment. *Cancers (Basel).* **6,** 1670–1690 (2014).

138. Kumar, V. & Gabrilovich, D. I. Hypoxia-inducible factors in regulation of immune responses in tumour microenvironment. *Immunology* **143,** 512–519 (2014).

139. Huang, Y. C., Parolini, O., Deng, L. & Yu, B. S. Should hypoxia preconditioning become the standardized procedure for bone marrow MSCs preparation for clinical use? *Stem Cells* **34,** 1992–1993 (2016).

140. Chinnadurai, R. *et al.* Cryopreserved Mesenchymal Stromal Cells Are Susceptible to T-Cell Mediated Apoptosis Which Is Partly Rescued by IFNγ Licensing. *Stem Cells* **34,** 2429–2442 (2016).

141. François, M. *et al.* Cryopreserved mesenchymal stromal cells display impaired immunosuppressive properties as a result of heat-shock response and impaired interferon-γ licensing. *Cytotherapy* **14,** 147–152 (2012).

142. Killer, M. C. *et al.* Immunosuppressive capacity of mesenchymal stem cells correlates

with metabolic activity and can be enhanced by valproic acid. *Stem Cell Res. Ther.* **8,** 100 (2017).

143. Kurtzberg, J. *et al.* Allogeneic human mesenchymal stem cell therapy (Remestemcel-L, Prochymal) as a rescue agent for severe refractory acute graft-versus-host disease in pediatric patients. *Biol. Blood Marrow Transplant.* **20,** 229–235 (2014).

144. Martin, P. J. J. *et al.* Prochymal Improves Response Rates In Patients With Steroid-Refractory Acute Graft Versus Host Disease (SR-GVHD) Involving The Liver And Gut: Results Of A Randomized, Placebo-Controlled, Multicenter Phase III Trial In GVHD. *Biol. Blood Marrow Transplant.* **16,** S169–S170 (2010).

145. Daly, A. Remestemcel-L, the first cellular therapy product for the treatment of graft-versus-host disease. *Drugs of Today* **48,** 773–783 (2012).

146. Guess, A. J. *et al.* Safety Profile of Good Manufacturing Practice Manufactured Interferon γ Primed Mesenchymal Stem/Stromal Cells for Clinical Trials. *Stem Cells Transl. Med.* (2017). doi:10.1002/sctm.16-0485

147. Kim, N. *et al.* Mesenchymal stem cells for the treatment and prevention of graft-versus-host disease: experiments and practice. *Ann. Hematol.* **92,** 1295–1308 (2013).

148. Ali, N. *et al.* Xenogeneic Graft-versus-Host-Disease in NOD-scid IL-2Rγnull Mice Display a T-Effector Memory Phenotype. *PLoS One* **7,** 1–10 (2012).

149. Vunjak-Novakovic, G., Bhatia, S. N., Chen, C. & Hirschi, K. HeLiVa platform : integrated heart – liver – vascular systems for drug testing in human health and disease. *Stem Cell Res. Ther.* **4,** 1–6 (2013).

150. Villasante, A., Marturano-Kruik, A. & Vunjak-Novakovic, G. Bioengineered human tumor within a bone niche. *Biomaterials* **35,** 5785–5794 (2014).

151. Sviland, L. & Dickinson, a. M. A human skin explant model for predicting graft-versus-host disease following bone marrow transplantation. *J. Clin. Pathol.* **52,** 910–913 (1999).

152. Itoh, M. *et al.* Generation of 3D Skin Equivalents Fully Reconstituted from Human Induced Pluripotent Stem Cells (iPSCs). *PLoS One* **8,** e77673 (2013).

153. Zhang, H. *et al.* Functional Analysis and Transcriptomic Profiling of iPSC-Derived Macrophages and Their Application in Modeling Mendelian Disease. *Circ. Res.* **117,** 17–28 (2015).

154. Seki, T., Yuasa, S. & Fukuda, K. Generation of induced pluripotent stem cells from a small amount of human peripheral blood using a combination of activated T cells and Sendai virus. *Nat. Protoc.* **7,** 718–28 (2012).

155. Itoh, M. *et al.* Generation of 3D Skin Equivalents Fully Reconstituted from Human Induced Pluripotent Stem Cells (iPSCs). *PLoS One* **8,** 1–9 (2013).

156. Mathewson, N. & Reddy, P. The Microbiome and Graft Versus Host Disease. *Curr. Stem Cell Reports* **1,** 39–47 (2015).

APPENDIX

SUPPLEMENTAL TABLES

Table S1 Flow cytometry antibody details for MSC and PBMC staining.

Target	Clone	Fluorophore	Antibody Dilution	Source
CD3	UCHT1	PerCP-Cy™5.5	1:20	BD
CD4	RPA-T4	PE-Cy7	1:80	BD
CD8	SK1	APC-Cy7	1:40	BD
CD107a	H4A3	PE	1:5	BD
CD25	M-A251	APC	1:5	BD
CD45RA	HI100	V500	1:20	BD
CCR7	150503	FITC	1:20	BD
HLA-G	MEM-G/9	FITC	1:10	Abcam
IDO	eyedio	eFluor660	1:20	eBioscience
CD274 (PD-L1)	MIH1	eFluor450	1:20	eBioscience
COX-2	AS66	FITC	1:20	Cayman
HLA-E	3D12	APC	1:10	Miltenyi
GLUT1	SPM498	APC	1:500	Abcam

Table S2 Forward and reverse primers for immunosuppressive genes

	Forward	Reverse
GAPDH	AAGGTGAAGGTCGGAGTCAAC	GGGGTCATTGATGGCAACAATA
HLA-G	GAAGAGGAGACACGGAACA	TGGCCTCATAGTCAAAGACA
HLA-E	ATGGAACCCTCCTTTTACTC	GGCTCCAGGTGAAGCAGC
HGF	GGTGACCAAACTCCTGCCA	ACCTCTGGATTGCTTGTGAAA
COX2	CAGCCATACAGCAAATCC	ATCCTGTCCGGGTACAAT
iNOS	TCATCCGCTATGCTGGCTAC	CCCGAAACCACTCGTATTTGG
IDO	TCTCATTTCGTGATGGAGACTGC	GTGTCCCGTTCTTGCATTTGC
LIF	CCAACGTGACGGACTTCCC	TACACGACTATGCGGTACAGC
IL-10	TCAAGGCGCATGTGAACTCC	GATGTCAAACTCACTCATGGCT
TGF-β	GGCCAGATCCTGTCCAAGC	GTGGGTTTCCACCATTAGCAC
TSG-6	GGGCAGAGTTGGATACCCC	TGCGTGTGGGTTGTAGCAATA
CD59	TTTTGATGCGTGTCTCATTACCA	ATTTTCCCTCAAGCGGGTTGT
PD-L1	GGACAAGCAGTGACCATCAAG	CCCAGAATTACCAAGTGAGTCCT
Arginase-1	GTGGAAACTTGCATGGACAAC	AATCCTGGCACATCGGGAATC
Galectin-1	TCGCCAGCAACCTGAATCTC	GCACGAAGCTCTTAGCGTCA
Galectin-3	GTGAAGCCCAATGCAAACAGA	AGCGTGGGTTAAAGTGGAAGG

Abbreviations: glyceraldehyde 3-phosphate dehydrogenase (GAPDH), human leukocyte antigen-G (HLA-G), human leukocyte antigen-E (HLA-E), hepatocyte growth factor (HGF), cyclo-oxgenase-2 (COX-2), inducible nitric oxide synthase (iNOS), indoleamine-2,3-dioxygenase (IDO), leukemia inhibitory factor (LIF), interleukin-10 (IL-10), transforming growth factor- β (TGF- β), tumor necrosis factor-inducible gene 6 (TSG-6), programmed death ligand 1 (PD-L1)

Table S3 Mean fluorescence intensity ± SD of GLUT1 expression on CD4+ and CD8+ T-cell subsets in MSC-MLR co-culture studies on days 1 and 3.

	CD4+		CD8+	
	Day 1	Day 3	Day 1	Day 3
Responder Only	2711 ± 958	2796 ± 938	2792 ± 1416	2482 ± 828
MLR	2792 ±1089	3792 ± 2360	2859 ± 1297	3649 ± 3000
MLR + C MSCs	3886 ± 1782	4166 ± 2444	4044 ± 1921	4176 ± 2702
MLR + I MSCs	3957 ± 1811	3809 ± 2352	4535 ± 2413	3895 ± 2664
MLR + H MSCs	3408 ± 1519	3838 ± 2361	3638 ± 1838	3610 ± 2106
MLR + D MSCs	2636 ± 1200	3170 ± 1728	2801 ± 1577	2884 ± 1889

Note: There were ~4,000 events in the CD4 gate and ~1,000 events in CD8 gate for each sample; ANOVA analysis showed that GLUT1 expression in the MLR + D MSCs condition was significantly lower (****) than all other MLR conditions; on Day 1, there was not even a significant difference between Responder Only and MLR + D MSC

Table S4 Mean fluorescence intensity ± SD for protein expression data shown in Figure 4.

	IDO	**HLA-G**	**HLA-E**	**COX-2**	**PD-L1**
C MSCs	299 ± 227	564 ± 570	2396 ± 3640	310 ± 2003	169 ± 288
I MSCs	20 900 ± 11 087	668 ± 680	8848 ± 7296	337 ± 796	611 ± 489
H MSCs	482 ± 2405	554 ±797	2375 ± 4580	358 ± 1222	167 ± 265
D MSCS	31,766 ± 16,677	796 ± 1212	9721 ± 6944	336 ± 827	575 ± 435

Table S5 Daily glucose consumption and lactate production in MSC-MLR experiments

	Daily Glucose Consumption		Daily Lactate Production	
	Day 1	Day 2-3 Avg	Day 1	Day 2-3 Avg
Responder Only	3.65	8.53	< 1	1.97
MLR Only	6.80	15.38	< 1	2.92
MLR + C MSCs	34.45	40.33	5.61	7.85
MLR + I MSCs	46.10	40.45	6.88	7.36
MLR + H MSCs	61.55	39.50	9.22	5.53
MLR + D MSCs	70.85	45.60	14.08	6.30

Table S6 Effect of lactate on intracellular pH as measured by the pHrodo Red dye intensity

[Lactate]	Median Fluorescence Intensity (pHrodo Red)
0 mM	4974
5 mM	5891
10 mM	6176
15 mM	7503
20 mM	8761
30 mM	14108

Table S7 Flow cytometry antibody details for dendritic cell characterization.

Target	Clone	Fluorophore	Concentration	Source
CD11c	3.9	APC	1:20	ebioscience
CD14	M5E2	FITC	1:5	BD
CD36	CB38	PE	1:5	BD
CD80	L307.4	FITC	1:5	BD
CD207 (Langerin)	2G3	PE	1:20	BD
CD209 (DC-SIGN)	DCN46	FITC	1:5	BD
CD324 (E-cadherin)	67A4	FITC	1:20	Biolegend
HLA-DR	G46-6	PE	1:20	BD

SUPPLEMENTAL FIGURES

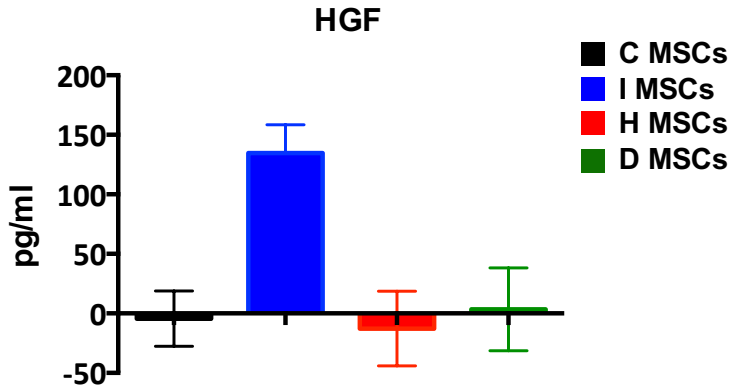

Figure S1 Supernatant HGF levels. Relative soluble HGF levels in conditioned media from MSCs primed for 48 hours.

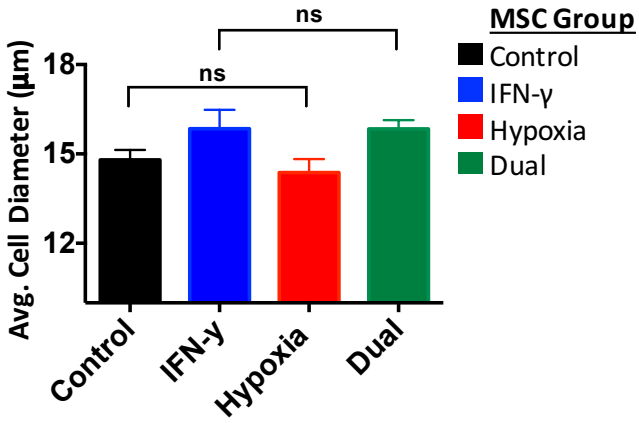

Figure S2 The effect of hypoxia and/or IFN-γ priming on the average cell diameter. Cell diameter was determined immediately after passaging using a Countess device. n=5 experiments were averaged. All pairwise comparisons were significant at $p<0.05$ except where indicated.

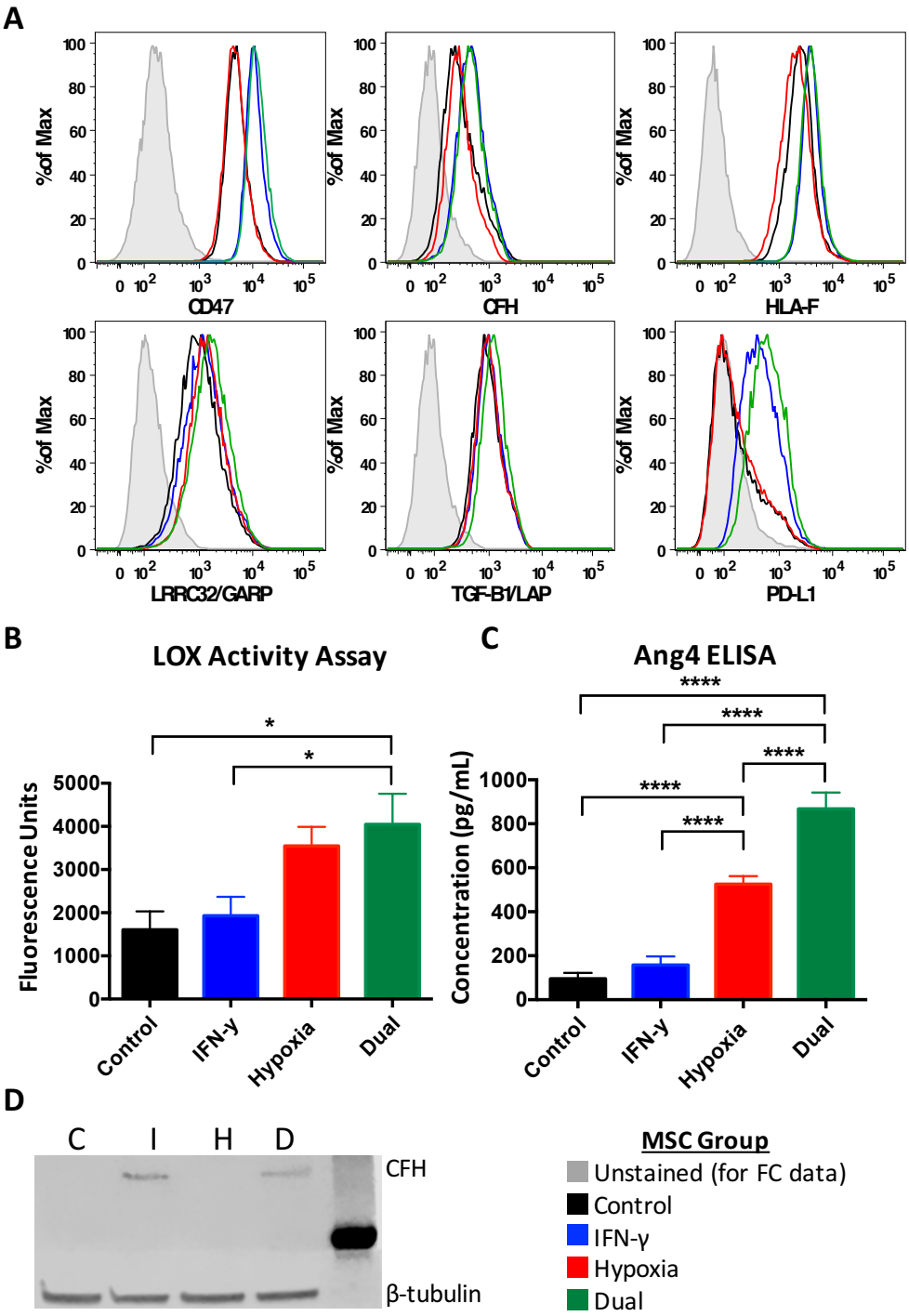

Figure S3 Confirming trends found via mass spectroscopy for select proteins. A) Flow cytometry was used to assess how IFN-γ and/or hypoxia affected expression of some proteins that had been detected by a single peptide via mass spectroscopy (CFH, HLA-F,PD-L1) or had shown a DE of small magnitude on mass spectroscopy (CD47, LRRC32, TGF-B1). **B)** Lysyl oxidase activity assay was used to confirm the increased activity/expression of this family of proteins upon exposure to hypoxia (or dual hypoxia/IFN-γ). **C)** ANGPTL4 ELISA was used to confirm the upregulation of this protein under hypoxia or dual hypoxia/IFN-γ priming. **D)** CFH Western Blot was a second means of confirming the upregulation by IFN-γ and dual priming seen from the mass spec data. * $p<0.05$, *** $p<0.0001$

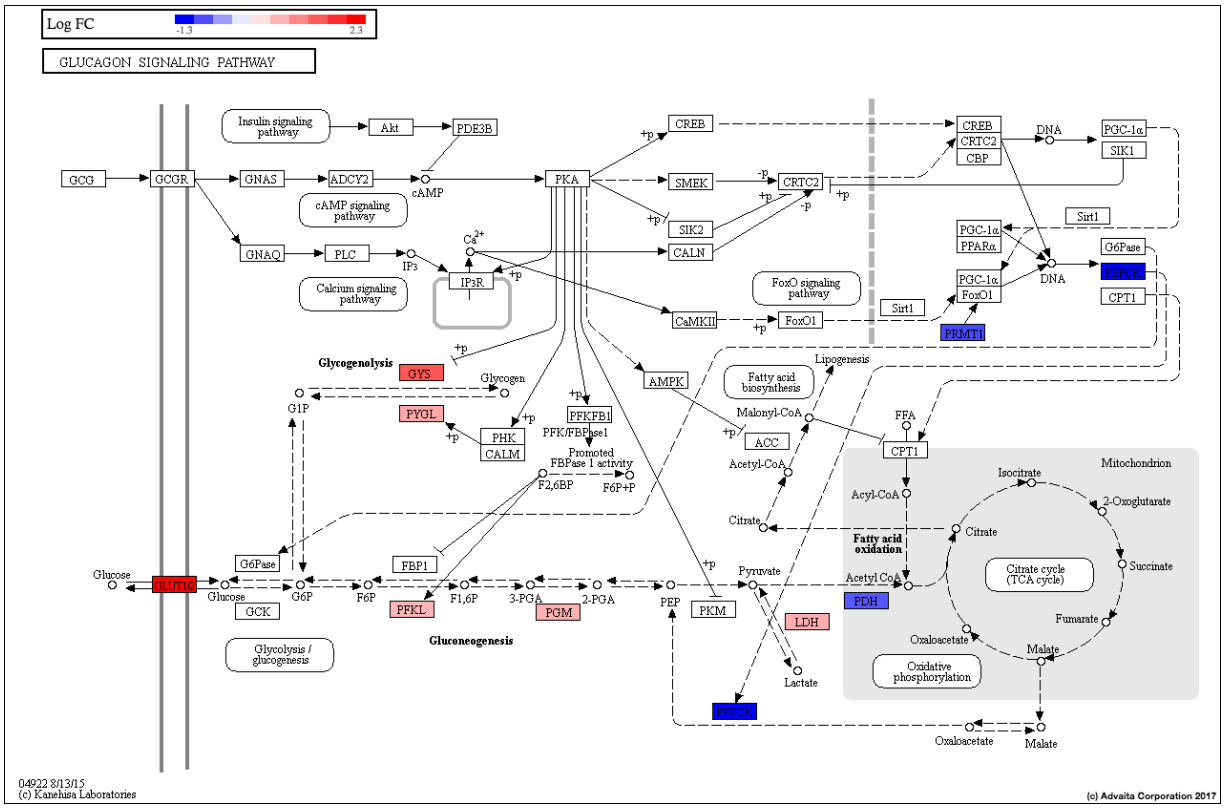

Figure S4 The effect of dual priming on the expression of proteins in the glucagon signaling pathway. The heat map at the top left shows the log2 fold change difference in expression of proteins, where blue indicates a down-regulated protein and red indicates an upregulated protein. Only those proteins that met our criteria for differential expression are shown (log2FC > 0.6 and p< 0.05)

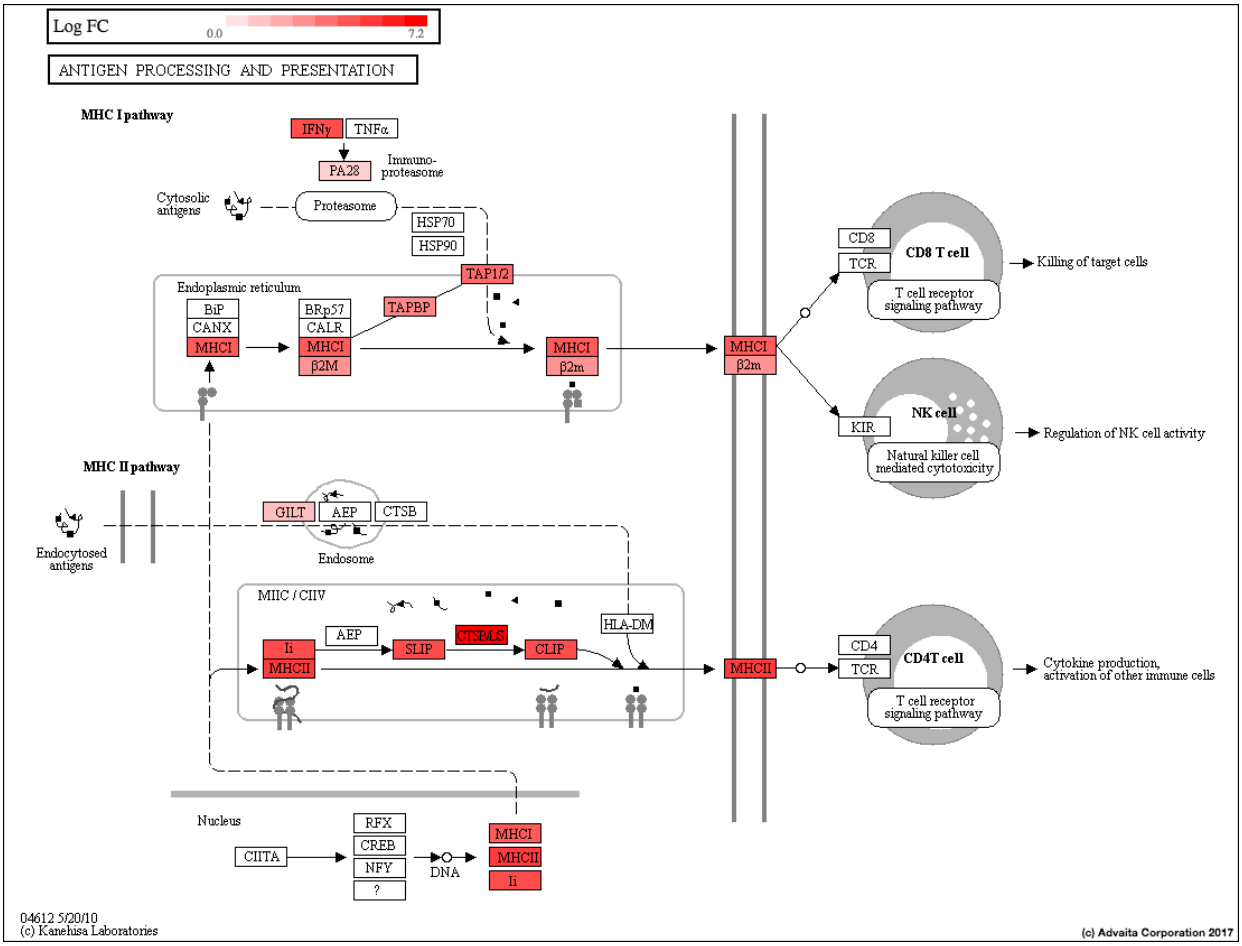

Figure S5 The effect of IFN-γ priming on the expression of proteins in the antigen presentation cascade. The heat map at the top left shows the log2 fold change difference in expression of proteins, where blue indicates a down-regulated protein and red indicates an upregulated protein. Only those proteins that met our criteria for differential expression are shown (log2FC > 0.6 and p< 0.05)